Cosmos Impact Factor - 6.987

ISSN 0970-6569 (Print)
ISSN 2320-3218 (Online)

Bulletin of Pure and Applied Sciences
Section D – Physics

July-December 2022
Volume 41D, Number 2

(A Peer Reviewed and Refereed Journal)

Editor-in-chief:
Prof. Madan jee

Published half-yearly in June and December Every Year

Website:
www.bpasjournals.com

Bulletin of Pure and Applied Sciences
Section D – Physics

EDITORIAL BOARD

Bulletin of Pure and Applied Sciences
Section D – Physics

Dr. R. Somashekar, Department of Physics, University of Mysore, Mysore, Karnataka 570005, India
E-mail: rs@uomphysics.ner
Dr. Amol V. Patil, Department of Physics, I.C.S. College of Arts, Commerce and Science, Khed, Dist. Ratnagiri , Maharashtra 415 709, India
E-mail: avpatil333@gmail.com; avpatil333@rediffmail.com
Dr. Uppara Naresh, BIT Institute of Technology, Hindupuram, Andhra Pradesh 515201, India
E-mail: nareshkkm@gmail.com

International Editorial Advisory Board

Editorial Office

Managing Editor: Prof. Dr. A K Sharma
E-mail: editorbulletin8@gmail.com

Publication Editor: Manoj Kumar Singh
E-mail: bpaspublications@gmail.com

Bulletin of Pure and Applied Sciences
Section D – Physics

About the Journal

Bulletin of Pure and Applied Sciences: Section-D- Physics is a Double-blind Peer Reviewed and Refereed Journal. It devoted to the international advancement of organized knowledge on all branches of Physics. It is an international journal committed to publish and disseminate original research in the field of physics (pure and applied) through a fair and rigorous review process. Scope of the journal includes: Atomic physics, molecular physics, condensed matter, elementary particles, nuclear physics, gases, fluid dynamics, plasmas, electromagnetism, optics, mathematical physics, interdisciplinary, classical and applied physics. It provides a forum for comments by publishing original research contributions, scientific survey, case studies, book review and letter to the Editor-in-Chief. **Bulletin of Pure and Applied Sciences: Section-D- Physics** is issued six monthly, i.e. June and December of every year. The Editor-in-Chief/Managing Editor/Editorial Board etc. assumes no responsibility for the statements and opinions advanced by the contributors. The editorial staff in its work of examining papers, received for possible publication is assisted, in an honorary capacity, by a large number of distinguished scientists working in various parts of the world.

(A Double-blind Peer Reviewed and Referred Journal)

Abstracting and Indexing information:
This publication is included in Abstracted/Indexed coverage of selected services i.e. Google Scholar; GALE group, Indian Science Abstract, ProQuest, USA; EBSCO Information Services, USA; Indian Citation Index, India; J-Gate, India; Scope database, India; Cosmos Impact Factor, Germany; Scientific Indexing Services (SIS), USA etc.

Annual Subscription Rates
Print version (For 2022)**-** India Rs.3200; Abroad $ 100 or equivalent
Print version (For 2023)**-** India Rs.3200; Abroad $ 100 or equivalent
Online version (For 2023)**-** India Rs.2000; Abroad $ 100 or equivalent

Online version available at- https://online.bpasjournals.com/journal/journals/year-2022/
Archive available at- http://www.bpasjournals.com/physics/journal-archive.php

Subscription Information

Institutional (1 year) INR3200/USD100

Here is payment instruction for your reference.

For Bank transactions: (RTGS, IMPS and NEFT transactions)
Complete Bank Account No. 916020035086217
Beneficiary Name: BPAS PUBLICATIONS
Bank & Branch Name: AXIS BANK Ltd. Laxmi Nagar, Delhi-110092
MICR Code: 110211163
SWIFT Code: AXISINBB166
IFSC Code: UTIB0002685 (used for RTGS and NEFT transactions)

For Bank Cheque/ Demand Draft:
Please send the US dollar check from outside India and INR check from India made
Payable to '**BPAS PUBLICATIONS'** at **Delhi**.

Online Payment Method (By Payment Gateway):
https://online.bpasjournals.com/payment/

**Please kindly add bank charge at your side if you pay by check or wire transfer.
Payment, orders and all correspondences should be sent to;

Mail all orders to
Subscription and Marketing Manager
BPAS PUBLICATIONS
115-RPS- DDA Flat, Mansarover Park,
Shahdara, Delhi-110032, India
Mob: +91- 9212200909
E-mail:
editorbulletin8@gmail.com
bpaspublications@gmail.com
bpassubscriptions@gmail.com
Website:
www.bpasjournals.com

Bulletin of Pure and Applied Sciences
Section D – Physics

July-December 2022
Volume 41D, Number 2

ISSN 0970-6569 (Print)
ISSN 2320-3218 (Online)

Contents

Original Articles

Bulletin of Pure and Applied Sciences
Section D – Physics

Address for communication:

Prof. Dr. A.K. Sharma,
BPAS Publications
115-RPS-DDA Flat, Mansarover Park, Shahdara, Delhi-110032, India
(Phone-011-22138726, 9212200909)
Email: editorbulletin8@gmail.com, bpaspublications@gmail.com
Website: www.bpasjournals.com

Bulletin of Pure and Applied Science
Physics, Vol.41D No.2,
July-December 2022 P.41-44
Original Research Article

Print version ISSN 0970 6569
Online version ISSN 2320 3218
DOI: 10.5958/2320-3218.2022.00008.2
Available online at www.bpasjournals.com

How Violation of Newton's Third Law Can Pave Way to New Space Propulsion Mechanism via Optical Diametric Drive Experiment

[1]Victor Christianto*, [2]Florentin Smarandache

Author's Affiliations: [1]Malang Institute of Agriculture, Indonesia. Halton Arp Institute, affiliated to International Mariinskaya Academy, St. Petersburg
[2]Dept. Mathematics & Sciences, University of New Mexico, Gallup, USA.

***Corresponding author:** **Victor Christianto**
Malang Institute of Agriculture, Indonesia. Halton Arp Institute, affiliated to International Mariinskaya Academy, St. Petersburg
E-mail: victorchristianto@gmail.com

Received on 21.03.2022
Revised on 29.08.2022
Accepted on 29.10.2022
Published on 15.12.2022

ABSTRACT In our initial paper discussing plausible steps toward workable warp drive machines. The following article express our view on this debate. While there are still objections toward existing *warp drive* proposals, such as by G. Landis, Harold White *etc*., because they are all based on GTR, nonetheless we think it is possible by starting to see if it is possible to deviate from Newton's third law. And we discuss possible a propulsion method based on negative masses, and discuss how optical diameter drive can be first step for realistic lab-scale version of negative mass propulsion.

KEYWORDS Negative Mass Propulsion, Negative Mass Particle, Phonon Roton Superfluidity, Lab-Scale Warp Drive Experiment, Optical Diameter Drive Experiment.

How to cite this article: Christianto V., Smarandache F. (2022). How Violation of Newton's Third Law Can Pave Way to New Space Propulsion Mechanism via Optical Diametric Drive Experiment. *Bulletin of Pure and Applied Sciences- Physics,* 41D (2), 41-44.

NEWTON'S THIRD LAW

Despite normally we think that action-reaction law is given, actually in some cases it can be violated, just like violation of Pauli principle (voP), perhaps we can call it with term: violation of Newton 3rd law (voN3L). In stating Newton's Third Law, we have assumed tacitly that (a) All forces are two-body forces, i.e. they act between a specified pair of objects and are not influenced by the presence of other objects; and (b) The net force on object i is the vector sum of the individual forces actingon it from all the other objects in the universe.

According to Ivlev *et al*. (2015), "There is a variety of situations in which Newton's third law is violated. Generally, the action-reaction symmetry can be broken for mesoscopic particles, when their effective interactions are mediated by a nonequilibrium environment."[1]

Terletsky/Winterberg's concept of negative mass particles

While only recently the experimental vindication of existence of negative mass particles are reported (see *Nature Communication*, 2021), actually it can be traced back to an eminent physicist from MSU, Yakov Terletsky, and also the late F. Winterberg (from University of Nevada).

Actually Terletsky wrote in his book, paradoxes in relativity theory, as follows:

"Along these lines, assuming that the parts of the vector are taken to be ar-
bitrary genuine numbers, then, at that point, equation concedes to three essen-
tially unique actual frameworks:
1. systems with positive proper mass, i.e., M2 ~ 0, E > 0;
2. systems with negative proper mass, i.e., M2 ~ 0, E < 0;
3. systems with an imaginary proper mass, i.e., M2 < o.

Thus, the system of the hypothesis of relativity advertisement
mits three sorts of basically various frameworks of which just sys-
tems of the principal kind are viewed as actually genuine."[7]

Although the notion of *negative mass* is quite controversial in the field of gravitation and cosmology studies, and by numerous authors its existence is forbidden, actually Pollard and Dunning-Davies show that it is possible to appear in Nature. [8]

Later on F. Winterberg, who was one of last finest students of W. Heisenberg, puts forth possible existence of phonon-roton model of superfluidity which are composed of positive and negative mass particles, which he coined as "*Planckions*."[8]

Although possibility of negative mass propulsion method has been discussed by several authors, including Winterberg [9]; among other things he wrote in abstract:
"Schrödinger's examination of the Dirac condition gives a clue for the presence of negative masses taken cover behind certain masses. Be that as it may, their utilization for impetus by decreasing the idleness of issue for instance, in the restriction of plainly visible bodied with zero rest mass, relies upon a specialized answer with the expectation of complimentary them from their detainment by sure masses. Apparently there are fundamentally two different ways this may be accomplished:
1. By the utilization of solid electromagnetic or gravitational fields or by high molecule energies.
2. Via looking for places in the universe where nature has effectively done this detachment, and from where the negative masses can be mined.
The first of these two prospects is for all viable means barred, since, in such a case that conceivable at all, it would rely upon electromagnetic or gravitational fields with strength past what is actually feasible, or on very huge in like manner not achievable molecule energies. As to the second chance, it has been seen that non-baryonic cold dim matter will in general aggregate close to the focal point of cosmic systems, or spots in the universe which have a huge gravitational potential
well "[9]

Although there are others who also investigate negative mass propulsion such as Robert L. Forward and Martin Tajmar and his team at Dresden University [10][11]; to these authors, an appropriate term is: "*Terletsky-Winterberg negative mass propulsion mechanism*." Nonetheless, to our knowledge we are still far to be in "operational scale" of negative mass propulsion engine as envisaged by F. Winterberg.[1]

Fortunately, there are recent lab-scale experiments using optical diametrical drive which made use of negative mass particle into practical lab experiments.

[1]This author is forever indebted to Prof. F. Winterberg who once sent his book, around 2010/2011, and to encourage him to continue further our investigation on superfluid phonon roton model of the Cosmos. But the book that he sent, with title something like: "Finititude theory of particles" was lost from trace.

OPTICAL DIAMETRIC DRIVE PROSPECT

Isaac Newton in his *Principia* expressed that for any activity there is an equivalent and inverse response. The consequences of this law of movement are presently being rethought by a group of specialists from the University of Central Florida and Germany who as of late completed an optical test that one day might help lead to new impetus frameworks.

"This strange interaction, which includes the idea of negative mass, imitates the conduct of a polar drive," said Professor Demetrios Christodoulides of UCF's College of Optics and Photonics. "Despite the fact that thoughts of this sort have been around for a long time, they have never been effectively sought after on the grounds that mass in nature is consistently a positive amount." Diametric drive alludes to the chance of an independent, space-impetus motor that works without the requirement for any outside fuel.

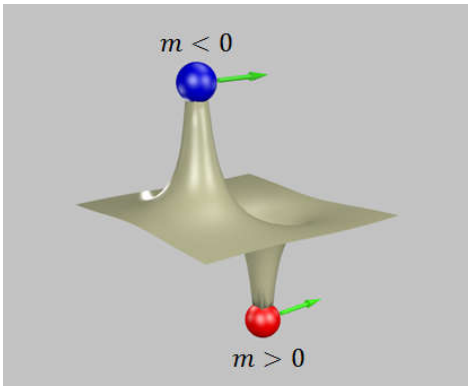

Figure 1: Diametric drive illustration [1]

The review "Optical polar drive speed increase by means of activity response balance breaking" as of late distributed on the site of *Nature Physics* and was important for a venture with other accomplice colleges. Mohammad-Ali Miri, a UCF graduate understudy in the Center for Research and Education in Optics and Lasers (CREOL), likewise took part in this work.

Another experiments, as reported by Pei *et al*.: "optical self-accelerating state driven by nonlinear coherent interaction of its constituting components with opposite "mass-sign". The coherent propulsion, highly immune to initial phase conditions, is surprisingly enhanced comparing to its incoherent counterpart."[4]

Acknowledgement
The present article is dedicated to VC's former professors at IGC, RUDN, including Prof. A. Yefremov (Director, IGC), Prof. Yu P. Rybakov, and also Prof. Yu Vladimirov. This writer can recall, back then to Dec. 2008 when he just arrived to Moscow and started to attending class of Prof. Yu Vladimirov, he asked this author: "*Where do you come from?*" I replied: "*Indonesia*." And the former professor replied: "*Ah, Indonesia? I remember Soekarno*." Although, in this article I don't cite any of his many publications on cosmology etc., but I recall that Terletsky also belonged to Moscow State University, as also great physicists like Prof. Lev Landau and Prof. Bogoliubov. MSU belongs to one of the best universities for physics studies in the world. Moreover, that simple comment by Prof. Vladimirov has motivated, somewhat in strange way, to do small experiment in Moscow streets, during early may 2009. In essence, Prof. Vladimirov helped him to become just an Indonesian scientist, not just trying to mimic someone else's figure. That is what he can say about Prof. Yu Vladimirov, he is one of such great teachers. To quote Plutarch: "*The mind is not a vessel to be fulfilled, but a fire to be rekindled*." [3]

Version 1.0: 29th January 2022, pk. 12:00
VC, FS

REFERENCES

[1] IvlevA.V. *et al*. (2015). Statistical Mechanics where Newton's Third Law is Broken. *PHYSICAL REVIEW* X 5, 011035.

[2] Gene Kruckmeyer. (2013). Optical Experiment Mimics Futuristic System for Space Propulsion. url: https://www.ucf.edu/news/optical-experiment-may-help-lead-to-new-space-propulsion-system/

[3] "The mind is not a vessel to be filled but a fire to be kindled." url: https://www.brainyquote.com/quotes/plutarch_161334

[4] Yumiao Pei et al. (2019). Coherent Propulsion with Negative-mass Fields in a Photonic Setting. *CLEO: QELS_Fundamental Science 2019*, San Jose, California United States, 5–10 May 2019, ISBN: 978-1-943580-57-6. OSA Technical Digest (Optica Publishing Group, 2019), paper FTh4B.2 https://doi.org/10.1364/CLEO_QELS.2019.FTh4B.2. url: https://opg.optica.org/abstract.cfm?uri=CLEO_QELS-2019-FTh4B.2

[5] V. Christianto & F. Smarandache. (2022). Plausible steps to make a workable warp drive machine, someday in the near future: Discussion and remark. Not yet submitted to any journal. (Jan. 2022)

[6] Yakov P. Terletsky. (1964). Cosmic rays and particles of negative mass *Annales de l'I. H. P., section A, tome 1*, no 4, p. 431-436 <http://www.numdam.org/item?id=AIHPA_1964__1_4_431_0

[7] Yakov P. Terletsky. (1968). *Paradoxes in the Theory of Relativity.* Springer Science+Business Media, LLC.

[8] G. Cavalleri & E. Tonni. Negative masses, even if it is isolated, imply self-acceleration, hence catastrophic world.

[9] F. Winterberg (2011). Negative Mass Propulsion. BIS, 64, 3-16.

[10] R.L. Forward. (1988). Negative mass propulsion.. Presented as Paper 88-3168 at the AIAA/ASME/SAE/ASEE 24th, Joint Propulsion Conference, Boston, MA, July 11-13, 1988; received July 15, 1988; revision received Dec. 12, J. Propulsion 6(1).

[11] M. Tajmar & A.K.T. (2015). Assis. Particles with Negative Mass: Production, Properties and Applications for Nuclear Fusion and Self-Acceleration. *Journal of Advanced Physics,* 4, 77-82. DOI: 10.1166/jap.2015.1159.

****

Bulletin of Pure and Applied Science
Physics, Vol.41D No.2,
July-December 2022 P.45-50
Original Research Article

Print version ISSN 0970 6569
Online version ISSN 2320 3218
DOI: 10.5958/2320-3218.2022.00009.4
Available online at www.bpasjournals.com

Computation of Phonon Density of States, Atomic Electrostatic Potential and Electric Field Gradient Tensor Using Single Crystal Data of Six Benzene Sulfonamide Based Compounds

[1]BN AnanthaKumar, [2]J Mahadeva, [3]MB Nandaprakash*, [4]GC Bharath, [5]R Somashekar

Author's Affiliations:
[1,2]Department of Physics, PES College of Arts, Science and Commerce, PET Research Foundation, Mandya–571401, Karnataka, India.
[3]Department of Physics, Karnataka State Open University, Mukthagangotri, Mysuru–570006, Karnataka, India.
[4]Department of Physics, Regional Institute of Education, University of Mysore, Mysuru–570006, Karnataka, India.
[5]DOS in Material Science and RIE, University of Mysore, Manasagangotri, Mysuru–570006, Karnataka, India.

***Corresponding author:**
MB Nandaprakash
Department of Physics, Karnataka State Open University, Mukthagangotri, Mysuru–570006, Karnataka, India.
E-mail: nandaprakash_mb@rediffmail.com

Received on 13.03.2022
Revised on 03.06.2022
Accepted on 05.08.2022
Published on 15.12.2022

ABSTRACT
Molecular dynamic study of benzene sulfonamide based compounds was carried out to compute several properties like phonon density of states, atomic electric potential and electric field gradient tensor components and then compared. This work establishes the correlation between physical properties and the quantity of carbon atoms in a molecule. The GULP program was used to do all the calculations and reported single crystal data.

KEYWORDS
GULP; benzene sulfonamide single crystals; Density of Phonon states; atomic electric potential; electric field gradient tensor

How to cite this article: AnanthaKumar BN, Mahadeva J, Nandaprakash MB, Bharath GC, Somashekar R. (2022). Computation of Phonon Density of States, Atomic Electrostatic Potential and Electric Field Gradient Tensor Using Single Crystal Data of Six Benzene Sulfonamide Based Compounds. *Bulletin of Pure and Applied Sciences- Physics,* 41D (2), 45-50.

INTRODUCTION

Benzyl sulfonamide based compounds were the initial materials for used for curing and preventing bacterial infection in human beings [1]. They exhibit antibacterial [2,3], antifungal [4], anti-inflammatory [5], antitumor[6], anticancer [7], anti-HIV [8] and antitubercular activities [9]. Since there is a continued interest in these Benzene sulfonamide based compounds, we have carried out molecular modeling method to simulate several physical properties like phonon density of states, atomic electric potential and electric field gradient tensor of these materials using General Utility Lattice Program (GULP), freely available software. Six single crystal data of benzene sulfonamide based compounds reported earlier were used in the following investigations. [10-14]

MATERIAL AND METHOD

Six single crystal data of benzene sulfonamide based compounds were used and they are [10-14]:
1)2,5-Dimethoxy-N-phenylbenzenesulfonamide($C_{14}H_{15}NO_4S$)(Monoclinic, $P_{21/c}$)
2)4-Bromo-N-(4-fluorophenyl)benzenesulfonamide ($C_{12}H_9BrFNO_2S$)(Orthorhombic, $P_{na}2_1$)
3) 3,5-dichloro-N-(2,3-dimethylphenyl)benzenesulfonamide ($C_{14}H_{13}Cl_2NO_2S$)(Monoclinic,$P_{21/n}$)
4) 3,5-dichloro-N-(2,6-dimethylphenyl)benzenesulfonamide ($C_{14}H_{13}Cl_2NO_2S$)(Triclinic, P1)
5) 3,5-dichloro-N-(3,5-dimethylphenyl)benzene-sulfonamide($C_{14}H_{13}Cl_2NO_2S$)(Monoclinic,$P_{21/c}$)
6)4-Bromo-N-(4-bromophenyl)benzenesulfonamide ($C_{12}H_9Br_2NO_2S$)(Monoclinic, $P_{21/n}$)

With experimental single crystal data reported earlier, we have simulated Phonon density of states, atomic electric potential and refractive index and dielectric constant of Prop-2-en-1-one based compounds [15]. For validation of the computed elastic constants in these compounds, we have referred to "Second and Higher Order Elastic Constants" by A. G. Every, A. K. McCurdy (auth.), D. F. Nelson (eds.) [16].

The phonon density of states for a solid as the number of frequencies against frequency value becomes a continuous function when integrated across the Brillouin zone.For carrying out these integrations, GULP employs a standard scheme method [17-19] for selecting grid points. We have employed this procedure to compute the phonon density of states for all the six compounds.

Atomic electrostatic site potential and electric field gradient tensor

The Coulombic interaction per unit charge experienced by an ion at a given position in space is measured by atomic electrostatic site potential.For this purpose, we have used Buckingham potential $U(r) = Ae^{-r/\rho} - C/r^6 + q_i q j e^2/r_{ij}$.The optimization of the lattice energy results in the components of the electric field gradient tensor.

RESULTS

There are six compounds, out of which, 3,4 and 5 compounds have the same composition, but different chemical and crystal structure as reported.

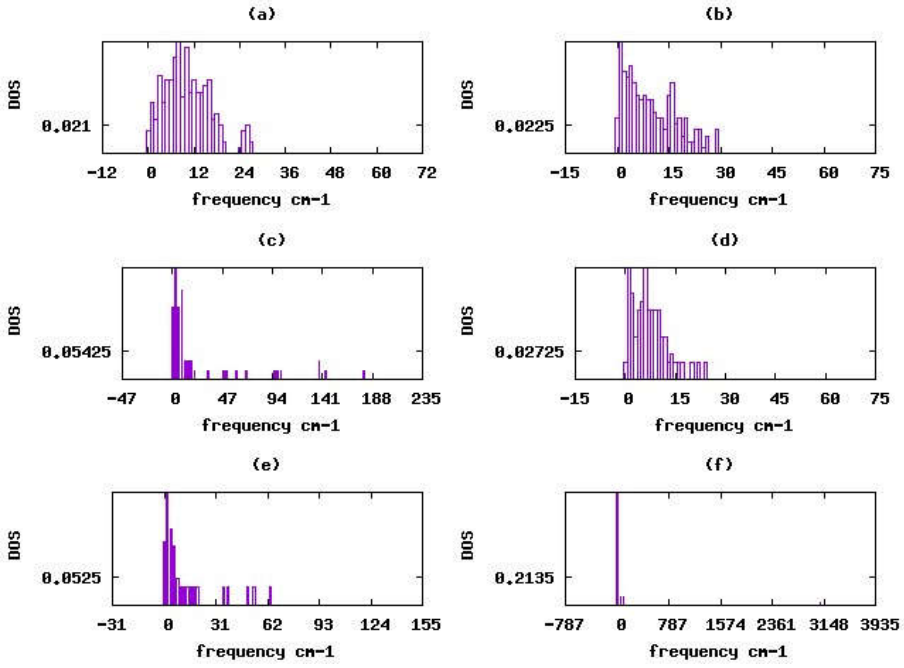

Figure 1: Variation of density of phonon states with frequency (a) compd.1 (b) compd.2 (c) compd.3 (d) compd.4 (e) compd.5 and (f) compd.6

Table 1: Phonon properties per mole of unit cells at T=300K

Sl. No.	**Compd.1**	**Compd.2**	**Compd.3**	**Compd.4**	**Compd.5**	**Compd.6**
Zero point energy(eV)	0.158	0.134	0.189	0.059	0.085	0.512
Entropy(eV/K)	0.083	0.076	0.037	0.045	0.042	0.029
Helmholtz free energy(eV)	-23.5	-28.7	-10.3	-12.3	-13.2	-6.7
Heat capacity at constant volume(eV/K)	0.021	0.017	0.009	0.010	0.010	0.007

Figure 1 shows the variation of density of phonons with frequency in all six compounds. We have made a comparison phonon property (per mole of unit cells) at Temperature 300K in Table 1.

In Figure 2 we have compared the atomic site potential of all the six compounds and Table 2 highlights the properties of atomic potential computed. This potential represents the coulomb interaction per unit charge experienced by an ion at a given location in space. Electronegativity of all compounds are approximately same whereas self-energy varies from -1.33 to -10.14 eV.

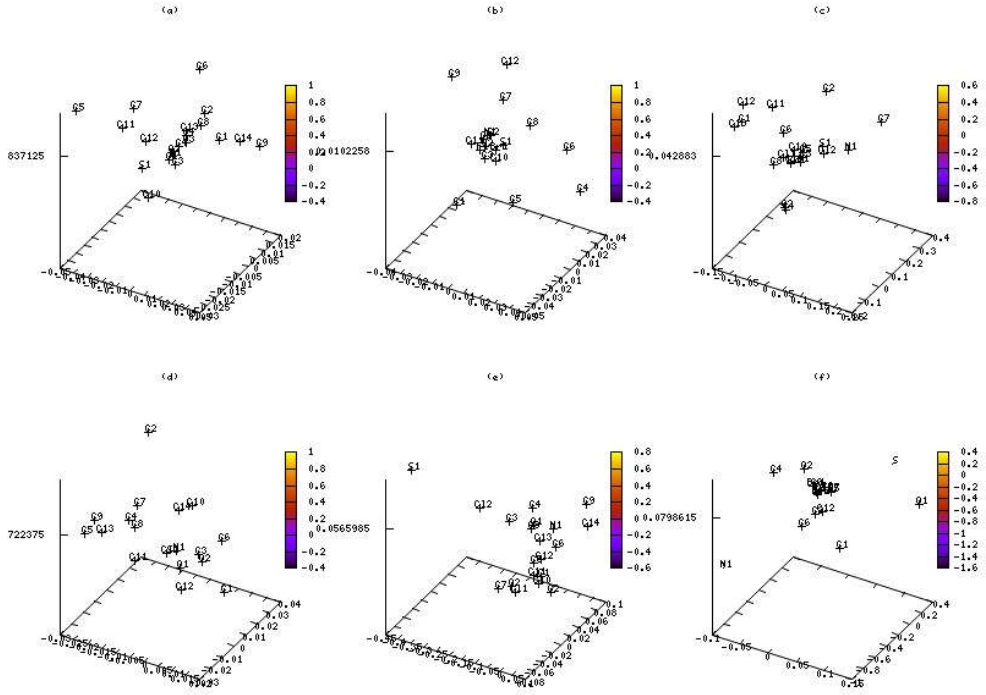

Figure 2: Atomic site electric potential of all compounds (a) compd.1 (b) compd.2 (c) compd.3 (d) compd.4 (e) compd.5 and (f) compd.6

T**able 2: Properties of atomic site potential**

Sl. No.	Compd.1	Compd.2	Compd.3	Compd.4	Compd.5	Compd.6
Electronegativity (eV)	6.31	6.29	6.23	6.13	6.27	6.07
Self energy(eV)	-3.43	-10.14	-2.71	-1.33	-2.39	-2.49

In Figure 3 we have compared the electric field gradients (EFG) at atomic positions of all the six components. Here x-axis refers to 0: xx, 1:xy, 2:yy, 3:xz, 4:yz, 5:zz and y axis refers atoms. For example in Figure 3(a) along y-axis, 0-13 refers to carbon atoms present in the molecule. Figures 2 and 3 do represent the structural optimisation of the lattice energy. Further even though the compounds 3, 4 and 5 have same number of atomic constituents, the higher Vzz component is found in compound 3 and lowest in compound 4. Here we have given a method to quantify the changes in the crystal structure in terms of EFG tensor components.

In Figure 3 EFG is different in each of the six specimens and the presence of heavy elements changes the nature of interatomic interactions. Compds 3,4 and 5 are important since they have same and similar number of atoms but chemical and crystal structures are different. EFG variations in these three compounds are quiet significant which shows that there are different lattice energy minimizations even though one has same molecular weight.

Further, for a better understanding the variations of these tensor components we have plotted higher value diagonalised zz-component of EFG tensor corresponding to the appropriate atom with the volume of the unit cell and we find an interesting result that Nitrogen atom with a reasonably higher volume has higher value.

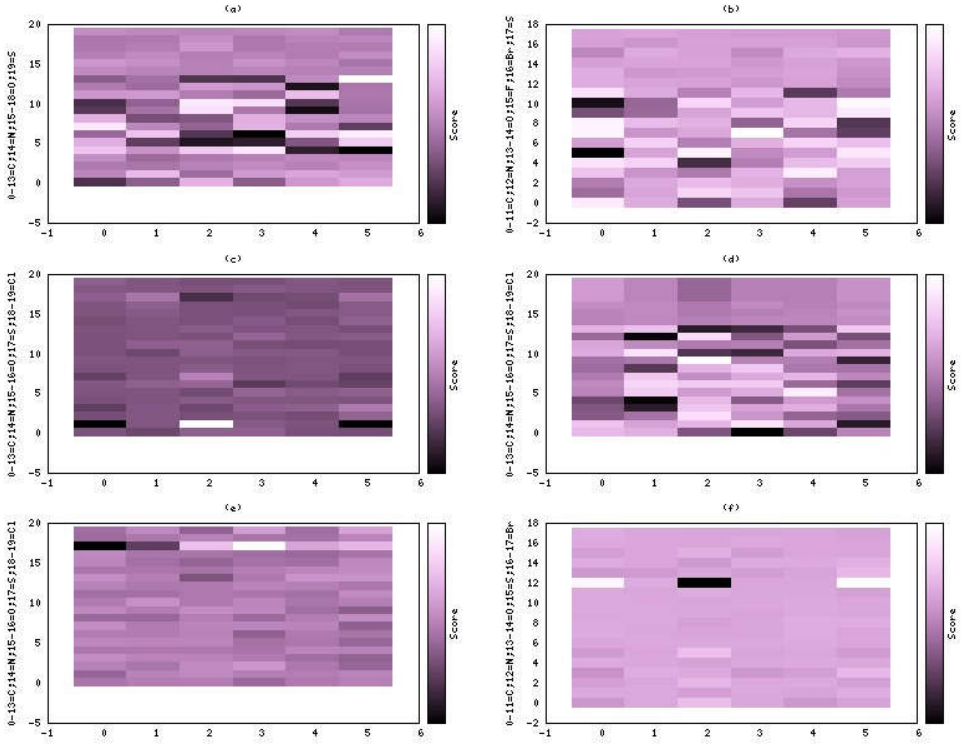

Figure 3: Electric field gradients (EFG) at each atomic positions in sulfonamide compounds based on single crystal data. (a) compd.1 (b)compd.2 (c)compd.3 (d) compd.4 (e) compd.5 and (f) compd.6

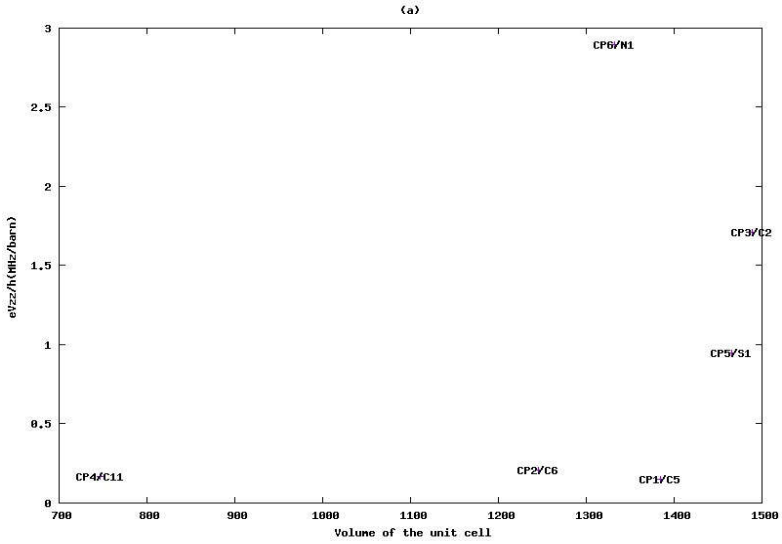

Figure 4: Diagonalised zz component of EFG tensor of all six compounds with unit cell volume.(exmaple CP4/C11 refer to compound 4 and carbon atom number 11 in the structure)

CONCLUSIONS

Using reported single crystal structure data for sulfonamide based compounds, we have computed density of phonon state, atomic site electric potential and electric field gradients at each atomic positions. For lower frequencies, the computed phonon density of states is maximum for compound six and minimum for compound two. This is due to the influence of the functional groups. The variation in electrostatic potential values at atomic positions in these six compounds indicates the sites of molecular interactions with the surroundings. The ESP is a useful tool for studying molecular reactivity in industrial research. In sulfonamide-based compounds, there is a clear representation of EFG for each atomic position, bringing out the atomic interactions in different environments. Figure 4 shows a correlation between one of the predicted physical parameters and molecular weight.

Acknowledgements:
Authors thank UGC, New Delhi for UPE/CPEPA projects to the University of Mysore, Mysuru.

REFERENCES

[1] Shiva Prasad, K., Shiva Kumar, L., Vinay, K. B., Chandra Shekar, S., Jayalakshmi, B. & Revanasiddappa, H. D. (2011). Int. J. Chem. Res,2, 1–6.

[2] Subhakara Reddy, N., Srinivas Rao, A., Adharvana Chari, M., Ravi Kumar, V., Jyothy, V. & Himabindu, V. (2012). J. Chem. Sci. 124,723–730

[3] Himel, C. M., Aboul-Saad, W. G. &Uk, S. (1971). J. Agric. Food Chem. 19, 1175–1180.

[4] Hanafy, A., Uno, J., Mitani, H., Kang, Y. &Mikami, Y. (2007). Nippon Ishinkin Gakkai Zasshi, 48, 47–50.

[5] Küçükgüzel, Ş. G., Coşkun, İ., Aydın, S., Aktay, G., Gürsoy, Şule,Çevik, Ö., Özakpınar, Ö. B., Özsavcı, D., Şener, A., Kaushik-Basu, N., Basu, A. &Talele, T. T. (2013). Molecules, 18, 3595–3614.

[6] Ghorab, M. M., Ragab, A. F., Heiba, I. H. & Agha, M. H. (2011). J.Basic Appl .Chem. 1(2), 8–14.

[7] Al-Said, M. S., Ghorab, M. M., Al-Dosari, M. S. & Hamed, M. M. (2011). Eur. J. Med. Chem. 46, 201–207.

[8] Sahu, K. K., Ravichandran, V., Mourya, V. K. & Agrawal, R. K. (2007). Med. Chem. Res. 15, 418–430.

[9] Vora, P. J. & Mehta, A. G. (2012). IOSR J. Appl. Chem. 1, 34–39.

[10] K. Shakuntala, Vijaya Kumari, N. K. Lokanath, S. Naveen and P. A. Suchetan,IUCrData (2017). 2, x170311

[11] Vinola Z. Rodrigues, P. A. Suchetan, L. Saritha, N. K. Lokanath and S. Naveen,IUCrData (2016). 1, x161256;

[12] K. Shakuntala, S. Naveen, N. K. Lokanath and P. A. Suchetan,Acta Cryst. (2017). E73, 673–677;

[13] K. Shakuntala, N. K. Lokanath, S. Naveen and P. A. Suchetan IUCrData (2017). 2, x170372;

[14] Vinola Z. Rodrigues, a S. Naveen, b N. K. Lokanath c and P. A. Suchetan d *,IUCrData (2016). 1, x160631)]

[15] B N Anantha Kumar, M Ramegowda, M.B Nandaprakash, H Somashekarappa, and R Somashekar, SN Appl. Sci. (2020)**2,** 1097.

[16] A. G. Every, A. K. McCurdy (auth.), D. F. Nelson (eds.) [6].Vol 29(IIIa),(1992),Landolt-Bomatein series.

[17] Monkhorst and Pack [Phys.Rev. B, 13(12), 5188-5192(1976)]

[18] Kapustinskii, A.F. (1956) "Lattice energy of ionic crystals", Q. Rev. Chem. Soc. 10, 283–294.

[19] Julian D. Gale † and Andrew L. Rohl, Molecular Simulation, 2003 Vol. 29 (5), pp. 291–341

****

Bulletin of Pure and Applied Science
Physics, Vol.41D No.2,
July-December 2022 P.51-58
Original Research Article

Print version ISSN 0970 6569
Online version ISSN 2320 3218
DOI: 10.5958/2320-3218.2022.00010.0
Available online at www.bpasjournals.com

Study of Electron Impact Ionization Cross-Sections of Nitrogen Molecule by Inelastic Collision

[1]Ritu Sharawat*, [2]Meenakshi, [3]Rajeev Kumar, [4]Ravinder Sharma

Author's Affiliations:
[1,2]Department of Physics, Baba Mastnath University, Rohtak, Haryana-124001, India
[3]Department of Physics, D. J. College, Baraut, Baghpat, Uttar Pradesh-250611, India
[4]Department of Biomedical Engineering, Deenbandhu Chhotu Ram University of Science & Technology, Murthal, Sonipat, Haryana-131039, India

***Corresponding author:**
Ritu Sharawat
Department of Physics, Baba Mastnath University, Rohtak, Haryana-124001, India
E-mail: ritusharawat21@gmail.com

Received on 20.04.2022
Revised on 26.06.2022
Accepted on 05.08.2022
Published on 15.12.2022

ABSTRACT

In this article, the calculation of ionization cross-section of N_2 molecule by electron impact is reviewed. The work on ionization cross-sections from threshold to high (10 KeV) incident electron energies are calculated and their applications are discussed. To find exact values of total ionization cross-sections for the N_2 molecule, a semi-empirical approach of Jain and Khare (1976) is adopted which is a modification to eliminate the error factors, and then it is compared with the existing experimental and/or theoretical data which gives satisfactory results

KEYWORDS Cross-section, Electron impact, Partial and total ionization.

How to cite this article: Sharawat R., Meenakshi, Kumar R., Sharma R. (2022). Study of Electron Impact Ionization Cross-Sections of Nitrogen Molecule by Inelastic Collision. *Bulletin of Pure and Applied Sciences- Physics,* 41D (2), 51-58.

INTRODUCTION

Nitrogen is the largely important chemical element present in our earth's atmosphere. Nitrogen has the application in auroral and ionospheric phenomena taking place in the uppermost atmosphere of earth, in electrical discharges, etc. The symbol for the nitrogen element is 'N' and its atomic number is '7'. Nitrogen has two stable isotopes N^{14} and N^{15}. Nitrogen in its elemental form is an odorless, colorless, tasteless, and inert diatomic gas at standard conditions. Out of the total volume of the earth's atmosphere Nitrogen constitutes 78.09%, these are some of the properties of nitrogen due to which it becomes an important

element. The data obtained on electron impact ionization of the molecular Nitrogen is of utmost importance in the field of astrophysics, atmospheric physic, and related applications such as space vehicle re-entry and many more.

The ionization process is the process in which targeting an incident particle on a bounding electron of the atom becomes free. This happens due to the transfer of energy from the incident particle to the bound electron when it exceeds electron binding energy. The data relating to the total electron impact ionization cross-section and the partial ionization cross-section of different molecules (fragmented ions) has a wide range of importance. These data can be of great use in the fields of collision theory, plasma physics, radiation chemistry, etc. The studies of electron impact ionization fall into two general classes, the first class to find the TICS "total ionization cross-section" and the second class to find the partial ionization cross-section. The findings of the total ionization cross-sections are a much simpler task and the agreement between the results is moderately satisfactory. The most comprehensive result of this class in starting is given by Rapp and Englander Golden in the year 1965 [1]. They experimentally find total ionization cross-section and partial ionization cross-section for N_2 in the very much limited energy range, it is mainly from threshold to 1000eV. The results of PICS are in disagreement, this is due to the reason it is very difficult to collect the fragments of the ions as they often formed with kinetic energy, thus ensuring the complete collection of fragments ions is a very difficult task due to which disparities occur in the estimation of PICS "Partial ionization cross-section".

Later on, in 1970 Khare and Padalia (1970) use the semi-empirical approach to give the total ionization cross-sections for the He, N_2, H_2, and O_2 molecules [2] from threshold to high incident electron energy. Opal et al. (1972), [3] investigate the total and differential ionization cross-section (50-2000 eV) of different atomic and molecular gaseous by experimentally using the crossed-beam analyzer. In 1992, Jain and Baluja (1992) [4] determine the elastic and inelastic cross-sections for N_2 (10 eV to 5000 eV) and other molecules using a complex optical potential methodology. In 1997, Saksena V. et al. improved the formula and repeated the calculation by using OOS (optical oscillator strength) instead of GOS (generalized oscillator strength) [5]. In 1995, Straub et al. (1995) [6] the absolute partial cross-section for N_2, H_2, and O_2 molecules was determined experimentally by the use of a time-of-flight mass spectrometer from threshold to 1000 eV. Brook et al. (1978) [7] also used the crossed beam method for the Nitrogen which was found to be in good agreement with data which is obtained from earlier crossed beams experiments that make use of the thermal energy atoms beams but the data recorded has a low value in magnitude at lower energies as compared to Rapp and Briglia (1965). Rapp and Briglia (1965) use the technique which is known as the static gas target technique. Then with the advancement in technology, the detection of the ionic fragments formed during partial ionization cross-section becomes easy and also the detection of the dissociation channels becomes possible by using an ion imaging mass spectrometer.

Theoretical approaches used classical computation for the electron impact ionization for almost a century. Thomson (1912) derived an equation based on which diverse models have been developed [8]. The further development embraced the progress of an examination by Bethe. Several non-perturbative methods that are used to calculate the ionization cross-sections of atoms/atomic ions in the last three decades show very good agreement with each other and with experimental results. Margreiter et al. (1990) [9] determine the electron impact ionization cross-section applying the newly developed semi-classical formula from threshold to a high value of 200 eV energy. After that, this semi-classical formula was updated by Deutsch et al. (2000) [10] and calculated 31 molecules from low to high incident electron energy including the N_2 molecule, and comparison showed good agreements. The various theoretical methods to calculate partial and total ionization cross-section include the methods of Partial Wave Approximation, Ab-Initio electrostatic method, R-matrix method, close-coupling method, coupled Integral-differential equation, Binary Encounter Bethe method, Born-Oppenheimer approximation, the

formalism of Kim and Rudd, the method involving Plane-wave born approximation, and semi-empirical methods. The close coupling and R-matrix yield results for a wide range of incident energies. The other theoretical method used by Joshipura (1993) [11] is the Complex Optical Potential approach. He adopted an additivity rule and work at high energy levels. G. Garcia et al. (1997), [12] theoretically evaluate the N_2 molecule scattering from 1 to 10 KeV using the method of Born-Bethe approximation. The total interaction with the target of the incident electron in this method is shown by the local, complex optical potential which is dependent on energy. Kothari and Joshipura (2011) [13] finds the total ionization cross-section of N_2 molecule by positron impact CSP-ic "Complex Scattering Potential-ionization contribution" method between the energy range 15 eV to 2000 eV. Besides this, Singh et al. (2016) [14] also estimate the positive scattering cross-section for Carbon, Nitrogen, Oxygen, and diatomic molecules that is C_2, N_2, and O_2 from 1eV to 5000 eV using SCOP "Spherical Complex Optical Potential" formalism. Shen et al. (2018) [15] also work on the partial and the total ionization cross-sections for gas-phase N_2 molecule by using the experimental electron impact method in a wide energy range from 250eV to 8000eV by ion imaging mass spectrometer. Stefan E. Huber et al. (2019) [16] estimate the partial and total ionization cross-section of the diatomic molecules which are fusion–relevant including N_2 molecule from threshold to10 KeV energy using BEB and DM formalism and also compared available data which gives a better agreement. So, there are many theoretical and experimental investigations for calculating the ionization cross-section of N_2 molecules. There is so abundant work done on this molecule, that it is difficult to include all the previous findings of the N_2 molecule. For this work, many techniques are used for better results. Hence, many improvements are there over earlier work. Because of the experimental difficulties the finding of the quantitative understanding of the electron impact ionization cross-sections of Nitrogen molecules is not sufficient for its applications. It became more interesting to review the total electron impact ionization cross-section of gaseous molecular Nitrogen. So, the ionization cross-section for N_2 is determined by using modified Jaina and Khere (1976) formalism which gives more accurate results than another comparison.

THEORETICAL METHODOLOGY

To investigate the total and partial electron impact ionization, we have applied the theoretical modified Jain and Khare methodology. In 1976 Khare *et al.* [17] provided this formula and improved it from time to time. In his, work Khare combined the Mott and Bethe theories, which describe ionization cross-section at high and low impact parameters respectively. They used the Inokuti formalism to determine an SDICS "single differential ionization cross-section" having the combination of the Mott cross-section and Bethe cross-section (Khare and Meath, 1987) [18] that is collectively shown in equation 1.

$$Q_i(E,\in)=\frac{4\pi.a_0^2R^2}{E}\left[\left(1-\frac{\in}{E-I_i}\right)\frac{R}{W}\frac{df_i(W,0)}{dW}.\ln\left[1+C_i(E-I_i)\right]+\frac{R}{E}S_i\frac{(E-I_i)}{(\in^3+\in_0^3)}\left(\in-\frac{\in^2}{(E-\in)}+\frac{\in^3}{(E-\in)^2}\right)\right] \quad \text{.....(1)}$$

The secondary electron(s) energies (ε) vary from minimum (zero) to maximum (incident electron energy E). In the calculations of the SDCS for the production of an i^{th} type of ion, we have replaced W with $(\varepsilon+I_i)$, the loss of energy suffered by the primary electron is from I_i to maximum i.e. E [19-26], that given in equation 2.

$$Q_i(E,W)=\frac{4\pi.a_0^2R^2}{E}\left[\left(1-\frac{\in}{E-I_i}\right)\frac{R}{W}\frac{df_i(W,0)}{dW}.\ln\left[1+C_i(E-I_i)\right]+\right.$$
$$\left.\frac{R}{E}S_i\frac{(E-I_i)}{(\in^3+\in_0^3)}\left(\in-\frac{\in^2}{(E-\in)}+\frac{\in^3}{(E-\in)^2}\right)\right] \quad \ldots\ldots(2)$$

The total single differential cross-section can be calculated by the summation of all i[th] type cross-sections i.e.

$$Q_i^T(E,W)=\sum_i Q_i(E,W) \quad \ldots..(3)$$

The integral cross-section i.e. the partial ionization cross-section is produced by the integral of equation (2) given the energy loss "W" from the ionization threshold to the maximum E.

$$Q_i(E)=\frac{4\pi a_0^2R}{E}\left[\frac{E}{(E-I_i)\left(1+\frac{I_i}{E}\right)}\left(M_i^2-\frac{R}{W}S_i\right)\ln\left[1+C_i(E-I_i)\right]+\right.$$
$$\left.\int_{I_i}^{E}\frac{R}{E}S_i\frac{(E-I_i)}{(\in_0^3+\in^3)}\left[\in-\frac{\in^2}{(E-\in)}+\frac{\in^3}{(E-\in)^2}\right]\right]dW \quad \ldots.(4)$$

The total ionization cross-section is given as

$$Q_i^T(E)=\sum_i Q_i(E) \quad \ldots..(5)$$

For the evaluation of ionization rate coefficients, we use Maxwell-Boltzmann distribution **[27-32]** as a function of temperature concerning the different types of cross-sections i.e.

$$R_i(E)=\int_{-\infty}^{+\infty}4\pi\left(\frac{1}{2\pi mkT}\right)^{\frac{3}{2}}me^{-E/kT}Q_i(E)EdE \quad \ldots..(6)$$

Where, T, k, and m are the absolute temperature, Boltzmann constant, and mass of the electron, respectively.

RESULTS AND DISCUSSION

We determine the total ionization cross-section of the Nitrogen Molecule by electron impact using modified Jain-Khere formulism from threshold up to high energy. The most important factor in the findings of the ionization cross-sections is the oscillator strength which is taken from Chain et al. (1993) **[33]** ranges from 13 to 40eV for N_2 molecule and higher energy oscillator strength is extrapolated up to desired energy loss using TRK sum rule. The Ionization potential has been taken for N_2 is 15.58 eV [4, 13, 14, 16]. The energy parameter and Collision parameters measured for the N_2 molecule are 50 eV and 0.02249 respectively. MATLAB codes have been developed to solve the above equations [24] and the calculated results are tabulated in Table 1 and graphically represented in Figure 1. We compared our results with National Institute of Standards and Technology (NIST) laboratory data [34] and one more theoretical data [4]. We also compared our results with available experimental data [1, 3, 6] which shows very good agreements and graphically are shown in Figure 2.

Table 1: Total Ionization Cross-Sections ($10^{-16}cm^2$) of N_2 molecule

Energy (eV)	TICS	Energy (eV)	TICS
20	0.089	250	2.699
22	0.103	300	2.493
24	0.136	350	2.312
26	0.152	400	2.153
28	0.424	450	2.015
30	0.665	500	1.895
32	0.880	550	1.788
34	1.091	600	1.694
36	1.276	650	1.610
38	1.440	700	1.534
40	1.585	750	1.466
45	1.884	800	1.404
50	2.112	850	1.348
60	2.360	900	1.296
65	2.526	950	1.249
70	2.660	1000	1.205
75	2.768	1100	1.126
80	2.855	1200	1.058
85	2.927	1300	0.999
90	2.983	1400	0.946
95	3.029	1500	0.899
100	3.064	1600	0.857
105	3.091	1700	0.819
110	3.110	1800	0.785
115	3.124	1900	0.754
120	3.132	2000	0.725
125	3.135	2100	0.698
130	3.134	2200	0.674
135	3.131	2300	0.651
140	3.124	2400	0.630
145	3.114	2500	0.611
150	3.103	2600	0.592
155	3.089	2700	0.575
160	3.074	2800	0.559
170	3.040	3000	0.530
180	3.002	4000	0.421
190	2.961	5000	0.352
200	2.918	6000	0.303
210	2.874	7000	0.267
220	2.830	8000	0.239
230	2.786	9000	0.217
240	2.742	10000	0.199

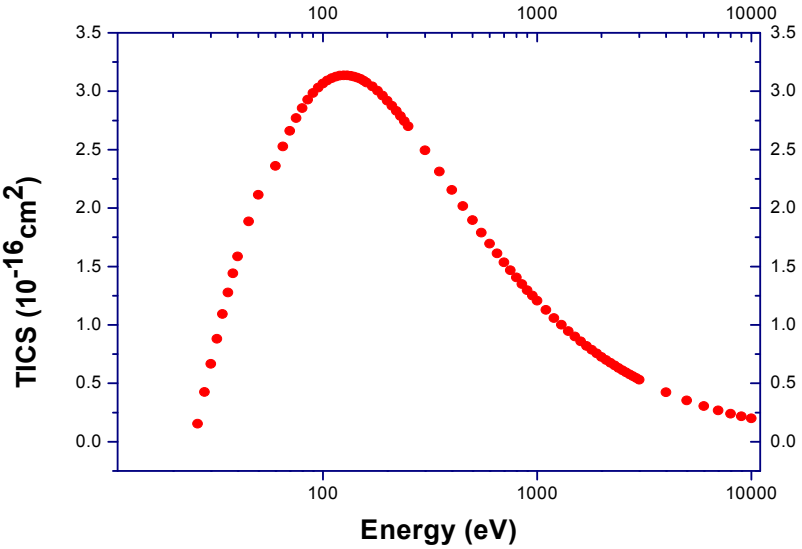

Figure 1: Total Ionization Cross-Section of N_2.

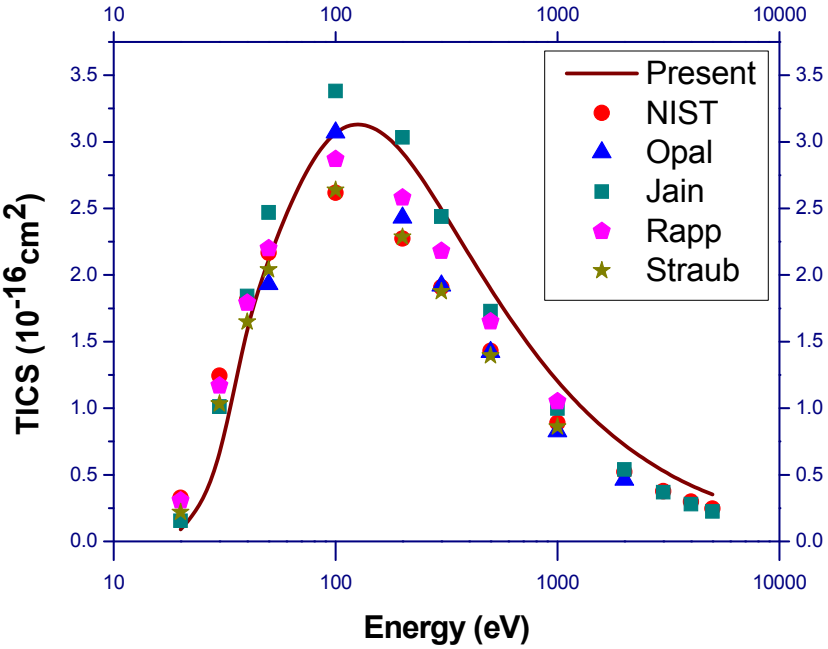

Figure 2: Comparison of N_2TICS: Solid line, Present result; Pentagon, Donald Rapp [1]; Triangle, C.B. Opal [3]; Squire, Ashok Jain[4]; Star, H.C. Straub [6]; Solid dot, NIST [34]

CONCLUSIONS

Satyendra Pal et al. (2020) determine both the single and double differential ionization cross-section for N_2 and O_2 molecules [25]. But the data for the Absolute ionization cross-section of these molecules are not available by using the modified Jain and Khere method. Here we have calculated the total ionization cross-section of the N_2 molecule using this approach. Comparing the results with theoretical and experimental data gives a good agreement. It is observed that at the low ionization energy, all the graphs show the peak whereas with the increase in the ionization energy the curve shows the decrease.

REFERENCES

[1] Rapp D, Briglia DD. (1965). Total cross sections for ionization and attachment in gases by electron impact. II. Negative ion formation. The Journal of Chemical Physics. 43(5),1480-9. https://doi.org/10.1063/1.1696958

[2] Khare SP, Padalia BD. (1970). Total ionization cross sections of He, N_2, H_2, and O_2 due to electron impact. Journal of Physics B: Atomic and Molecular Physics (1968-1987). 3(8), 1073.

[3] Opal CB, Beaty EC, Peterson WK. (1972). Tables of secondary-electron-production cross sections. Atomic Data and Nuclear Data Tables. 4, 209-53.

[4] Jain A, Baluja KL. (1992). Total (elastic plus inelastic) cross sections for electron scattering from diatomic and polyatomic molecules at 10–5000 eV: H_2, Li_2, HF, CH_4, N_2, CO, C_2 H_2, HCN, O_2, HCl, H_2S, PH_3, SiH_4, and CO_2. Physical review A. 45(1), 202.

[5] Saksena V, Kushwaha MS, Khare SP. (1997). Ionization cross-sections of molecules due to electron impact. Physica B: Condensed Matter. 233(2-3), 201-12.

[6] Straub HC. Absolute partial cross sections for electron-impact ionization of argon, hydrogen, nitrogen, oxygen, and carbon dioxide from threshold to 1000 eV (Doctoral dissertation, Rice University).

[7] Brook E, Harrison MF, Smith AC. (1978). Measurements of the electron impact ionisation cross sections of He, C, O and N atoms. Journal of Physics B: Atomic and Molecular Physics (1968-1987). 11(17), 3115.

[8] Mark TD. (1992). Ionization by electron impact. Plasma Physics and Controlled Fusion. 34(13), 2083.

[9] Margreiter D, Deutsch H, Schmidt M, Märk TD. (1990). Electron impact ionization cross sections of molecules: Part II. Theoretical determination of total (counting) ionization cross sections of molecules: a new approach. International journal of mass spectrometry and ion processes. 100, 157-76. Https://doi.org/10.1016/0168-1176(90)85074-c

[10] Deutsch H, Becker K, Matt S, Märk TD. (2000). Theoretical determination of absolute electron-impact ionization cross sections of molecules. International Journal of Mass Spectrometry. 197(1-3), 37-69.https://doi.org/10.1016/S1387-3806(99)00257-2

[11] Joshipura KN, Patel PM. (1994). Electron impact total (elastic+ inelastic) cross-sections of C, N & O atoms and their simple molecules. Zeitschrift für Physik D Atoms, Molecules and Clusters. 29(4), 269-73.

[12] García G, Roteta M, Manero F. (1997). Electron scattering by N2 and CO at intermediate energies: 1–10 keV. Chemical physics letters. 264(6), 589-95.

[13] Kothari HN, Joshipura KN. (2011). Total and ionization cross-sections of N_2 and CO by positron impact: Theoretical investigations. Pramana. 76(3), 477-88. https://doi.org/10.1007/s12043-011-0049-8

[14] Singh S, Dutta S, Naghma R, Antony B. (2016). Theoretical formalism to estimate the positron scattering cross section. The Journal of Physical Chemistry A. 120(28), 5685-92. https://doi.org/10.1021/acs.jpca.6b04150

[15] Shen Z, Wang E, Gong M, Shan X, Chen X. (2018). Electron-impact ionization cross sections for nitrogen molecule from 250 to 8000 eV. Journal of Electron Spectroscopy and Related Phenomena. 225, 42-8.

[16] Huber SE, Mauracher A, Süß D, Sukuba I, Urban J, Borodin D, Probst M. (2019). Total and partial electron impact ionization cross sections of fusion-relevant diatomic molecules. The Journal of Chemical Physics. 150(2), 024306. https://doi.org/10.1063/1.5063767

[17] Jain, D. K., & Khare, S. P. (1976). Ionizing collisions of electrons with CO_2, CO, H_2O, CH_4 and NH_3. Journal of Physics B: Atomic and Molecular Physics, 9(8), 1429.

[18] Khare SP, Meath WJ. (1987). Cross sections for the direct and dissociative ionisation of NH_3, H_2O and H_2S by electron impact. Journal of Physics B: Atomic and Molecular Physics (1968-1987). 20(9), 2101.

[19] Pal S, Prakash S, Kumar S. (1999). Differential cross sections for the ionization of the CO molecule by electron impact. International journal of mass spectrometry. 184(2-3), 201-5. https://doi.org/10.1016/S1387-3806(99)00003-2

[20] Pal S. (1999). Partial double-and single-differential cross-sections for CO_2 by electron collision. Chemical physics letters. 308(5-6), 428-36. https://doi.org/10.1016/S0009-2614(99)00590-4

[21] Pal, S., Singh, R., Kumar, M., & Kumar, N. (2020). Ionization cross-sections for C_2H_2 and C_2H_5OH by electron-impact. Radiation Physics and Chemistry, 173, 108877.

[22] Sharma, R., & Sharma, S. P. (2019). Direct and dissociative ionization cross-section of oxygen molecule from threshold to 10 KeV. International Journal of Engineering and Advanced Technology, 8(6 Special Issue 3), 1365–1368. https://doi.org/10.35940/ijeat.F1241.0986S319

[23] Sharma R, Kumar R, Sharma SP. (2020). Absolute ionization cross sections of hydrogen bromide by electron impact. In AIP Conference Proceedings. 2220(1), 130024. AIP Publishing LLC. https://doi.org/10.1063/5.0001800

[24] Sharma R, Sharma SP. (2019). Absolute Ionization Cross Sections of Hydrogen Chloride Gaseous Molecule by Electron Impact. In International Conference on Sustainable and Innovative Solutions for Current Challenges in Engineering & Technology. pp. 77-87. Springer, Cham. https://doi.org/10.1007/978-3-030-44758-8_8

[25] Kumar R, Sharma SP, Sharma R. (2020). Electron impact ionization cross sections of hydrogen fluoride molecule. European Journal of Mass Spectrometry. 26(3), 195-203. https://doi.org/10.1177/1469066719893230

[26] Pal S, Kumar J, Bhatt P. (2003). Electron impact ionization cross-sections for the N2 and O2 molecules. Journal of electron spectroscopy and related phenomena. 129(1), 35-41.

[27] Pal S. (2008). Differential and partial ionization cross sections for electron impact ionization of plasma processing molecules: CF_4 and PF_5. Physica Scripta. 77(5), 055304. https://doi.org/10.1088/0031-8949/77/05/055304

[28] Pal, S., Kumar, N., & Anshu. (2009). Electron-collision-induced dissociative ionization cross-sections for silane. Advances in Physical Chemistry, 2009. https://doi.org/10.1155/2009/309292

[29] Kumar R, Pal S. (2013). Evaluation of electron ionization cross sections of methyl halides. Rapid Communications in Mass Spectrometry. 27(1), 223-37. https://doi.org/10.1002/ rcm.6433.

[30] Kumar R, Pal S. (2011). Electron ionization cross-sections and rate coefficients for the N_2O molecule. Indian Journal of Physics. 85(12), 1767-74. https://doi.org/10.1007/s12648-011-0197-1

[31] Kumar R. (2015). Electron ionization cross sections of PF_3 molecule. Journal of Applied Mathematics and Physics. 3(12), 1671-8. https://doi.org/10.4236/jamp.2015.312192

[32] Pal S, Kumar M, Singh R, Kumar N. (2019). Evaluation of electron-impact ionization cross sections for molecules. The Journal of Physical Chemistry A. 123(19), 4314-21.

[33] Chan WF, Cooper G, Sodhi RN, Brion CE. (1993). Absolute optical oscillator strengths for discrete and continuum photoabsorption of molecular nitrogen (11–200 eV). Chemical physics. 170(1), 81-97.

[34] https://physics.nist.gov/cgi-bin/Ionization/table.pl?ionization=N_2

****

Bulletin of Pure and Applied Science
Physics, Vol.41D No.2,
July-December 2022 P.59-64
Original Research Article

Print version ISSN 0970 6569
Online version ISSN 2320 3218
DOI: 10.5958/2320-3218.2022.00011.2
Available online at www.bpasjournals.com

On Some Ground State and Finite Temperature Properties of Mixed-Valence Compounds Induced by Next to Next-Nearest-Neighbor (NNNN) Hopping

[1]Piyali Ghosh, [2]Nanda Kumar Ghosh*

Author's Affiliations: [1,2]Department of Physics, University of Kalyani, Kalyani-741235, West Bengal, India

***Corresponding author:** **Nanda Kumar Ghosh**
Department of Physics, University of Kalyani, Kalyani-741235, West Bengal, India
E-mail: nkg@klyuniv.ac.in

Received on 08.05.2022
Revised on 01.09.2022
Accepted on 29.10.2022
Published on 15.12.2022

ABSTRACT In the present study, effects of next to next-nearest-neighbor (NNNN) hopping of *d*-electrons in the crystal of mixed valence compounds has been discussed. For convenient theoretical calculation and computer simulation within exact diagonalization method, a small cluster of eight lattice sites is considered here to investigate the valence transition through the study of the inter-site and on-site *f-d* correlation functions. Unusual magnetic behavior of mixed valence compoundsh as also been examined. Antiferromagnetic (AF) order has been developed in the compounds of rare earth elements with the addition of NNNN hopping interaction within the extended Falicov-Kimball model. The extrapolation of the curves of the reciprocal susceptibility (χ^{-1}) intercept at a negative temperature which confirms AF order in the system.

KEYWORDS Mixed valence compound, Extended Falicov-Kimball model, Exact diagonalization method, Valence transition, Antiferromagnetic nature.

How to cite this article: Ghosh P., Ghosh N.K. (2022). On Some Ground State and Finite Temperature Properties of Mixed-Valence Compounds Induced by Next to Next-Nearest-Neighbor (NNNN) Hopping. *Bulletin of Pure and Applied Sciences- Physics,* 41D (2), 59-64.

INTRODUCTION

Significantly increasing tendency to use the rare-earth elements in modern technologies and life-styles catches the attention of new researchers [1]. The rare-earth elements, especially Lanthanum (La), Samarium (Sm), Thulium (Tm) etc. exhibit the fluctuating configuration of electrons [2]. The general outermost shell configuration of the rare-earth compounds is$(4f)^n(sd)^m$. By using external pressure or temperature, the *f*-level energy *E* is increased, as a consequence the stability of the *4f* shell is lost. Due to the coexistence of two valence states $(4f)^n(sd)^m$ and $(4f)^{n-1}(sd)^{m-1}$, the rare-earth compounds are called mixed-valence compounds. A partially band like nature is developed in rare-earth compounds (i.e., *SmS*, SmB_6, *SmSe, SmTe* etc.). As a consequence, the number of *f*-electrons at each site in the crystal becomes non-integral [2]. This unusual valency is the main reason behind unusual

characteristics of the mixed-valence compounds. Various experiments like edge spectrum of L_{III} X-ray absorption of Samarium hexaboride [3,4] prove the anomalous behaviour of MV compounds. The temperature dependent resistivity [5], Schottky typed specific heat [6], linear type specific heat coefficient [7] etc. also support the existence of unusualness of thermodynamical, electrical and magnetic properties of mixed valence compounds. Density-matrix-renormalization-group (DMRG) study has been applied within extended Falicov-Kimball model to study the stability of the excitonic phase [8]. Exact-diagonalization method on small-cluster, DMRG method and an approximate numerical method are used to study the effect of the *f*-electron hoppingwith the support of extended Falicov-Kimball model [9]. A combined approach using exact diagonalization and quantum Monte Carlo methodshas been applied to study magnetization effects of rare-earth tetraborides [10]. An exact diagonalization method along with an approximate method being well-controlled have been used to examine the effects of magnetic field and induced pressure in valence transition with the support of spin one and half Falicov-Kimball model [11]. Many interactions like correlated hopping [12-13], non-local coulomb interaction [14-15], nearest-neighbor (NN) hopping of *d*-electrons [16] and *f*-electrons [17], next-nearest-neighbor (NNN) hopping of *d*-electrons [18], NNN coulomb interaction [19] etc. have already been studied. We observe the fact that the Falicov-Kimball model is a very convenient, appropriate as well as realistic model to investigate the effects of various types of interactions within two band square lattice cluster. So, we decide to use the extension of the conventional Falicov-Kimball model [20] to examine the effect of next-to-next-nearest-neighbor (NNNN) hopping of *d*-electrons which is unexplored still now.

In the present work, the influence of the NNNN coulomb interaction on some ground state and finite temperature properties of the MV systems has been addressed. The calculations have been made within an 8-site cluster using ED technique. Though finite size effect can't be ignored, but the qualitative nature of the characteristics is almost the same with larger size clusters [21]. Finite-size effect is largely reduced in the thermodynamic limit. Analyzing the results and discussion part, a conclusion has been made at the end.

HAMILTONIAN AND FORMULATION

A cluster of a two-dimensional square lattice with two bands and eight sites is considered here. Taking the total Hamiltonian to be

$$H=H_0+H' \quad (1)$$

Where,

$$H_0=E\sum_{i\sigma} f_{i\sigma}^{+} f_{i\sigma}+U\sum_i f_{i\uparrow}^{+} f_{i\uparrow} f_{i\downarrow}^{+} f_{i\downarrow}+G\sum_{i\sigma\sigma'} f_{i\sigma}^{+} f_{i\sigma} d_{i\sigma}^{+} d_{i\sigma'}+ V\sum_{<i,j>\sigma}(f_{i\sigma}^{+} d_{j\sigma}+d_{j\sigma}^{+} f_{i\sigma})-t_1\sum_{<i,j>\sigma} d_{i\sigma}^{+} d_{j\sigma}-t_2\sum_{<pq>\sigma} d_{p\sigma}^{+} d_{q\sigma} \quad (2)$$

And

$$H'=-t_3\sum_{<m,n>\sigma} d_{m\sigma}^{+} d_{n\sigma} \quad (3)$$

Where, <*i*, j >, <p,q> and < m, n > are NN, NNN and NNNN pairs of sites respectively. $f_{i\sigma}^{+}$ ($f_{i\sigma}$) is the creation (annihilation) operator for the localized f-electrons with spin σ at lattice site *i*. Similarly, $d_{i\sigma}^{+}(d_{i\sigma})$ is the creation (annihilation) operator for the itinerant *d*-electrons, (σ,σ'=spin). *U, G, V* are the interaction strengths for on-site Coulomb repulsion, inter-site Coulomb repulsion, and hybridization between *f*- and *d*-states respectively. t_1, t_2 and t_3 represent the itinerant *d*-electrons' quantum-mechanical hopping between NN, NNN and NNNN sites respectively.

The representative basis state is taken as

$$|n_{1\uparrow}^{f} n_{1\downarrow}^{f} n_{1\uparrow}^{d} n_{1\downarrow}^{d} n_{2\uparrow}^{f} n_{2\downarrow}^{f} n_{2\uparrow}^{d} n_{2\downarrow}^{d} n_{3\uparrow}^{f} n_{3\downarrow}^{f} n_{3\uparrow}^{d} n_{3\downarrow}^{d} \ldots\ldots\ldots n_{8\uparrow}^{f} n_{8\downarrow}^{f} n_{8\uparrow}^{d} n_{8\downarrow}^{d}> \quad (4)$$

The eigen states of H are suitable linear combinations of the basis states.

The on-site *f-d* correlation functionc_d^f= <$n_{i\sigma}^f n_{i\sigma'}^d$> = <$f_{i\sigma}^+ f_{i\sigma} d_{i\sigma'}^+ d_{i\sigma'}$>

The inter-site *f-d* correlation functionc_{fd}=<$f_{i\sigma}^+ d_{j\sigma}$>

For *f*-electrons, spin susceptibility is defined asχ=β< $\left(n_{i\uparrow}^f - n_{i\downarrow}^f\right)$ >^{2}, where $\beta = \frac{1}{k_B T}$; k_B is Boltzmann constant. The reciprocal susceptibility is denoted by $1/\chi$.

RESULTS AND DISCUSSIONS

In the present calculation, the total number of electrons is restricted to 2. The strengths of the interactions are measured with respect to NN hopping interaction. Here,V=0.5, G=1, U=5, t_1=1, t_2=-0.4. All are measured in eV.

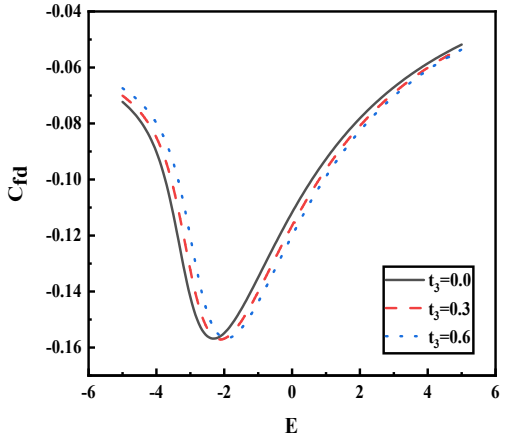

Figure 1: Variation of c_{fd} vs. E for distinct values of NNNN hopping interactions t_3.

The variation of inter-site *f-d* correlation function C_{fd} is plotted against *f*-level energy E in Fig. 1 and the next-to-next-nearest-neighbour hopping interaction (t_3) is used here as variable. Generally, the non-zero value of the *f-d* correlation function confirms the occurrence of insulator to metallic valence transition of the system [22]. Initially, from a value near equals to zero, c_{fd} starts to decline as E is increased. After a crucial value of $E(E_c)$, c_{fd}increases towards zero. The observation is consistent with the concept that c_{fd}should be closer to zero in the metallic or insulating phase [22]. The splitting of these graphs also supports the fact that the NNNN hopping interaction effects on the valence transition from insulator to metal in mixed valence compounds. E_c differs depending on the value of t_3 and it shifts to the higher value of E with the higher value of t_3.Another observation of figure 1, for smaller values of t_3 the system is less insulating within the region $E<E_c$ and more metallic for the region $E>E_c$.

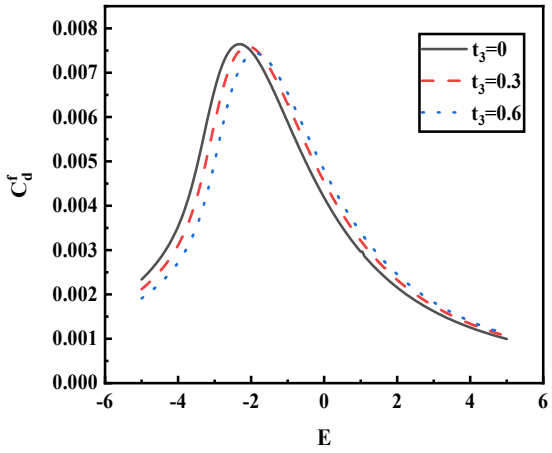

Figure 2: On site *f-d* corelation function c_d^f vs. *E* for distinct values of t_3.

Initially the onsite *f-d* correlation function rises with the increasing value of E. Attaining a high peak value, the value of the f-d correlation function decreases with increasing value of E. The height of the peak of each graph is almost same but it shifts to the higher value of E with the higher value of t_3. The nature of the figure 2 also supports the valence transition from insulating to metallic state of the system. From the observation of figure 2, it also reveals the fact that for smaller values of t_3, the system is more insulating for $E<E_c$ whereas less metallic for $E>E_c$. Figure 3 shows the variation of spin susceptibility χ with temperature (T) for different values of t_3. The peak of spin susceptibility versus temperature graph proves the antiferromagnetic property of the material [23, 24]. It is observed that the peak of all graphs is very sharp. Neel temperature (T_N) at which the spin susceptibility is maximum, is almost equal for each graph [23] but the peak height increases with the increasing value of t_3. These observations are coincided with the magnetic behaviour of mixed valence compounds [2]. Above the Neel temperature, the nature of the graphs exhibits the paramagnetic behaviour following Curie-Wiess law [23]. Furthermore, it is also observed that there is a miraculous coincidence of all graphs towards zero-spin susceptibility in the region $T< T_N$.

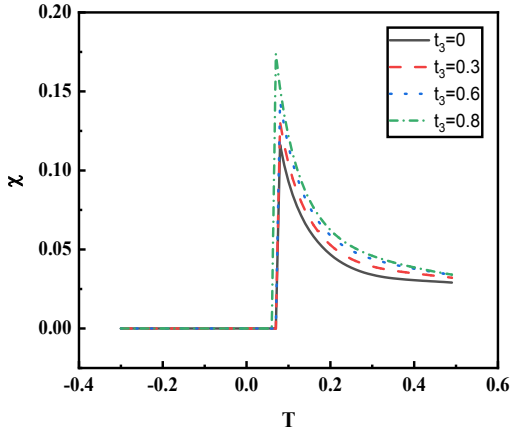

Figure 3: Graph of temperature dependent spin susceptibility for different values of t_3.

From the Curie-Wiess plot ($1/\chi$~T) for different values of t_3, it is noted that the reciprocal susceptibility curves intercept at a negative temperature which also confirms the antiferromagnetic nature of the system. All graphs intersect to each other at near equals to zero temperature. Above the intersection point of temperature, for the lower value of t_3, the value of $1/\chi$ shows is increasing property and below it, $1/\chi$ shows decreasing nature.

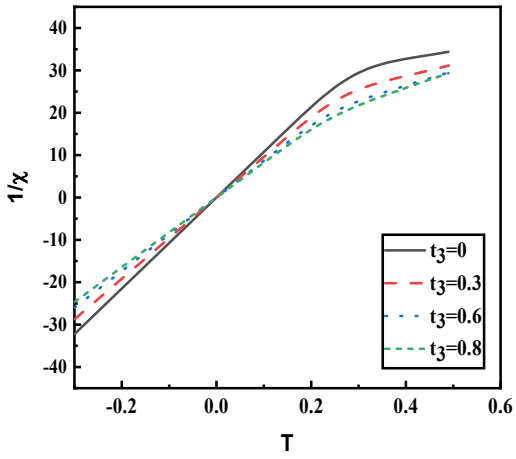

Figure 4: Graph of temperature dependence of reciprocal spin susceptibility ($1/\chi$) for different values of t_3.

CONCLUSIONS

Studying the ground state and temperature dependent magnetic properties of the mixed valence compounds, we can conclude that the NNNN hopping interaction is very significant in the compounds of fluctuating valency such as samarium hexaborides, samarium sulphide etc. Both the inter-site and onsite *f-d* correlation functions exhibit the valence transition from insulator to metal phase. With the increasing value of *f*-level energy *E*, the inter-site *f-d* correlation function becomes negative in value. Whereas with the increasing value of E, the value of on-site *f-d* correlation function is always positive. Owing to their unusual magnetic properties, rare earth elements have many applications. Rare earth magnets are used in hard drives, CD-ROM drives and DVD disc drives etc. In our present study, we also analyse the graphs of spin susceptibility versus temperature and Curie-Wiess plot. Observations of these two types of graphs also confirm the antiferromagnetic nature of the system by the inclusion of NNNN hopping interaction term t_3 to the extended Falicov-Kimball model.

Funding declaration
The work has been financially supported under RUSA 10 component (CH & E) No. IP/RUSA (C-10)/05/2021 of the University of Kalyani.

REFERENCES

[1] Balaram V., (2019), Geoscience Frontiers 10, 1285.
[2] Varma C. M., (1976), Rev. Mod. Phys. 48, 219.
[3] Vainshtein E.E., Blokhin S.M., and Paderno Yu. B., (1965), Sov. Phys. Solid State 6, 2318.
[4] Kasuya T., Takegahara K., Fujita T., Tanaka T., and Bannai E., (1979), J. Phys. (Paris) 40,308.
[5] Bader. S. D, Phillips. N.E, and McWhan. D. B, (1973), Phys. Rev. B 7, 4686.
[6] Cencarikova H., and Farkasovsky P., (2015), Phys. Stat. Sol. (b) 252, 333.

[7] Gmitra M., Cencarikova H., and Farkasovsky P., (2014), Acta Physica Polonica A 126, 298.
[8] Farkasovsky P., (2021), Condensed Matter Physics 23, 43709.
[9] Farkasovsky P., and Cencarikova H., (2014), Eur. Phys. J. B 87, 209.
[10] Farkasovsky P., and Regeciova L., (2020), Journal of Superconductivity and Novel Magnetism 33, 3463.
[11] Farkasovsky P., (2021), Eur. Phys. J.B 94, 61.
[12] Ghosh N.K., Bhowmick S.K., and Mondal N. S., (2011), Pramana- J. of Phys. 76, 139.
[13] Cencarikova H., and Farkasovsky P., (2005), Phys. Stat. Sol(b) 242, 2061.
[14] Farkasovsky P., (2019), Eur. Phys. J.B 92, 141.
[15] Bhowmick S.K., and Ghosh N.K., (2012), Pramana- J. of Phys. 78, 289.
[16] Ghosh N.K., and Mukherjee P., (2016), AIP Conf. Proc. 1728, 020016.
[17] Mukherjee P., and Ghosh N.K., (2017), Bull. Of Pure and Appl. Sc. 36D, 80.
[18] Bhowmick S.K., and Ghosh N.K., (2012) Indian J. Phys. 86, 345.
[19] Mukherjee P., and Ghosh N.K., (2018) Int. J. of Current Trends in Sc. and Technology 8, 20195.
[20] Falicov L.M., and Kimball J.C., (1969), Phys. Rev. Lett. 22, 997.
[21] Roy K., Ghosh S., Nath S., and Ghosh N. K., (2019), Eur. Phys. J. B 92, 270
[22] Entel P., Leder H. J., and Grewe N., (1978), Z. Phys. B 30, 277.
[23] Kittel C., (2007). Introduction to Solid State Physics (7th ed.). New Delhi: Wiley India Pvt. Ltd.
[24] Farkasovsky P., *et al.* (2022) J. Phys.: Condens. Matter (inpress) https://doi.org/10.1088/1361-648X/ac8bbf

****

Bulletin of Pure and Applied Science
Physics, Vol.41D No.2,
July-December 2022 P.65-69
Original Research Article

Print version ISSN 0970 6569
Online version ISSN 2320 3218
DOI: 10.5958/2320-3218.2022.00013.6
Available online at www.bpasjournals.com

Strong Correlation Effects and Localization in Metallic Systems

Amita Sharma*

Author's Affiliations: Department of Physics, R. D. S. College, Muzaffarpur, B.R.A.B.U., Muzaffarpur, Bihar 842001, India.

***Corresponding author:** **Amita Sharma**
Department of Physics, R. D. S. College, Muzaffarpur, B.R.A.B.U., Muzaffarpur, Bihar 842001, India.
E-mail: dramitasharma63@gmail.com

Received on 28.04.2022
Revised on 21.09.2022
Accepted on 29.10.2022
Published on 15.12.2022

ABSTRACT We have studied strong correlation effects and localization in metallic systems. Strong correlation effects and localization occurred in metallic systems due to strong electron-electron interactions and strong electron phonon coupling. Strong electron-phonon interactions have been found in such materials as cuprates, fullerides and manganites. The interplay of electron-electron and electron-phonon interactions in these correlated systems leaded to coexistence of or competition between various phases such as super conductivity, charge-density-wave or spin–density wave phases or formation of novel non Fermi liquid phases, polarons, bipolarons and so on. We have considered Holstein-Hubbard model for our work. The Holstein-Hubbard model provides on over simplified description of both electron-electron and electron-phonon interactions, it retains to be the relevant ingredients of a system in which electrons experience simultaneously an instantaneous short range repulsion and a phonon-mediated retarded attraction. In spite of its formal simplicity, it is not exactly solvable even in one dimension. So quantum simulators of Fermi-Hubbard modes based on either fermionic atoms inoptical lattice or electrons in artificial quantum dot crystals have been used. In our work a classical analog simulator was theoretically proposed for the two site Holstein-Hubbard model based on light transport in engineered waveguide lattices, which is capable of reproducing the temporal dynamics of the quantum model in Fock space as spatial evolution in photonic lattice. We have found that in the strong correlation regime the periodic temporal dynamics exhibited by the Holstein-Hubbard Hamiltonian, related to the excitation Holstein polarons has been explained in terms of generalized Bloch oscillations of a single particle in a semi-infinite inhomogeneous tight binding lattice. Light transport in two dimensional photonic lattices simulated in Fock space the hopping dynamics of two correlated electrons on a one dimensional lattice and exploited to visualize such phenomena as correlated tunneling of bond electron-electron molecules and their coherent motion under the action of d.c. or a.c. fields. The obtained results were found in good agreement with previous results.

KEYWORDS Strong Correlation, Localization, Electron-Electron Interaction, Electron-Phonon Coupling, Fermi Liquid, Polaron, Quantum Simulation, Quantum Dot, Photonic Lattice, Fock Space, Tunneling.

How to cite this article: Sharma A. (2022). Strong Correlation Effects and Localization in Metallic Systems. *Bulletin of Pure and Applied Sciences- Physics,* 41D (2), 65-69.

INTRODUCTION

Realization of quantum analog simulators of many body problems have been based mainly on atoms [1-3], trapped ions [4-6], nuclear magnetic resonance [7] and single photons [8,9]. At the few photon level interaction is generally mimicked using purely linear optical systems by measurement-induced non linearity [10]. Simplified models of many body condensed matter physics have been simulated such as frustrated Heisenberg dynamics in a spin $-\frac{1}{2}$ tetramer. The propagation of classical light in waveguide based optical lattices has provided an experimentally accessible test bed to mimic in a purely classical setting single particle coherent phenomena of solid state physics [11-12], such as Bloch oscillations [13], dynamic localization [14] and Anderson localization [15] to mention a few. The possibility to simulate Bose-Hubbard models of few interacting bosons or fermions in coupled waveguide linear optical structures using classical light beams has been proposed by Longhi [16]. The main idea is that the temporal evolution of a few interacting particles in Fock space can be conveniently mapped into linear spatial propagation [17]. One of the simplest theoretical model that accounts for the interplay between these two types of interactions is the Holstein-Hubbard model [18-20]. As quantum simulators of Fermi-Hubbard models based on either fermionic atoms in optical lattices [21-22] or electrons in artificial quantum dot crystals have taken into account for our work.

METHOD

The two site Holstein-Habbard model has been considered for our work. This describes two correlated electron hopping between two adjacent sites of a diatomic molecule, each of which exhibited an optical mode with frequency Ω. This model has been often used in condensed matter physics as a simplified model to describe some basic features of polaron and bipolaron dynamics. The two site Holstein-Hubbard Hamiltonian have has been separated into two terms. One describes a shifted oscillator that does not couple to the electronic degrees of freedom and has been disgarded. The other describes the effective electron-phonon system where phonon couple directly with electronic degree of freedom. The corresponding Hamiltonian with $\hbar = 1$ is written as

$$\hat{H} = \hat{H}_e + \hat{H}_{ph} + \hat{V}_{e-ph}$$

Where

$$\hat{H}_e = -t\sum_{\sigma\uparrow,\downarrow}\left(\hat{c}^{\dagger}_{1,\sigma}\hat{c}^{\dagger}_{2,\sigma} + \hat{c}^{\dagger}_{2,\sigma}\hat{c}_{1,\sigma}\right) + U\left(\hat{n}_{1.\uparrow}\hat{n}_{1.\downarrow} + \hat{n}_{2.\uparrow}\hat{n}_{2.\downarrow}\right)$$

$$\hat{H}_{ph} = \Omega\hat{b}^{\dagger}\hat{b}$$

$$\hat{V}_{e-ph} = \frac{g}{\sqrt{2}}\left(\hat{n}_1 - \hat{n}_2\right)\left(\hat{b} + \hat{b}^{\dagger}\right)$$

$\hat{c}^{\dagger}_{i,\sigma}\left(\hat{c}_{1,\sigma}\right)$ are the fermionic creation (annihilation) operators for the electron at site 1 with spin σ. $\hat{n}_{1,\sigma} = \hat{c}_{1,\sigma}\hat{c}^{\dagger}_{1,\sigma}$ and $\hat{n}_1 = \hat{n}_{1.\uparrow} + \hat{n}_{1.\downarrow}$ are the electron occupation numbers, g is the one site electron-phonon coupling strength t_d is the hopping amplitude between adjacent sites, U is the onsite coulomb interaction energy and $\hat{b}^{\dagger}\hat{b}$ is creation (annihilation) bosonic operator for the oscillator. For the two site two electron system there are six electronic states. Three of these states are degenerate with zero energy $\hat{H}_e\left|\psi_{Ti}\right\rangle = 0$ where $i = 1,2,3$ and belong to the triplet states. The triplet states are not coupled with the 'b' oscillator and can be disgarded. The three other eigen states of $\hat{H}_e$ denoted by $\left|-\right\rangle, \left|s+\right\rangle$ and $\left|s-\right\rangle$ have been constructed from the singlet states. The electron-phonon interaction term $\hat{V}_{e-ph}$ couples the electronic eigen states

$|-\rangle$ and $|s\pm\rangle$ of $\hat{H}_e$ with the phonon states $|n\rangle_{ph} = \left(1/\sqrt{n!}\right)\hat{b}^{\dagger n}|0\rangle_{ph}$ of $\hat{H}_{ph}$ have been taken into account for our work.

RESULTS AND DISCUSSION

Graph (1) shows results obtained in the moderate correlated regime $U = 0.2mm^{-1}$, corresponding to $\cos\theta \approx 0.851$, $\sin\theta \approx 0.526$. In this case $k_n \neq \rho_n$ and thus the two zigzag chains forming the array are noticeably asymmetric. The strong correlation regime is attained when the on-site interaction strength *U* is much larger than the hopping amplitude '*t*' corresponding to $\cos\theta \approx 1$ and $\sin\theta \approx 0$. In this case $\rho_n \approx 0$ and thus the phonon modes are coupled to the electronic degree of freedoms solely via the two dressed states $|-\rangle$ and $|s+\rangle \approx -|+\rangle$, whose energy levels are nearly degenerate and equal to *U* and $E_+ \approx U\left(\frac{1+4t^2}{U^2}\right)$ respectively. In Fock space, the electron-phonon coupling dynamics is thus reduced to the coupled equations for occupation amplitudes 'f_n' and 'g_n'.

$$i\frac{df_n}{dt} = \left(U + \Omega_n\right)f_n - k_n g_{n-1} - k_{n+1}g_{n+1}$$

$$i\frac{dg_n}{dt} = \left(E_+ + n\Omega\right)g_n - k_n f_{n-1} - k_{n+1}f_{n+1}$$

Where $k_n = \sqrt{2ng}$, correspondingly, the optical analog simulator reduces to a simple linear chain of wave guides with nonuniform spacing as shown in graph (2)(a). The optical simulation of the Holstein-Hubbard model in the strong correlation regime is shown in graph (2) for parameters values $g = 0.1mm^{-1}$, $t = 0.1mm^{-1}$, $\Omega = 0.2mm^{-1}$ and $U = 10mm^{-1}$. The dynamics of occupation amplitudes shows in this case is a tpical periodical behavior with a period given by $\frac{2\pi}{\Omega}$. In our optical simulator the periodic revival is clearly visualized by the self imaging property of the waveguide array in which the initial light periodically returns into the initially excited waveguide as shown in graph (2). Such a periodic behavior has been explained after obtaining that in the strong correlation regime $U \to \infty$, the phonon modes couple solely to two dressed electronic states $|-\rangle$ and $|+\rangle$. The obtained results were compared with previously obtained results of theoretical and experimental research works and found in good agreement.

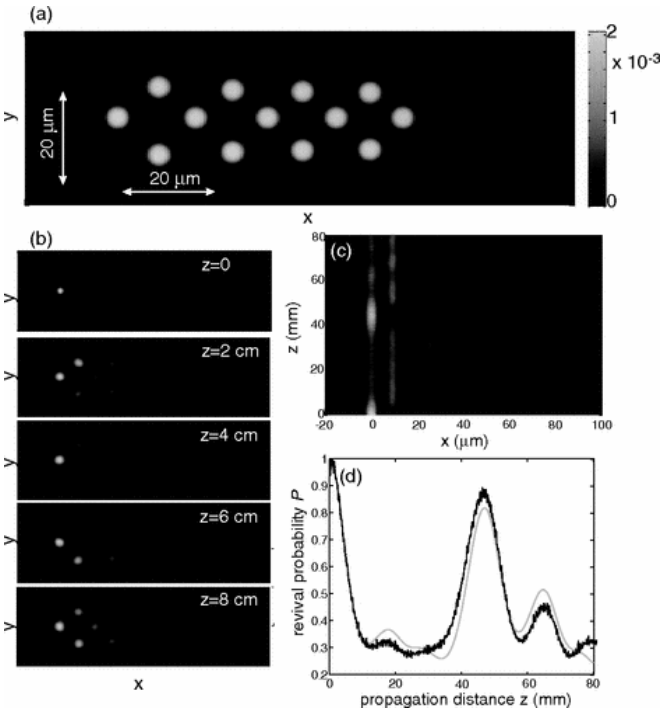

Graph 1: Optical simulation in the intermediate correlation regime (U=0.2mm^{-1})

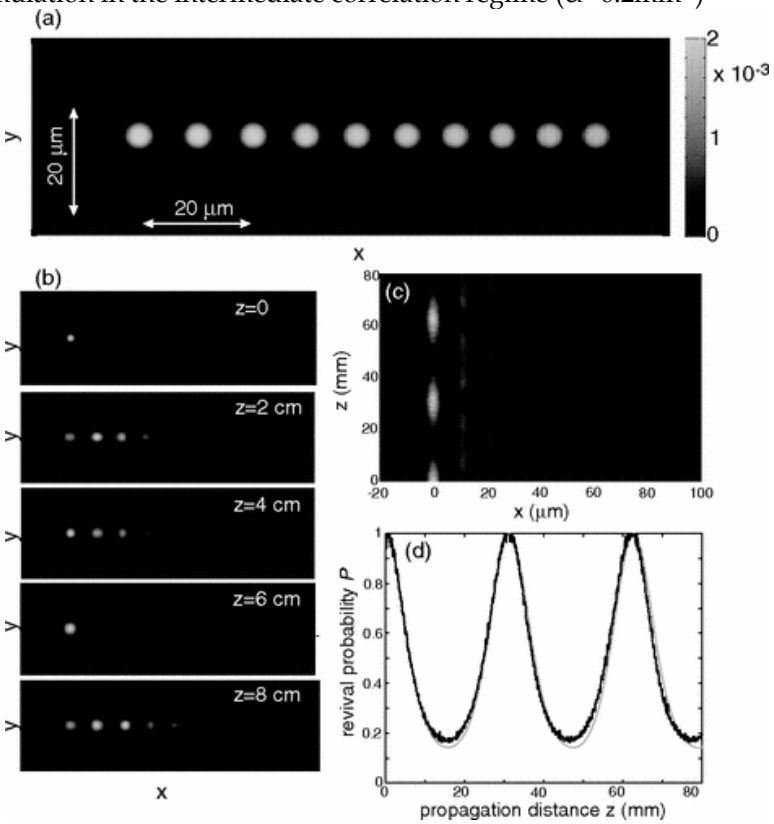

Graph 2: The Strong correlation regime (U = 10mm^{-1}) with the oscillation frequency Ω=0.2mm^{-1}

CONCLUSION

We have studied strong correlation effects and localization in metallic systems due to strong electron-electron interactions and strong electron-phonon coupling. Our photonic analog simulator enabled to map the temporal dynamics of the quantum system in Fock space spatial propagation of classical light waves in the evanescently coupled wave-guides of the array. We have found that in the strong correlation regime the periodic temporal dynamics related to the excitation of Holstein polarons with equal energy spacing were obtained as a periodic self imaging phenomenon of the light beam along the waveguide array in terms of generalized Block oscillations of a single particle in bending lattice. The obtained results were found in good agreement with previously obtained results.

REFERENCES

[1] M. Lewenstein, Adv. Phys. 56, 247, (2007).
[2] S. Trotzky et al., Nat. Phy. 6, 998, (2010).
[3] H. Weimer, M. Miller, I. Lesanovsky, P. Zoller and H. P. Bchler, Nat. Phys. 6, 382, (2010).
[4] M. Johanning, A. F. Varon and C. Wunderlich, J. Phys. B, 42, 154009, (2009).
[5] A. Friedenauer, H. Schmitz, J. T. Glueckert, D. Porras and T. Schaetz, Nat. Phys. 4, 757, (2008).
[6] K. Kim, M. S. Chang, S. Korenblit, R. Islam, E. E. and C. Monroe, Nature 465, 590, (2010).
[7] J. Zhang, T. C. Wei and R. Laflamme, Phys. Rev. Lett. 107, 010501, (2011).
[8] R. Kaltenbaek, J. Lavoie, B. Zeng, S. D. Bartlett and K. J. Resch, Nat. Phys. 6, 850, (2010).
[9] X. S. Ma, B, Dakic, W. Naylor, A. Zeiling and P. Walther, Nat. Phys. 7, 399, (2011).
[10] E. Knill, R. Laflamme and G. J. Milburn, Nature, 409, 46, (2001).
[11] S. Longhi, Laser Photon, Rev. 3, 243, (2009).
[12] A. Szameit and S. Nolte, J. Phy. B, 43, 163001, (2010).
[13] R. Morandotti etal, Phys. Rev. Lett. 83, 4756, (1999).
[14] S. Longhi etal, Phys. Rev. Lett. 96, 243901, (2006).
[15] T. Schwartz etal, Nature 446, 55, (2007).
[16] S. Longhi, J. Phys. B, 44, 051001, (2011).
[17] D. N. Christodoulides, F. Lederer and Y. Silberberg, Nature 424, 817, (2003).
[18] G. D. Mohan, Many Particle Physics (Kluwer Academic/ Plenum, New York, 2000)
[19] J. Zhong and H. B. Schutter, Phys. Rev. Lett. 69, 1600, (1992).
[20] C. R. Proetto and L. M. Falicov, Phys. Rev. B, 39, 7545, (1989).
[21] T. Esslinger, Ann. Rev. Cond. Matter Phys. 1, 129, (2010).
[22] T. Byrnes, N. Y. Kim, K. Kusudo and Y. Yamamoto, Phys. Rev. B, 78, 075320, (2008), A. Singha etal, Science 332, 1176, (2011).

****

Bulletin of Pure and Applied Science
Physics, Vol.41D No.2,
July-December 2022 P.70-74
Original Research Article

Print version ISSN 0970 6569
Online version ISSN 2320 3218
DOI: 10.5958/2320-3218.2022.00012.4
Available online at www.bpasjournals.com

Electronic Structure of Phosphorous Doped Bulk Silicon and Its Use for Spin Qubits for Quantum Computation

[1]Anupam Amar*, [2]Anuradha Amar

Author's Affiliations:
[1]Research Scholar, University Department of Physics, B.N. Mandal University, Madhepura, 852128, North Campus, Singheshwar, Bihar, India.
E-mail: anupam9215@gmail.com
[2]Research Scholar, University Department of Physics, B.N. Mandal University, Madhepura, 852128, North Campus, Singheshwar, Bihar, India.
E-mail: anuradhaamar654@gmail.com

***Corresponding author:**
Anupam Amar
Research Scholar, University Department of Physics, B.N. Mandal University, Madhepura, 852128, North Campus, Singheshwar, Bihar, India.
E-mail: anupam9215@gmail.com

Received on 29.06.2022
Revised on 21.09.2022
Accepted on 29.10.2022
Published on 15.12.2022

ABSTRACT

We have studied the electronic structure of silicon dopants which is necessary for implementation of spin based qubits in silicon. Description of dopant in silicon is therefore useful both as a benchmark and for determining the details of the electronic structure of an isolated dopant which can subsequently be used to calculate more accurate spin dependent scattering cross sections. These calculation have been able to perform large scale calculations using the computational resources. We have performed two electron Hartree-Fock calculations within effective mass theory. These efforts include calculating the effects of applied electric and magnetic fields and the coupling of two donors via exchange interaction. Tight binding calculations have also been performed including a calculation of the quadratic stark coefficient of the hyper interaction. We have found an unprecedented level of structure in the doping potentials and densities and wave functions. Due to oscillatory nature of doping potentials, the exchange coupling between qubits obtained by extrapolating our results to smaller distances was found to be less than estimates based on the Heitler-London approximation. The obtained results were found in good agreement with previously obtained results.

KEYWORDS

Electronic structure, Dopant, isolated scattering, effective mass, quadratic stark coefficient, interaction, doping potential, qubits.

How to cite this article: Amar A, Amar A. (2022). Electronic Structure of Phosphorous Doped Bulk Silicon and Its Use for Spin Qubits for Quantum Computation. *Bulletin of Pure and Applied Sciences-Physics,* 41D (2), 70-74.

INTRODUCTION

Kohn and Luttinger [1] studied that the theory of group-v dopants such as phosphorus in silicon is useful for describing the quantum nature of the electrons in these systems as well as for developing schemes to circumvent one of the most challenging aspects of solid-state quantum computers, namely environmental decoherence [2-5]. In order to provide a bench mark for such theories and also to use as a starting point for building efficient and accurate tight binding methods, an ab initio description of dopants in silicon is desired. The size of the systems required to describe doped silicon at or near the single dopant limit is large, making such a description computationally expansive. In this work, we have presented large scale density functional theory calculations for phosphorous doped silicon suprecells with up to 432 atoms. We have made comparisons to other theoretical works [6-9] to determine what can and cannot be captured by approximate or single-electron theories for the doped silicon systems. Previous efforts to describe the electronic structure of silicon dopants included effective mass approaches beginning with the work of Kohn and Luttinger and continuing with many others [10-15] including Fang etal, who performed two electron Hartree Fock calculations within effective mass theory [16]. Tight binding calculations have also been performed [17-19] including a calculation of the quadratic stark coefficient of the hyperfine interaction which has reproduced experimentally measured values more accurately than effective mass theory [20]. Density functional theory studies [21] evaluated the use of mixed Pseudopotentials which treated the dopant and silicon atoms in the layer using the same core potential and compared them to all atom calculations. These density functional theory calculations and a number of additional calculations [22] showed a large amount of disagreement for calculated properties such as the valley splitting.

METHOD

Face-centered cubic lattices of doped silicon were considered for variable dopant ratios by substituted one phosphorous atom in unit cells with 53, 127, 249 and 431 silicon atoms. We have used Perdew-Burke-Ernze-rhof density functional with an ultrasoft Pseudopotential for phosphorous and a norm-conserving Pseudopotential was calculated using FHI98PP for silicon. A plane wave energy cutoff of 65 Ry was chosen based on convergence of the total energy and pressure in the smallest supercell- K-space sampling was performed using a Monkhorst pack grid of $8\times8\times8$ of 54 atoms, $6\times6\times6$ of 128 atoms $4\times4\times4$ of 250atoms and $2\times2\times2$ of 432 atoms grid points. For the energy and properties of bulk silicon, a two atom silicon cell was used with a grid of $20\times20\times20$ k-points. In this cell one silicon is placed at the origin and another is placed at the point $\left(\frac{a}{4},\frac{a}{4},\frac{a}{4}\right)$ where a is the lattice constant. The basis vector of the fcc cell are $\left(\frac{a}{2},\frac{a}{2},o\right)$, $\left(\frac{a}{2},o,\frac{a}{2}\right)$ and $\left(o,\frac{a}{2},\frac{a}{2}\right)$, the two silicon atoms are repeated at every integer multiple of the basis vectors. The lattice constant of the doped supercells was determined as multiples of the 5.46Å lattice constant for bulk silicon computed with the Pseudopotential used in this stuydy. The phosphorous dopants repeat along the directions of the basis vectors. The Gram Schmidt procedure was used to find the orthogonal direction. $([-1\,2\,0])$. In the calculations with $N<432$ atoms, all of the atoms were allowed to move during the simulation.

RESULTS AND DISCUSSION

Graph (1) shows the plot of the doping potential as a function of distance from (001) layer of dopants. In graph (1) (a) a full two dimensional cut through the potential is given in the plane perpendicular to the (001) plane, and the in graph (1)(b) and (1)(c) the potential is shown in a slice of this plane which connects two dopants. In graph (2) the mixed Pseudopotential doping potentials are much smoother then in graph (1) (b), especially in the region around the dopant. In graph (1) (b) there is a significant amount of structure in the potential near the dopant itself. Minor effects of the silicon atoms in the next layer of the crystal are also evident in graph (1) (c) when the effects of geometric relaxation are included. These results are for doping densities near the single dopant limit, a study of the effect of δ -layer of dopants would require very large cells which would likely have thousands of atoms. Additionally, the dopant potentials are plane averaged while we have plotted straight point potentials. Averaging does not eliminate the structure in our potentials but instead reduces the peak potential relative to the somewhat noisy structure of the atomic lattice. Oscillations are due to interactions with electrons in the shells below the valence shell. If these calculations were performed without using Pseudopotentials, which reduce oscillations from core electrons and replace them with a smooth potential the potential would most likely oscillate to an even greater degree. These oscillations, as well as possible in optimized geometries due to the silicon lattice distortions represent qualitative differences between density functional theory and effective mass theory. Mixed Pseudopotential in order to estimate the potential as a function of the distance from a layer of dopants. The obtained results were compared with previously obtained results of theoretical and experimental research works and found in good agreement.

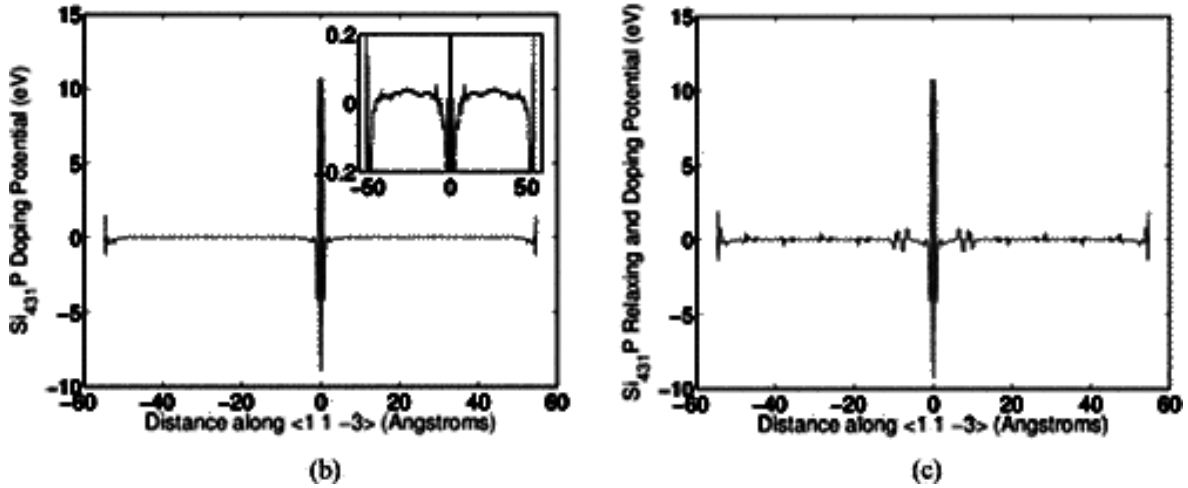

Graph 1: The doping potentials $\left(V_{si_{431}P} - V_{si}\right)$ as function of distance from the doping layer.

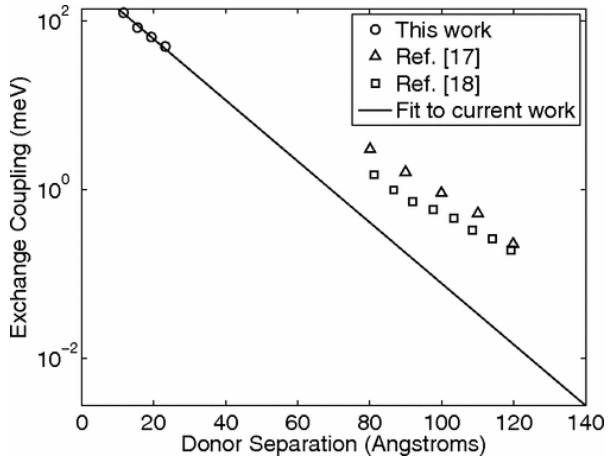

Graph 2: Magnitude of the zero-field exchange coupling calculated by density functional theory in this work (Circles), and in the Heitler-London approximation with effective mass theory wave functions.

CONCLUSION

We have studied electronic structure of phosphorous doped bulk silicon and its use in spin qubits for quantum computation. Several properties relating to their use as spin qubits for quantum computation were found. We have found that the electron density around the dopant leaded to non spherical features in the doping potentials, such a trigonal lobes in the (001) plane at energy scales of +12 eV near the nucleolus and of -700 meV extending away from the dopants. These features are generally neglected in effective mass theory and affected the coupling between the donor electron and the phosphorous nucleus. Our density functional calculations reveled in the densities and potential of the dopants which are not evident in calculations that do not include explicit treatment of the phosphorous donor atom and relaxation of the crystal lattice. The doping potentials provide input for scattering calculations, including calculations in which the current carrying electrons are confirmed to a two dimensional plane to model electrical readout schemes for silicon quantum computation. The obtained results were found in good agreement with previously obtained results.

REFERENCES

[1] W. Kohn and J. M. Luttinger, Phys. Rev. 98, 915, (1955).

[2] J. J. L. Morton, D. R. McCaney, M. A. Eriksson and S. A. Lyon, Nature (London) 479, 345, (2011).

[3] G. Feher and E. A. Gere, Phys. Rev. B, 114, 1245, (1959).

[4] W. M. Witzel and S. Das Sarma, Phys. Rev. B, 74, 035322, (2006).

[5] E. Abe, A. M. Tyrshkin, S. Tojo, J. J. L. Morton, W. M. Witzel, A. Fujimoto etal, Phys. Rev. B, 82, 12101, (2010).

[6] B. Koiller, R. B. Capaz, X. Hu and S. Das Sarma, Phys. Rev. B, 70, 115207, (2004).

[7] D. J. Carter, N. A. Marks, O. Warschkow and D. R. Mc. Kenzie, Nanotechnol, 22, 065701, (2011).

[8] L. M. Kettle, H. S. Goan, S. C. Smit, L. C. L. Hollenberg and C. J. Wellard, J. Phys. Condens Matter, 16, 1011, (2004).

[9] C. J. Wellard, L. C. L. Hollenberg, F. Parisoli, L. Kettle, H. S. Goan, J. A. L. Mctosh and D. N. Jamieson, Phys. Rev. B, 68, 195209. (2003).

[10] D. B. Mac Millen and U. Landman, Phys. Rev. B, 29, 4524, (1984).

[11] L. M. Kettle, H. S. Goan, S. C. Smith, C. J. Wellard, L. C. L. Hollenberg and C. I. Pakes, Phys. Rev. B, 68, 075317, (2003).

[12] C. J. Wellard, L. C. L. Hollengberg, L. M. Kettle and H. S. Goan, J. Phys.: Condens Matter 16, 5697, (2004).

[13] M. J. Calderon, B. Koiller, X. Hu and S. Das Sarma, Phys. Rev. Lett. 96, 096802, (2006).

[14] M. J. Calderon, B. Koiller and S. Das Sarma, Phys. Rev. B, 75, 125311, (2007).

[15] Y. L. Hao, A. A. Djotyan, A. A. Avetisyan and F. M. Peeters, Phys. Rev. B, 80, 035329, (2009).

[16] A. Fang, Y. C. Chang and J. R. Tuuker, Phys. Rev. B, 66, 155331, (2002).

[17] G. P. Lansbergen, R. Rahman, C. J. Wellard, I. Woo, J. Caro, N. Collaert, S. Biesemans, G. Klimeck, L. C. L. Hollenberg and S. Rogge, Nature, Phys, 656, (2008).

[18] R. Rahman, S. H. Park, J. H. Cole, A. D. Greentree, R. P. Muller, G. Klimeck and L. C.L. Hollenberg, Phys. Rev. B, 80, 035302, (2009).

[19] R. Rahman, R. P. Muller, J. E. Levy, M. S. Carroll, G. Klimeck, A. D. Greentree and L. C. L. Hollengerg, Phys. Rev. B, 82, 155315, (2010).

[20] R. Rahman, C. J. Wellard, F. R. Bradbury, M. Prada, J. H. Cole, G. Klimeck and L. C. L. Hollenberg, Phys. Rev. Lett. 99, 036403, (2007).

[21] D. J. Carter, O. Warschkow, N. A. Marks and D. R. Mckenzie, Phys. Rev. B, 87, 045204, (2013).

[22] D. W. Drumm, A. Budi, M. C. Per, S. P. Russo and L. C. L. Hollenberg, Nano. Res. Lett. 8, 111, (2013).

****

Bulletin of Pure and Applied Science
Physics, Vol.41D No.2,
July-December 2022 P.75-80
Original Research Article

Print version ISSN 0970 6569
Online version ISSN 2320 3218
DOI: 10.5958/2320-3218.2022.00014.8
Available online at www.bpasjournals.com

Radiation Leakage Images For Two Different Dielectric-Loaded Surface Plasmon Polariton Waveguides

[1]Jay Shankar Kumar*, [2]Ashok Kumar

Author's Affiliations:
[1]Research Scholar, University Department of Physics, B.N. Mandal University, Madhepura, North Campus, Singheshwar, Bihar 852128, India.
E-mail: jayphysics108@gmail.com
[2]University Department of Physics, B.N. Mandal University, Madhepura, North Campus, Singheshwar, Bihar 852128, India.
E-mail: ashokabnu@yahoo.co.in

***Corresponding author:**
Jay Shankar Kumar
Research Scholar, University Department of Physics, B.N. Mandal University, Madhepura, North Campus, Singheshwar, Bihar 852128, India.
E-mail: jayphysics108@gmail.com

Received on 26.05.2022
Revised on 21.09.2022
Accepted on 29.10.2022
Published on 15.12.2022

ABSTRACT

We have studied about leakage radiation images obtained for two different dielectric-loaded surface plasmon polariton waveguides based on routing structures; linear couplers and bent waveguides. By simultaneously imaging the conjugated aperture and field planes of the microscope, we unambiguously quantify the degeneracy lift occurring for strongly interacting dielectric loaded surface plasmon polariton waveguides and visualize the symmetry of the coupled modes. We have obtained the wave vector distribution and showed its evolution with the bend radius. We have developed a numerical and an analytical analysis for momentum distribution. We have found that for large radii i.e. for vanishing bending loss, we can link the plasmon in Fourier space with the geometrical and modal properties of the bend structure. It was also found that the radial dependence of the wave vector distribution is governed by the phase difference. The obtained results were found in good agreement with previously obtained results.

KEYWORDS

Radian leakage, dielectric, surface plasmon, polariton, wave guide, routing structure, degeneracy, Fourier space.

How to cite this article: Kumar J.S., Kumar A. (2022). Radiation Leakage Images For Two Different Dielectric-Loaded Surface Plasmon Polariton Waveguides. *Bulletin of Pure and Applied Sciences- Physics,* 41D (2), 75-80.

INTRODUCTION

The different geometries capable of routing the flow of surface plasmons, dielectric loaded surface plasmon polariton wave-guides [1-3] have emerged as a potential plasmonic architecture that can be integrated seamlessly with current silicon on insulator photonic circuits [4,5] and can sustain transfer of information at high date rates [6]. A dielectric loaded surface plasmon polariton loaded surface plasmon polariton waveguide is made of a rectangular dielectric rib deposited on a metal film or strip [7]. The surface plasmon required for an optimum confinement of the mode compare well with state of the art silicon on insulator waveguides operating in the telecom bands. Despite higher losses, the advantage of such a plasmonic platform is that the optical index of the dielectric material used to confined the mode can be controlled extremely to realize active dielectric loaded surface plasmon polariton waveguide-based devices [8-12]. Near field optical microscopy and far field leakage radiation microscopy [13] are instrumental for visualizing the confinement and propagation details of surface plasmons supported by this geometry [14,15]. For thin metal films, leakage radiation microscopy is an especially useful characterization tool. Effective indices of the different modes and interactions developing in a given structure can be readily determined [16-18].

METHOD

Optical characterization is performed by using homemade leakage radiation microscopy. An incident tunable laser beam is focused by 100x microscope objective on the extremity of a dielectric loaded surface plasmon polariton waveguide. The sharp discontinuity by the polymer structure acted a local scatterer and produced a spread of wave vectors, some of which resonated with the surface plasmon modes supported by the geometry. By controlling the incident polarization parallel to the longitudinal axis of the waveguide, the dielectric loaded surface plasmon polariton waveguide mode can readily be excited. The leakage radiation microscopy provided a far field imaging technique to directly visualized surface plasmon propagation. This method relies on the collection of radiation losses occurring in the waveguide during propagation. These losses were emitted in the substrate at an angle phase matched with the in plane wave vector of the surface plasmon polariton mode. In our leakage radiation microscopic, the plasmon radiation losses were collected by an oil-immersion objective with numerical aperture. the plane provided direct information about the propagation of the surface plasmon mode developing in dielectric loaded surface plasmon polariton waveguide. To complete the analysis we have used the Fourier transforming property of the ovbjective to access the wave vector distribution of the emitted light. The angular distribution of the radiation in the substrate collected by the object transformed to a lateral distribution at the objective back focal plane. We obtained the quantitative result of the complex surface plasmon wave vector in complex effective index consisting of the radial distance with respect to optical axis. Access to momentum space was performed by inserting a beam splitter in the optical path and a set of Fourier transforming relay. The obtained results were compared with previously obtained results.

RESULTS AND DISCUSSION

Graph (1) (a) and graph (1)(b) show images of the leakage radiation intensity of a single mode dielectric loaded surface plasmon polariton waveguide in conjugated image and Fourier planes respectively. The plasmon mode was launched at the bottom of the structure and propagated up the waveguide with an exponentially decaying intensity. The image of graph (1)(b) is the wave vector content of the intensity distribution shown in graph (1)(a). Both Fourier plane and image plane images, a calibration was performed prior to any data extraction. For calibrating image plane images we have used the known waveguide length as a standard with the system magnification, one pixle represents $\square\ 0.6\mu m$. For Fourier plane

images the numerical aperture of the objective was used. The largest ring in graph (1)(b) represents the numerical aperture 1.49 specified. The central disc is the numerical aperture of the x100 excitation objective at numerical aperture 0.52. On pixle provided a $\Delta N.A \square 0.012$. The dielectric loaded surface plasmon polariton waveguide mode propagating along this straight waveguide is shown in graph (3). The Fourier plane image is shown in graph (1)(b) contains more information than a direct space image since the real part and imaginary part of the effective index can be obtained directly. The mode is represented by a single line at a constant $n_{eff} = \frac{k_y}{k_0} = 1.262 \pm 0.006$. The intensity along $\frac{k_y}{k_0}$ at $k_x = 0$ is related to the surface plasmon through the following formula:

$$I\left(k_x, k_y\right) \alpha \left|\tilde{H}_0\left(k_x\right)\right|^2 / \left[\left(k_y - \beta'\right)^2 + \left(1/2L_{spp}\right)^2\right]$$

$H_0\left(k_x\right)$ is the k_x Fourier transform of the guided magnetic field at the objective focal point. The imaginary party of the effective index was estimated precisely through a Lorentzian fit. Graph (2) shows the benefit of performing momentum spectroscopy. Grpah (2)(a) and (2)(b) are leakage radiation images obtained at the conjugated Fourier plane and image plane for a linear coupler with d=440nm. The coupling length L_C was evaluated using the relation

$$L_c = \frac{\pi}{\left|\beta_s^{'} - \beta_{as}^{'}\right|}$$

Where $\beta_s^{'} = k_0 \times n_{eff}^{s}$ and $\beta_{as}^{'} = k_o \times n_{eff}^{as}$. then

$$L_c = \frac{\lambda_0}{2\left|n_{eff}^{s} - n_{eff}^{as}\right|} = 15.2\mu m$$

We have proposed a simple analytical model that explains the main features of obtained Fourier plane images. We have approximated the mode that propagated in the bend structure by a Guassian profile with a finite propagation length. To simulate the curved dielectric loaded surface plasmon polariton waveguide we have maintained the complex propagation constant in the curved section equal to that of the straight waveguides. The assumption remained valid for $R_c > R_l$ where R_l is the liming radius where bend losses can be neglected. Graph (3) shows the impact of the integration boundaries on the momentum space representation of a single straight wave guide for a fixed propagation length of 40 µm. There is a perfect agreement between numerically calculated Fourier transform and its analytical solution. For integration boundries greater than the propagation length, the two calculations matched with the Lorentz function which are generally used. The obtained results were compared with previously obtained results of theoretical and experimental research works and were found in good agreement.

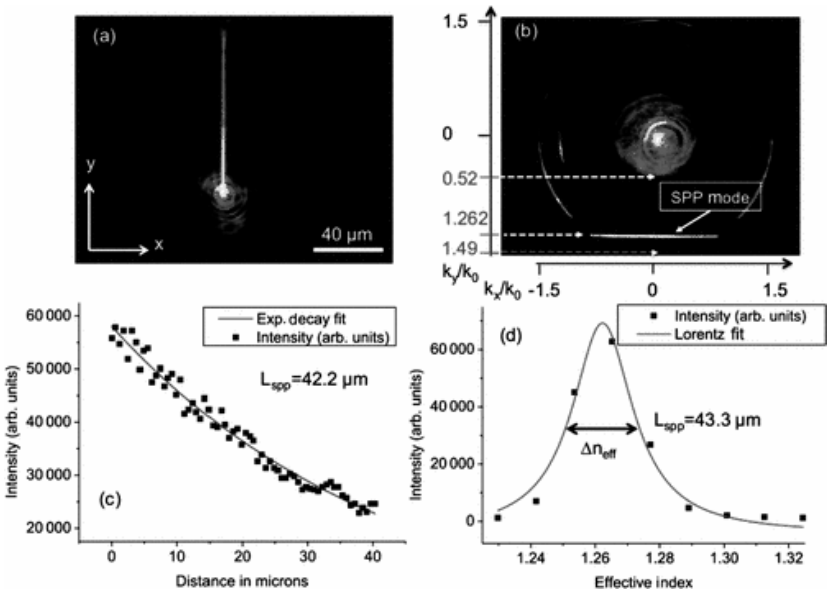

Graph 1: (a) Intensity distribution at the image plane of a surface plasmon mode propagating along a straight dielectric loaded surface plasmon polariton waveguide. The excitation spot is readily visible at the lower portion of the waveguide. (b) Corresponding wave-vector distribution. The central disk represents the numerical aperture of the illumination objective (0.52). The dielectric loaded surface plasmon polariton mode is recognized as a bright line at constant k_y / k_x.

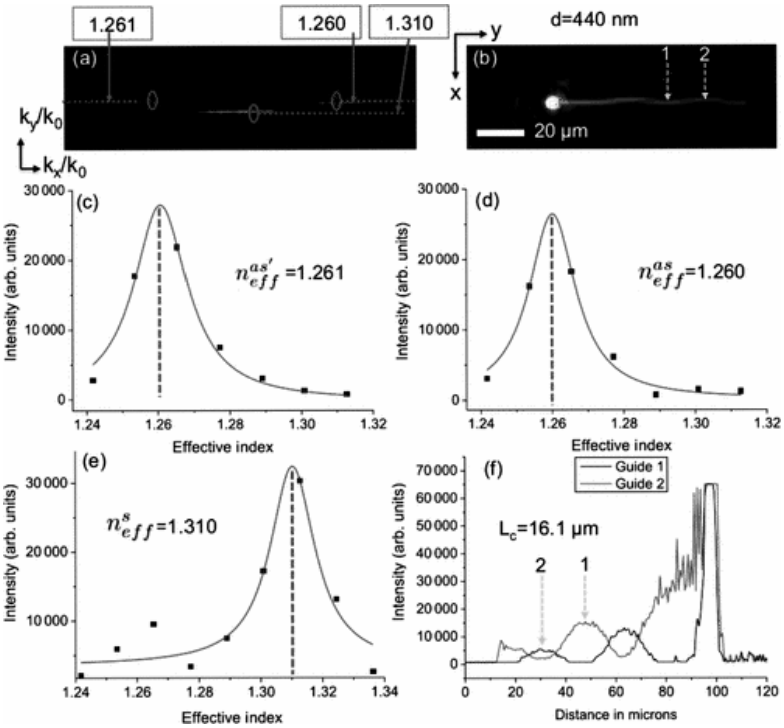

Graph 2: (a)+(b) are leakage radiation Fourier and image planes obtained from a linear Dielectric loaded surface plasmon polariton waveguide coupler width d =440nm. (c) and (d) are Lorentzian fits of the asymmetric mode at the location marked by the circle in (a). (e) is a Lorentzian fit of the symmetric mode. (f) Longitudinal intensity cross sections taken along the two cupled waveguides in (b) showing the energy transfer from one Dielectric loaded surface plasmon polariton waveguide to the other defining the coupling length L_c.

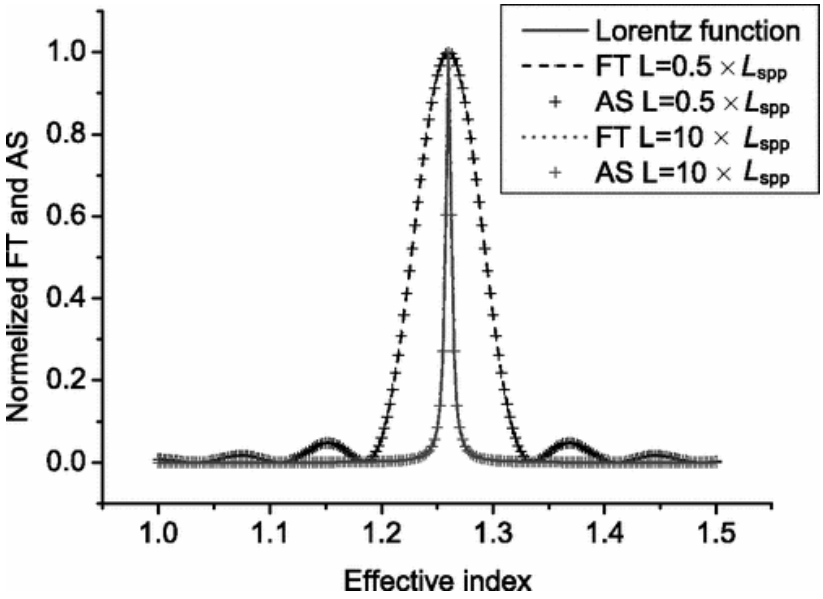

Graph 3: Effect of the Dielectric loaded surface plasmon polariton waveguide length on Fourier-plane calculations. Dashed line: calculated Fourier plane (FT) cross section for $L = 0.5 \times L_{spp}$ and $L = 10 \times L_{spp}$.

CONCLUSION

We have studied the leakage radiation images obtained for two different dielectric loaded surface plasmon polariton waveguides based on routing structures. We have analysed the energy transfer between coupled waveguides as function of gap distance and revealed the momentum distribution of curved geometries. We have found a clear degeneracy lift of the effective indices for strongly interacting waveguides in agreement with coupled mode theory. We have found that for large radii, we can link the plasmon in Fourier space with the geometrical and modal properties of the band structure. The radial dependence of the wave vector distribution was governed by phase difference. This corresponds to the resonance condition of a ring resonator. We have considered each part of the waveguide straight and bend independently from each other. The straight parts were approximately 30μm long, a length smaller than the longitudinal decay of the supported mode. For a long waveguide no oscillation of the wave vector distribution was found. The obtained results were found in good agreement with previously obtained results.

REFERENCES

[1] A. Honenau, J. R. Krenn, A. L. Stepanov. et al, Opt. Lett. 30, 893, (2005).
[2] T. Holmgaad, S. I. Bozhevolnyi, L. Markey and A. Dereux. Appl. Phys. Lett. 92, 011124, (2008).
[3] J. Grandidieretal, Phys. Rev. B. 78, 245419, (2008).
[4] R. M. Briggs, et al., Nano Lett. 10, 4851, (2010).
[5] D. Kalavrouziotis et al., IEEE, Photonics Technol, Lett. 24, 1036, (2012).
[6] S. Papaionannou et al., IEEEJ, Light Wave Technol. 29, 3185, (2011).
[7] J. Grandidier, G. Colas des Francs, L. Markey, A. Bouhelier, S. Massenot, J. C. Weeber and A. Dereux, Appl. Phys. Lett. 96, 063105, (2010).
[8] J. Gosciniak, S. I. Bozhenvolnyi et al., Opt. Express 18, 1207, (2010).
[9] S. Randhawa et al., Opt. Express, 20, 2354, (2012).
[10] D. Perron, M. Wu, C. Horvath, D. Bachman and V. Van, Opt. Lett. 36, 2731, (2011).
[11] A. V. Krasavin, S. Randhawa, J. S. Bouillard, J. Renger, R. Quidant and A. V. Zayats, Opt. Express. 19, 25222, (2011).
[12] K. Hassan, J. C. Weeber, L. Markey and A. Dereux, J. Appl. Phys. 110, 023106, (2011).

[13] B. Hecht, H. Bielefeldt, L. Novotny, Y. Inouye and D. W. Pohl, Phys. Rev. Lett. 77, 1889, (1996).

[14] T. Holmgaard et al. Phys. Rev. B, 78, 165431, (2008).

[15] B. Steinberger, A. Hohenau et al., Appl. Phys. Lett. 91, 081111, (2007).

[16] A. Krishnan, C. J. Regan, L. G. De peralta and A. A. Bernussi, Appl. Phys. Lett. 97, 231110, (2010).

[17] J. Berthelot, A. Bouhelier, G. Colasdes Francs, J. C. Weeber and A. Dereux, Opt. Express. 19, 5303, (2011).

[18] C. J. Regan, O. Thiabgoh, L. G. De Peralta and A. Bernussi, Opt. Express, 20, 8658, (2010).

****

Bulletin of Pure and Applied Science
Physics, Vol.41D No.2,
July-December 2022 P.81-85
Original Research Article

Print version ISSN 0970 6569
Online version ISSN 2320 3218
DOI: 10.5958/2320-3218.2022.00015.X
Available online at www.bpasjournals.com

Band Structure and Spatial Localization of Electrons in Twisted Bilayer Graphene Nanoribbons

[1]Aradhna Mishra*, [2]Jay Prakash Yadav, [3]Ashok Kumar

Author's Affiliations:
[1]Research Scholar, University Department of Physics, B.N. Mandal University, Madhepura, North Campus, Singheshwar, Bihar 852128, India.
E-mail: aradhnamishrabgp@gmail.com
[2]Saharsha College of Engineering, Saharsa, Bihar 852201, India.
E-mail: jayprakashyadav2003@gmail.com
[3]University Department of Physics, B.N. Mandal University, Madhepura, North Campus, Singheshwar, Bihar 852128, India.
E-mail: ashokabnu@yahoo.co.in

***Corresponding author:**
Aradhna Mishra
Research Scholar, University Department of Physics, B.N. Mandal University, Madhepura, North Campus, Singheshwar, Bihar 852128, India.
E-mail: aradhnamishrabgp@gmail.com

Received on 28.07.2022
Revised on 30.09.2022
Accepted on 30.10.2022
Published on 15.12.2022

ABSTRACT

We have studied the band structure, density of states and spatial localization of electron in twisted bilayer nanoribbons by means of tight binding calculation. In Chiral geometries, edge states are also related to the presence of zig-zag edge atoms, although they presented remarkable size effects. Physical properties of chiral graphene nanoribbons and general edges can have a stong dependence on chirality. We have analysed the properties of edge states in twisted bilayaer ribbons, explaining their energy dispersion and spatial localization. The different splittings were found in edge bands due to the inhomogeneous interplay coupling. For stacked zig-zag atoms the coupling was larger than corresponding edge states splitted apart, but edge states stemming from regions with stacking, where the interlayer coupling was smaller and gave rise to zero energy bands. We have also been found that in the edge regions where top and bottom zig-zag terminations were stacked, inter-ribbon tunneling between the dispersions less zero energy states created bonding and antibonding combination with energies away from the energy of the Dirac point. The obtained results were found in good agreement with previously obtained results.

KEYWORDS

Band Structure, Saptial localization, twisted bilayer, nanoribbon, chiral graphene, energy dispersion, splitting edge band, Dirac Point.

How to cite this article: Mishra A., Yadav J.P., Kumar A. (2022). Band Structure and Spatial Localization of Electrons in Twisted Bilayer Graphene Nanoribbons. *Bulletin of Pure and Applied Sciences- Physics,* 41D (2), 81-85.

INTRODUCTION

Trambly et al. (2010) [1] and Morell et al. (20202) [2] presented that for low rotation angles states near the Fermi level are mostly localized, with a strong localization, giving rise to the bright areas of the Moire pattern. The flattering of the bands with diminishing angle has been experimentally observed in angle-dependent Van-Hove singularities revealed in density of states measured by scanning tunneling spectroscopy [3-5] and by an increase of the intensity of Raman modes measured in twisted bilayer graphene samples [6-7]. There is not a controllable way to produce twisted bilayer graphene with a given angle, although some growth methods are more prone to yield twisted bilayers [8]. It was shown that graphene nanoribbons can be obtained by unzipping carbon nanotubes [9-10]. In this way twisted bilayer nanoribbons have been obtained by unzipping chiral multiwalled nanotubes [11]. Chiral graphene nanoribbons have edges with a mixture of armchair and zig-zag components. It has been theoretically established that all edges, with the exception of the pure armchair, presented zero energy localization state with a predominant weight at the edge atoms [12-13]. In pure zig-zag nanoribbons zero energy states were strongly localized at these atoms [14-15]. The dependence of the electronic properties of twisted bilayer graphene on the relative rotation angle between layers has attracted many theoretical [16-24] and experimental works [25-27]. If the rotation angle between the two graphene layers is large the system behaves as if it were composed of two uncoupled layers [28] with a linear dispersion relation and the same Fermi velocity as monolayer graphene. Singh et al. [29] developed a model for the miniband gap and related non parabolic dispersions at the limiting of bismuth-antimony. They have studied band edges and electronic phases as function of grow the orientation. They have found that layer width has large variation of phases and orientationless. Mishra and Kumar (2021) [30] studied electronic properties of graphene. The graphene nanoribbon sensitivity was dependent on matching condition and it was also found that conductivity was reduced.

METHOD

Unit cell of a commensurate twisted bilayer graphene was obtained by rotating a Bernal-Stacked bilayer. The rotation axis passes through a site which has an atom in a layer situated at the center of a hexagon of the other layer. In order to choose commensurate unit cell, a point of the crystal with co-ordinates $r = ma_1 + na_2$, where *m* and *n* are integers, was rotated to an equivalent site $t_1 = na_1 + ma_2$. The graphene lattice vectors are given by $a_1 = \frac{a}{2}\left(\sqrt{3} - 1\right)$ and $a_2 = \frac{a}{2}\left(\sqrt{3}, 1\right)$ and $a = 2.46\text{Å}$ is the graphene lattice constant. The unit cell vectors of the bilayer twisted cell can be chosen as $t_1 = na_1 + ma_2$ and $t_2 = -ma_1 + \left(n + m\right)a_2$. Bilayer unit cells built in this way are usually labeled by the indices $\left(n, m\right)$. The corresponding relative rotation angle between layers is given by $\cos\theta = \left(n^2 + 4mn + m^2\right) / 2\left(n^2 + mn + m^2\right)$. The repetition of twisted bilayer graphene cell with $n = \left(m + 1\right)$ along either t_1 or t_2, yielded a chirial ribbon with edges having a predominantly armchair component. We have considered ribbons with minimal edges i.e. those with a minimum number of edge nodes with co-ordination number 2. The width of the ribbon was given by an integer multiple N of its width vector t_1. We have labeled the ribbons as $N\left(2m + n, n - m\right)\left[\left(n, m\right)\right]$, where $\left(2m + n, n - m\right)$ are the edge, *N* the width and $\left(n, m\right)$ identities the Moire geometry. For sufficiently small relative rotation angle, below 10^o, distinct regions were found in twisted bilayer graphenes. There are areas with stacking, others with stacking and there are also regions which were seemed to be obtained by a relative translation, called slip. The obtained results were compared with previously obtained results.

RESULTS AND DISCUSSION

Graph (1) shows the bilayer geometry and the two components monolayer ribbons separately, which also shows their corresponding band structures. The (4,1) edge was decomposed as (3,0) + (1,1) in the right panels of graph (1), it is seen that the edge has only one armchair (1,1) step. This step is located at different parts of the suspended edges, so that they do not lie on top of each other. The orientation of the (1,1) steps is different in the two nanoribbons, in order to super impose them with a perfect stacking, a mirror reflection on a plane perpendicular to that of the ribbon is needed, in addition to a translation. Being related by a mirror reflection, the band structure of the two monolayer ribbons are equal. Having a (3,0) zigzag component, the (4,1) edge has the zero energy band. The monolayer ribbon should have two edge bands and therefore the bilayer ribbon has four. These edge bands are split apart and is seen in the left panels as shown in graph (1). The behavior is different from that of zigzag ribbons, due to the boundary condition for chiral edges mixes both sublattices. Such mixing leaded to the coupling of edge states at opposite sides of each monolayer ribbon, so that size effects produced the opening of a gap. The gap between the two edge bands in the monolayer ribbon is wider than for the bilayer ribbon. Coupling between the two ribbons splits the bands but the ribbon is so narrow. The 2(4,1)[(2,1)] twisted bilayer nanoribbons shown in graph (2). In the monolayer ribbon, the two edge bands are coupled, they touch at the edge of the Brillounin zone as $m = 1$, M is at the Brillounin zone boundary × and their splitting at T is also smaller. With a (13,1)[(5,4)] twisted bilayer nanoribbons is splited from a (5,4) twisted bilayer graphene which has relative rotation angle $\theta = 7.34^{o}$ and 244 atoms in the unit cell. The corresponding ribbon have a (13,1) edge, which decomposed as a (12,0)+(1,1). This bilayer ribbon has 16 edge states. For smaller relative rotation angles as in the case in the unit cell for the ribbon m=4 so the M point is folded at T is shown in graph (3). The obtained results were compared with previously obtained results of theoretical and experimental research works and were found in good agreement.

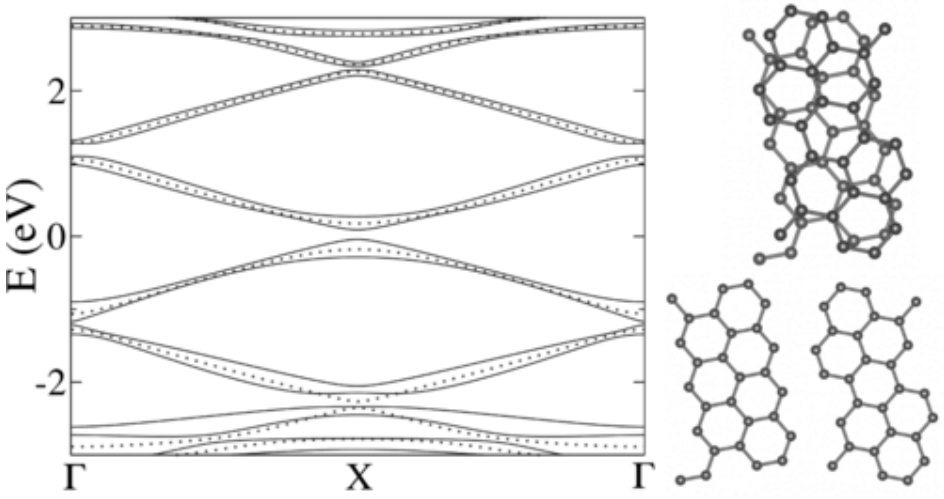

Graph 1: Band structures of the 1(4,1)[(2,1)] twisted bilayer nanoribbon (solid lines) and of the corresponding monolayer ribbon (dotted lines). The geometry of the unit cell and its constituent monolayers are shown on the right.

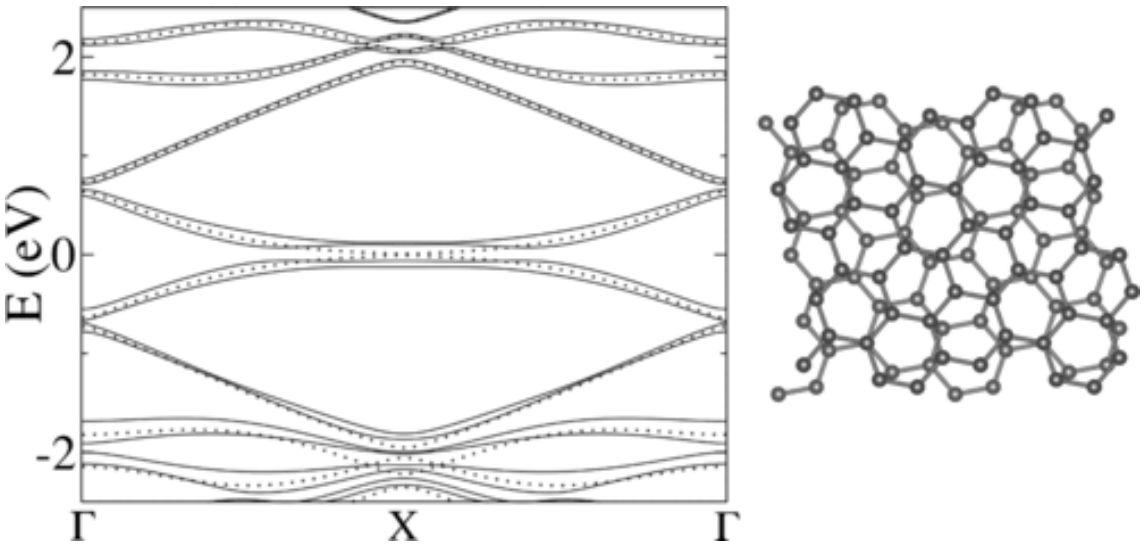

Graph 2: Left Panel: Band structures of the 2(4,1)[(2,1)] twisted bilayer nanoribbon (solid lines) and of the corresponding monolayer ribbon (dotted lines). Right panel: Unit cell of the 2(4,1)[(2,1)] twisted bilayer nanoribbon.

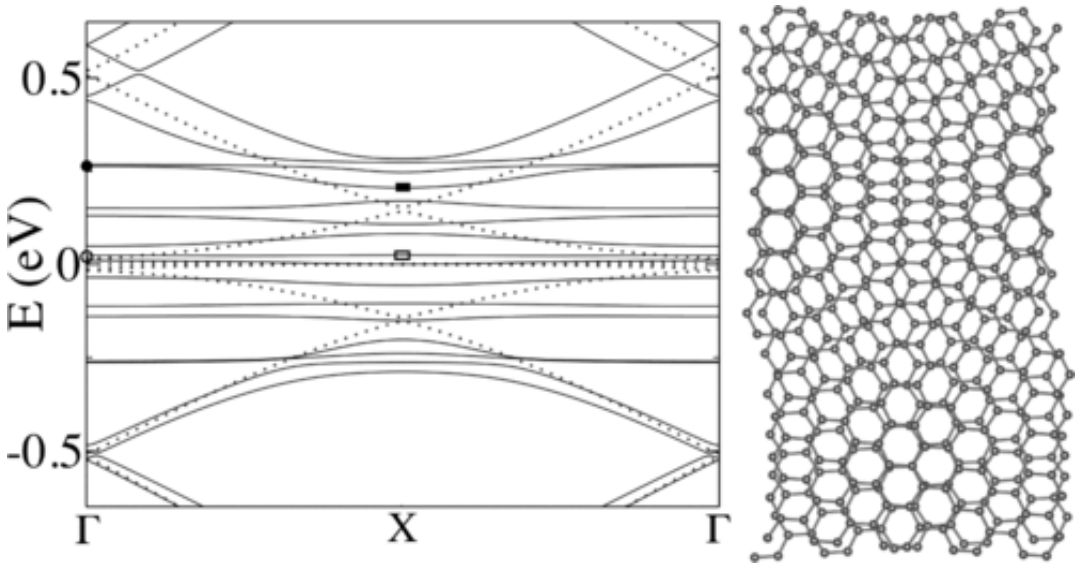

Graph 3: Left panel: Band structure of the 1(13,1) [(5,4)] twisted bilayer nanoribbon (solid lines) and of the corresponding monolayer ribbon (dotted lines). Small circles and boxes indicate the *k* point of the bands selected to show the local density of states.

CONCLUSION

We have studied band structure and spatial localization of electrons in twisted bilayer graphene nanoribbons. We have found that due to the spatially inhomogeneous interlayer coupling, edge states streaming from regions with stacking are closer to the energy of the Dirac point, where as those arising from stacked edge states are splitted in energy due to the stronger interlayer coupling. We have found that the bands with energies less than 0.2 eV are mainly localized in the regions of the edges while edge bands farther from Fermilevel energy corresponding to the edge sites following the moire pattern of the bulk. As opposed to

bulk bilayer graphene for which states near the Dirac point are localized in stacked regions. The obtained results were found in good agreement with previously obtained results.

REFERENCES

[1] Trambly. G. De Laissardiere, Mayon. D and Magand. L., (2010), Nano. Lett. 10, 804.

[2] Morell. E. Suanrez., Borrea. J. D., Vargas. P, Pacheco. M, ABarticevic. Z, (2010), Phys. Rev. B, 82, 121407.

[3] Trambly. G. De Laissar Diere et al., (2012), Phys. Rev. B, 86, 125413.

[4] Li. G, Luican. A, Lopes. J. M. B. dossantos, Castro. Neto. A.H, Reina. A, Kong. J. and Ander E.Y., (2010), Nat. Phys. 6, 109.

[5] Yan. W., Liu. M., Dou. R. F., Meng. L, Feng. L, Chu. Z. D., Zhang. Y, Liu. Z., Nie. J. C. and He. L., (2012), Phys. Rev. Lett. 109, 126801.

[6] Sato. K, Saito. R, Cong. C, Yu. T., and Dresselhaus. M. S., (2012), Phys. Rev. B, 86, 125414.

[7] Kim. K, Coh. S., Tan. L-Z, Regan. W, Yuk. J. M., Laie. S. G., Chatterjee. E, Crommee. M. F., Cohen. M. L. and Zettl. A, (2012), Phys. Rev. Lett. 108, 246103.

[8] Varchon. F, Mallet. P, Magaud. L. and Venillen. J. Y., (2008), Phys. Rev. B, 77, 165415.

[9] Kosynkin. D. V., Higginbotham, A. L. Sinitski. A, Lomeda. J. R., Dimiev. A., Price. B. K. and Tour. J. M., (2009), Nature (London), 458, 872.

[10] Jiao. L., Zhang. L., Wang. X., Diaakiv. G. and Dai. H, (2009), Nature (London), 458, 877.

[11] Xie. L, Wang. H, Jin. C, Wnag. X, Jiao. L, Suenaga. K and Dai.H, (2011), J. Am Chem. Soc. 133, 10394.

[12] Akhmerov. A. R. and Beenakker. C. W. J, (2008), Phys. Rev. B, 77, 085423.

[13] Jaskolski. W, Aynela. A, Pele. M, Santos. H, and Chico. L, (2011), Phys. Rev. B, 83, 235424.

[14] Nakada. K, Fujita. M, Dresselhaus. G and Dresselhaus. M. S, (1996), Phys. Rev. B, 54, 17954.

[15] Brey. L and Fertig. H. A., (2006), Phys. Rev. B, 73, 235411.

[16] Lopes. J. M. B., Dos Santos, Peres. N. M. R. and Castro. A.H. Neto, (2007), Phys. Rev. Lett. 99, 256802.

[17] Shallcross. S, Sharma. S and Pankratov. O. A., (2008), Phys. Rev. Lett. 101, 056803.

[18] Shallcross. S, Sharma. S, Kaneiaki. E and Pankrativ. O. A, (2010), Phys. Rev. B, 81, 165105.

[19] Bistritzer. R and Mac Donald. A. H, (2011), Proc. Natl. Acad. Sci, U. S. A., 108, 12233.

[20] Lopes. J. M. B. dos santos, Peres. N. M. R. and Castro. A. H. Neta, (2012), Phys. Rev. B, 86 155449.

[21] San-Jose. P, Gonzaliz. J and Guinea. F, (2012), Phys. Rev. Lett. 108, 216802.

[22] Morell. E. Sunarez, Pacheco. M, Chico. L and Breyy. L. B, (2013) Phys. Rev. B, 87, 125414.

[23] Stauber. T, San-Jose. P and Brecy. L, (2013), New. J. Phys. 15, 113050.

[24] Correa. J. D, Pacheco. M and Morell. E. Suarez, (2014), J. Mater. Sc. 49, 642.

[25] Luican. A, Li. G, Eeina. A, Kong. J. Nair. R. R, Novoselov. K. S, Geim. A. K and Andrei. E. Y, (2011), Phys. Rev. Lett. 106, 126802.

[26] Brihuega. I et al, (2012), Phys. Rev. Lett. 109, 196802.

[27] Xian. L, Barraza. Lopez-S and Chou. M. Y, (2011), Phys. Rev. B, 84, 075425.

[28] Morell. E. Suarez, Vargas. P et al, (2014), Phys. Rev. B, 84, 195421.

[29] Singh Kumar Ashok, Ahmad Ali and Jagriti, (2017), B. P. A. S. Phys. No-1, 36D, 75.

[30] Mishra. A and Kumar. A, (2021), B. P. A. S., 40D, Phy. No-1, 44.

****

Bulletin of Pure and Applied Science
Physics, Vol.41D No.2,
July-December 2022 P.86-92
Original Research Article

Print version ISSN 0970 6569
Online version ISSN 2320 3218
DOI: 10.5958/2320-3218.2022.00016.1
Available online at www.bpasjournals.com

Internal Energy, Enthalpy and Gibb's Free Energy of Spinning Black Hole in Active Galactic Nuclei

[1]Dipo Mahto*, [2]Rakesh Paswan

Author's Affiliations:
[1]Professor & Head, Dept. of Physics, Bhagalpur College of Engineering under Department of Science and Technology, Bhagalpur, Bihar 812001, India.
And
[1]Former Head, Department of Physics, Marwari College Bhagalpur, (TMBU, Bhagalpur) Bihar 812007, India.
[2]Assistant Professor & Head, Department of Mathematics, DSM College (Munger University, Munger) Jhajha, Bihar 811308, India.

***Corresponding author:**
Dipo Mahto
Professor & Head, Dept. of Physics, Bhagalpur College of Engineering under Department of Science and Technology, Bhagalpur, Bihar 812001, India.
E-mail: dipomahto@hotmail.com

Received on 28.08.2022
Revised on 30.10.2022
Accepted on 26.11.2022
Published on 15.12.2022

ABSTRACT
The present paper gives a model for the change in the internal energy and enthalpy (Mahto et al., 2016) and reviews it to propose a model for change in Gibb's free energy of the Reissnner-Nordstrom black hole. This also calculates their values in AGN concluding that the enthalpy and internal energy has the same values and they are just double to that of Gibb's free energy for the same mass.

KEYWORDS
Hawking radiation, Black holes & Super Nova Explosion

How to cite this article: Mahto D, Paswan R. (2022). Internal Energy and Enthalpy of Spinning Black Hole in Active Galactic Nuclei. *Bulletin of Pure and Applied Sciences- Physics,* 41D (2), 86-92.

INTRODUCTION

Black hole is a gift of nature. This is created after super- nova explosion and belongs to a category of dead stars [1]. It has mass greater than 5 of the solar mass. As per classical theory, the black hole is a perfect absorber and emits nothing. But the quantum theory suggests that the black hole emits Hawking radiation. [2,3, 4]. Kanak et al. proposed a model for the energy of non-spinning black holes (E_{BH}) in terms of the radius of the event horizon [5]. Mahto et al. gave a model for the energy of spinning black holes in terms of the event horizon [6]. Mahto et al. gave a model for the change in energy and entropy of Non-spinning black holes by the use of first law of the black hole mechanics and well-known relation $E=mc^2$[7]. David Hochberg (1994), Shen & Chang-Jun (2001), David Kastor et al. (2011)

and Beauchesne and Edery (2012) had done their works related to Gibb's free energy [8,9,10,11].

In the present work, we have used a model for the change in the internal energy and enthalpy (Mahto et al., 2016) and reviewed it to propose a model for change in Gibb's free energy of the Reissnner-Nordstrom black hole and calculated their values in AGN.

THEORETICAL DISCUSSION

In the case of spinning black holes with half spin, the internal energy and enthalpy is given by the following equation [12].

$$dU_{BHs} = dH_{BHs} = \frac{0.2320}{M} R_{bhs}^2 \quad \text{……(1)}$$

The change in the internal energy of black holes from first law of black hole thermodynamics is given by the following equation (Dolan et al., 2012).

$$dM = dU = TdS \quad \text{…….(2)}$$

The change in free energy of the Reissnner-Nordstrom black hole due to change in the mass of black hole can be obtained by differentiating the above equation

$$dG = \frac{1}{2} dM \quad \text{.....(3)}$$

Using equation (1) & (2) in the above equation and solving, we have

$$dG_{BHs} = \frac{0.1160}{M} R_{bhs}^2 \quad \text{……...(4)}$$

For half spinning black holes, we have

$$R_{bhs} = M \quad \text{……..(5)}$$

Putting above value in equation (1), the internal energy and enthalpy is given by the following equation

$$dU_{BHs} = dH_{BHs} = 0.2320M \quad \text{……(6)}$$

Putting (5) in equation (4), we have

$$dG_{BHs} = 0.1160M \quad \text{…….(7)}$$

The equation (6) represents the change in internal energy and enthalpy, while equation (7) represents the Gibb's free energy of spinning black holes. Hence, the required model for the change in internal energy and enthalpy & Gibb's free energy of spinning black hole is summarized in the following box.

$dU_{BHs} = dH_{BHs} = 0.2320M$ for internal energy and enthalpy

$dG_{BHs} = 0.1160M$ for Gibb's free energy

Data in support of mass of black holes in XRBs and AGN and Sun:

M ~ 5 - 20 $M_\odot$ in XRBs, M ~ 10^6 – $10^{9.5}$ $M_\odot$ in AGN and Mass of sun ($M_\odot$) = 1.99 x 10^{30} kg. [13]

Calculations:

dU=0.2320M= 0.2320x10^6 solar mass= 0.2320x10^6x1.99x10^{30}kg =0.46168x10^{36} Joule

dH=0.2320M= 0.2320x10^6 solar mass= 0.2320x10^6x1.99x10^{30}kg =0.46168x10^{36} Joule

dG=0.1160M= 0.1160x10^6 solar mass= 0.1160x10^6x1.99x10^{30}kg =0.23084x10^{36} J/mole

lly other values of internal energy/enthalpy and Gibb's Free energy can be calculated

Table 1: Change in enthalpy/internal and free energy of spinning black holes in AGN.

Sl. No.	Mass of BHs (M)	Mass of BHs in terms of solar mass ($M_\odot$ x 10^7)	dU_{BHsb}(in Joule)	dH_{BHs} (in Joule)	dG_{BHs} (in Joule/mole)
1	1 x 10^6 $M_\odot$	0.1	0.046168x 10^{37}	0.046168x 10^{37}	0.023084 x 10^{37}
2	2 x 10^6 $M_\odot$	0.2	0.092336x 10^{37}	0.092336x 10^{37}	0.046165 x 10^{37}
3	3 x 10^6 $M_\odot$	0.3	0.138504x 10^{37}	0.138504x 10^{37}	0.069252 x 10^{37}
4	4 x 10^6 $M_\odot$	0.4	0.184672x 10^{37}	0.184672x 10^{37}	0.092336 x 10^{37}
5	5 x 10^6 $M_\odot$	0.5	0.230840x 10^{37}	0.230840x 10^{37}	0.115420 x 10^{37}
6	6 x 10^6 $M_\odot$	0.6	0.277008x 10^{37}	0.277008x 10^{37}	0.138504 x 10^{37}
7	7 x 10^6 $M_\odot$	0.7	0.323176x 10^{37}	0.323176x 10^{37}	0.161588 x 10^{37}
8	8 x 10^6 $M_\odot$	0.8	0.369344x 10^{37}	0.369344x 10^{37}	0.184672 x 10^{37}
9	9 x 10^6 $M_\odot$	0.9	0.415512x 10^{37}	0.415512x 10^{37}	0.207756 x 10^{37}
10	1 x 10^7 $M_\odot$	1	0.461680x 10^{37}	0.461680x 10^{37}	0.230840 x 10^{37}
11	2 x 10^7 $M_\odot$	2	0.923360x 10^{37}	0.923360x 10^{37}	0.461650 x 10^{37}
12	3 x 10^7 $M_\odot$	3	1.385040x 10^{37}	1.385040x 10^{37}	0.692520 x 10^{37}
13	4 x 10^7 $M_\odot$	4	1.846720x 10^{37}	1.846720x 10^{37}	0.923360 x 10^{37}
14	5 x 10^7 $M_\odot$	5	2.30840x 10^{37}	2.30840x 10^{37}	1.154200 x 10^{37}
15	6 x 10^7 $M_\odot$	6	2.77008x 10^{37}	2.77008x 10^{37}	1.385040 x 10^{37}
16	7 x 10^7 $M_\odot$	7	3.23176x 10^{37}	3.23176x 10^{37}	1.615880 x 10^{37}
17	8 x 10^7 $M_\odot$	8	3.69344x 10^{37}	3.69344x 10^{37}	1.846720 x 10^{37}
18	9 x 10^7 $M_\odot$	9	4.15512x 10^{37}	4.15512x 10^{37}	2.077560 x 10^{37}
19	1 x 10^8 $M_\odot$	10	4.61680x 10^{37}	4.61680x 10^{37}	2.308400 x 10^{37}
20	2 x 10^8 $M_\odot$	20	9.23360x 10^{37}	9.23360x 10^{37}	4.616500 x 10^{37}
21	3 x 10^8 $M_\odot$	30	13.85040x 10^{37}	13.85040x 10^{37}	6.925200 x 10^{37}
22	4 x 10^8 $M_\odot$	40	18.46720x 10^{37}	18.46720x 10^{37}	9.233600 x 10^{37}
23	5 x 10^8 $M_\odot$	50	23.08400x 10^{37}	23.08400x 10^{37}	11.542000 x 10^{37}
24	6 x 10^8 $M_\odot$	60	27.70080x 10^{37}	27.70080x 10^{37}	13.850400 x 10^{37}
25	7 x 10^8 $M_\odot$	70	32.31760x 10^{37}	32.31760x 10^{37}	16.158800 x 10^{37}
26	8 x 10^8 $M_\odot$	80	36.93440x 10^{37}	36.93440x 10^{37}	18.467200 x 10^{37}
27	9 x 10^8 $M_\odot$	90	41.55120x 10^{37}	41.55120x 10^{37}	20.775600 x 10^{37}
28	1 x 10^9 $M_\odot$	100	46.16800x 10^{37}	46.16800x 10^{37}	23.084000 x 10^{37}
29	2 x 10^9 $M_\odot$	200	92.33600x 10^{37}	92.33600x 10^{37}	46.165000 x 10^{37}
30	3 x 10^9 $M_\odot$	300	138.50400x 10^{37}	138.50400x 10^{37}	69.252000 x 10^{37}

Graph 1: Fit 1: Linear, Equation, y = (0.46168) x + 4.440892099E-017, NDPU = 10, $\bar{X}$ = 0.55, $\bar{Y}$ =0.253924, RLSS = 1.40593E-032, RSS = 0.175847, COD = 1.000, Residual mean square, sigma-hat-squared = 1.75741E-033.

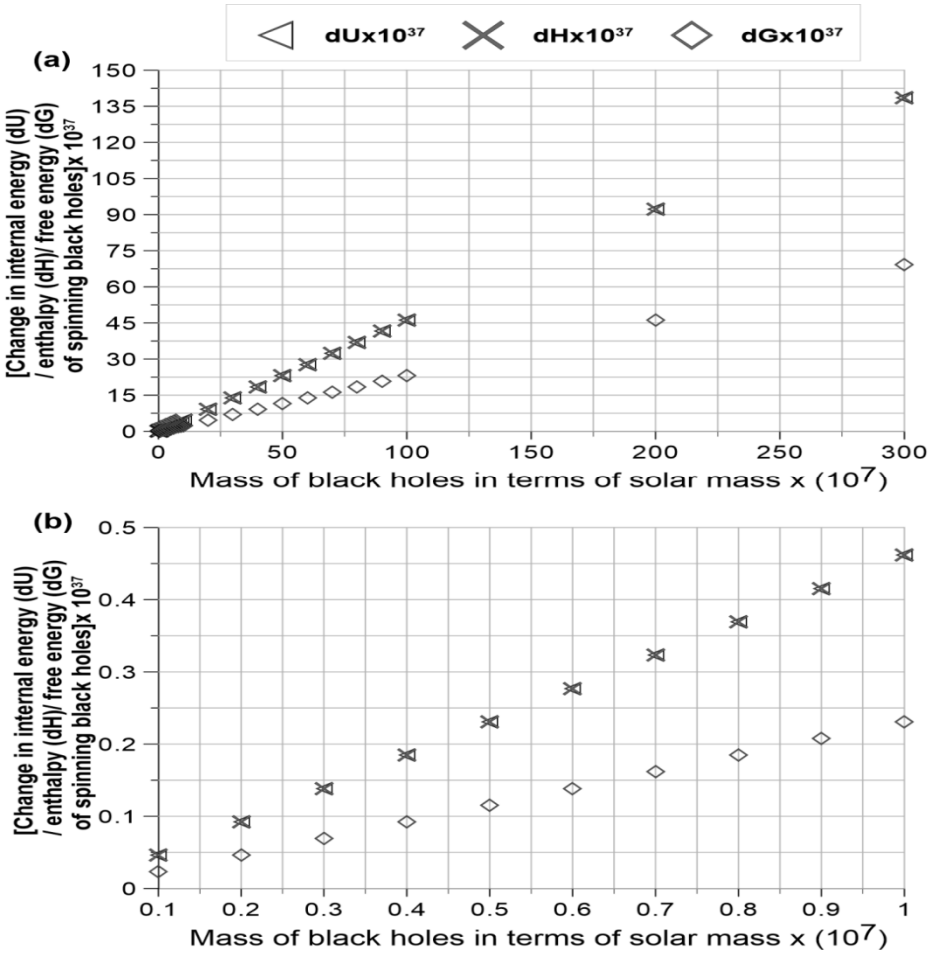

Graph 1: The Graph (a) shows that the change in internal energy/enthalpy/free energy of spinning black holes for different mass of black holes in AGN in ranging from 10^6 to $10^{9.5}$ solar mass, while the Graph (b) shows that the change in internal energy/enthalpy/free energy of spinning black holes for different mass of black holes in AGN in ranging from (0.1 to 1)x10^7 solar mass for better and clear visual representation.

Graph 2: Fit 1: Linear, Equation, y = (0.2308412727 x -1E-006, NDPU = 10, $\bar{X}$ = 0.55, Average $\bar{Y}$ = 0.126962, RLSS = 6.76364E-012, RSS = 0.0439623, COD = 1.000, Residual mean square, sigma-hat-squared = 8.45455E-013.

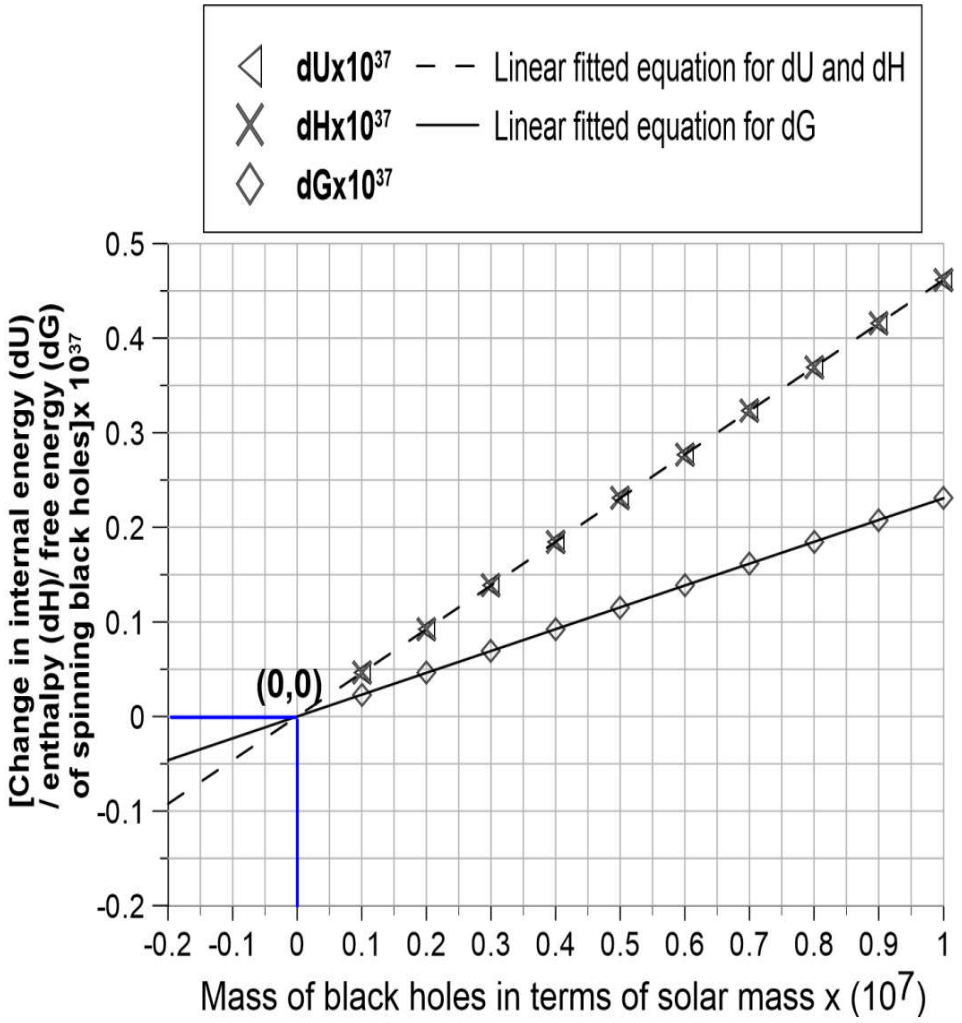

Graph 2: The figure shows that the change in internal energy/enthalpy/free energy of spinning black holes for different mass of black holes in AGN.

RESULT AND DISCUSSION

In the present work, we have used a model $dH / dR_{bh} = dU / dR_{bh} = 0.2320(R_{bhs}^2 / M)$ for the change in the internal energy and enthalpy of the spinning black holes and further this model is extended to obtain the change in the internal energy, enthalpy and Gibb's free energy of the spinning black holes in terms of mass. The new model for the change in the internal energy, enthalpy and Gibb's free energy of the spinning black holes is given below:

$$dU_{BHs} = dH_{BHs} = 0.2320M \quad \text{for internal energy and enthalpy}$$
$$dG_{BHs} = 0.1160M \quad \text{for Gibb's free energy}$$

After obtaining this model, we have calculated their values in AGN and plotted the graphs between the change in internal energy, enthalpy and free energy of spinning black holes for different values of mass of black holes.

From the graph plotted between the change in internal energy, enthalpy and free energy of spinning black holes & different values of mass in AGN, it is obvious that the change in internal energy and enthalpy for different masses are the

same and the Gibb's free energy of the spinning black holes have half value to that of the internal energy and enthalpy.

From graph, it is clear that there is an uniform variation in the change of internal energy, enthalpy and Gibb's free energy of the spinning black holes with increasing the mass of black holes.

The Graph (a) shows that the change in internal energy/enthalpy/free energy of spinning black holes for different mass of black holes in AGN in ranging from 10^6 to $10^{9.5}$solar mass, while the Graph (b) shows that the change in internal energy/enthalpy/free energy of spinning black holes for different mass of black holes in AGN in ranging from (0.1 to 1)x10^7 solar mass for better and clear visual representation.

In this case, when the nature of the graph plotted be t^n the mass of spinning black holes and their corresponding internal energy/enthalpy in AGN is observed, we see that there is an uniform variation of internal energy/enthalpy with different masses followed by the linear equation represented by dUx 10^{37}J =0.46168 x 10^7 $M_\odot$ + 4.440892099E-017 for internal energy & dH x 10^{37}J =0.46168 x $10^7 M_\odot$ + 4.440892099E-017 for enthalpy with slope 0.46168 and fitting accuracy equal to 1.000 showing that the proposed model is very good fit for the data and indicates that 100% of the variation in the outcome has been explained just by predicting the outcome using the covariates included in the model. Similarly there is also an uniform variation of free energy with different masses followed by the linear equation represented by dGx10^{37}J =0.2304812727 x 10^7 $M_\odot$ - 1E-006 with slope 0.2304812727 and fitting accuracy equal to 1.000 showing that the proposed model is very good fit for the data and indicates that 100% of the variation in the outcome has been explained just by predicting the outcome using the covariates included in the model.

CONCLUSION

1. The change in internal energy and enthalpy of spinning black holes for different values of mass are the same.
2. The change in enthalpy as well internal energy increase with increasing the mass of spinning black holes.
3. The enthalpy and internal energy has the same values and they are just double to that of Gibb's free energy for the same mass of black holes.
4. The enthalpy and internal energy of spinning black holes are the manifestation of the same thing.
5. There is an uniform variation in the change of internal energy, enthalpy and Gibb's free energy of the spinning black holes with increasing the mass of black holes.

REFERENCES

[1] Dipo Mahto & G.K. Jha (2000). Study of Mathematical analysis of Black hole. Bulletin of Pure and Applied Science, 19B(2), 125-128.

[2] S. W. Hawking (1975). Particle creation by Black hole, Comm. Math. Phys. 43, 199-220.

[3] Hawking. S.W., (1974). Black hole explosions?. Nature, 248, 30-31.

[4] R.M. Wald, R. M. Wald. (2001). The Thermodynamics of black holes, Living reviews in relativity.

[5] Kumari, K. et al. (2010). Study of Schwarzschild radius with reference to the non-spinning black holes, Bulletin of Pure and applied sciences, 29D(2), 183-187.

[6] Mahto, D. et al. (2011). Study of Schwarzschild radius with reference to the spinning black holes. Bulletein of Pure and applied sciences, 30D(1), 157-162.

[7] Mahto et al, (2012). Study of Non-spinning black holes with reference to the change in energy and entropy & Space Sciences, Astrophys Space Sci, 337, 685–691, DOI 10.1007/s10509-011-0883-7.

[8] David Hochberg. Free energy and entropy for semi-classical Black Holes in the Canonical Ensemble. arXiv:gr-qc/941003401. 1994.

[9] You-Gen Shen, Chang, Jun Gao. (2001). Entropy of Diatomic Black Hole due to Arbitrary Spin Fields. Chinees Journal of Astronomy and Astrophysics. 1(4), 357–364.

[10] David Kastor, Sourya Ray, Jennie Traschen. Mass and free energy of Lovelock Black Holes. arXiv:1106.2764v2. 2011.

[11] Hugues Beauchense and Ariel Edery. Black hole free energy during charged Collapse: numerical study. arXiv:1203.2279v2. 2012.

[12] Mahto D, Singh A.K., Kumari N. (2016). Change in Internal Energy and Enthalpy of Spinning Black Hole with Half Spin Parameter in XRBs, International Journal of Astronomy and Astrophysics, 6, 328-333,

[13] Narayan R. (2005). Black holes in Astrophysics. arXiv: gr-qc/0506078V1,14 Jan, 2005

****

Bulletin of Pure and Applied Science
Physics, Vol.41D No.2,
July-December 2022 P.93-110
Original Research Article

Print version ISSN 0970 6569
Online version ISSN 2320 3218
DOI: 10.5958/2320-3218.2022.00017.3
Available online at www.bpasjournals.com

Theory of Harmonic Oscillations: A Gross Error in Physics

Temur Z. Kalanov*

Author's Affiliations: Home of Physical Problems, Yozuvchilar (Pisatelskaya) 6a, 100128 Tashkent, Uzbekistan

***Corresponding author:** **Temur Z. Kalanov**
Home of Physical Problems, Yozuvchilar (Pisatelskaya) 6a, 100128 Tashkent, Uzbekistan
E-mail: tzk_uz@yahoo.com, t.z.kalanov@mail.ru, t.z.kalanov@rambler.ru

Received on 29.08.2022
Revised on 27.10.2022
Accepted on 28.11.2022
Published on 15.12.2022

ABSTRACT The critical analysis of the foundations of the standard theory of harmonic oscillations is proposed. The unity of formal logic and rational dialectics is methodological basis of the analysis. The analysis leads to the conclusion that this theory represents gross error. The substantiation (validation) of this statement is the following main results. I. In the case of the material point suspended on the elastic spring, the linear differential equation of harmonic oscillations is the equation (condition) of balance of Newton's force (Newton's second law) and "Hooke's force" ("Hooke's law" as pseudolaw). This equation contains the following gross methodological errors: (a) the differential equation of motion of the material point does not satisfy the dialectical principle of the unity of the qualitative and quantitative determinacy of physical quantities (i.e., Newton's force and Hooke's force). In other words, the left and right sides of the differential equation (i.e., the equation of balance of the forces) have no identical qualitative determinacy: the left side of the the equation of balance of the forces represents Newton's force, and the right side of the the equation of balance of the forces represents the "Hooke's force" (as pseudolaw); (b) the sum of Newton's force and the "Hooke force" (as pseudolaw) in the the equation of balance of the forces is equal to zero. This means that the sum of the numerical values of Newton's force and "Hooke's force" (as pseudolaw) is equal to zero. Consequently, the numerical values of Newton's force and "Hooke's force" (as pseudolaw) are equal to zero in the region of neutral real numbers. This means that the equation of balance of the forces is incorrect; (c) "Hooke's force" (as pseudolaw) in the equation of balance of the forces represents the product of the spring constant (coefficient of stiffness of the spring) and the coordinate of the material point. In this case, "Hooke's force" (as pseudolaw) does not represent Hooke's law. "Hooke's force" (as pseudolaw) contradicts to Hooke's law because the coordinate of rhe material point does not determine the spring constant (coefficient of stiffness of the spring). "Hooke's force" (as pseudolaw) has the dimension of Newton's force. But, as the practice of measurement of Hooke's force with the help of a dynamometer shows, the dynamometer readings are real neutral numbers with the dimension "kilogram-force"; (d) the mathematical operation of division of the equation of balance of the forces by the mass of the material point leads to the linear equation of balance of

the accelerations of the material point. In this case, the mathematical operation gives rise to the term "frequency": (spring stiffness coefficient)-to-(mass) ratio is "squared frequency". But the spring stiffness coefficient is the constant that does not define the concept of frequency. Therefore, the quantity of the acceleration of the material point does not define the concept of the frequency of periodic motion; (e) the solution of the linear differential equation of balance of the accelerations of the material point has imaginary roots. This leads to the following contradiction: the coordinate of the material point is both an exponential function and a trigonometric function. II. In the case of oscillations of the mathematical pendulum, the linear differential equation of harmonic oscillations of the material point suspended on the inextensible thread represents a mathematical description of the angular displacement of the inextensible thread in the Cartesian coordinate system. This equation is a mathematical consequence of the standard differential equation of the rotational motion dynamics and contains the following gross methodological errors: (a) the differential equation of motion of the material point suspended on the inextensible thread does not satisfy the dialectical principle of the unity of the qualitative and quantitative determinacy of physical quantities (i.e., the physical quantity of rate of change of the angular momentum (moment of momentum) and the physical quantity of moment of the acting force). This equation expresses the condition of balance of the rate of change of the angular momentum (moment of momentum) and the moment of the acting force. Gross error is that the left and right sides of the balance equation have no identical qualitative determinacy: the left side of the balance equation is the rate of change of the angular momentum (moment of momentum), and the right side of the balance equation is the moment of the acting force; (b) the sum of the rate of change of the angular momentum and the moment of the acting force is equal to zero in the balance equation. This means that the sum of the numerical values of the rate of change of the angular momentum and the moment of the acting force is equal to zero. Consequently, the numerical values of the rate of change of the angular momentum and the moment of the acting force are equal to zero in the region of neutral real numbers. This means that the balance equation is incorrect; (c) the mathematical operation of division of the equation of balance of the rate of change of the angular momentum and the moment of the acting force by the mass of the material point and the square of the thread length results in the equation of balance of the angular accelerations. In this case, the mathematical operation results in the term "frequency" ("squared frequency"). But the quantity of the angular acceleration does not determine the frequency of the periodic motion; (d) the linear differential equation of balance of the angular accelerations is analogous to the linear differential equation of balance of the accelerations of the material point suspended on the spring. Therefore, the solution of the linear differential equation of balance of the angular accelerations has imaginary roots and leads to the following contradiction: the angle of displacement of the pendulum from the equilibrium position is both an exponential function and a trigonometric function.

KEYWORDS General physics, Classical Mechanics, Formalisms in Classical Mechanics, Newtonian Mechanics, Harmonic Oscillations, Engineering, Technology, General Mathematics, Methodology of Mathematics, General Applied Mathematics,Philosophy of Mathematics, Education, Philosophy of Science, Logic in the Philosophy of Science, History of Science.

PACS: 01.40.-d, 01.55.+b, 01.65.+g, 01.70.+w, 02.90.+p, 45.05.+x, 45.20.-d, 45.20.D- . 45.20.dc, 89.20.Kk

How to cite this article: Temur Z. Kalanov (2022). Theory of Harmonic Oscillations: A Gross Error in Physics. *Bulletin of Pure and Applied Sciences- Physics,* 41D (2), 93-110.

INTRODUCTION

As is known, the theory of harmonic oscillations is an important part of the foundations of physics and mathematics [1-10]. This theory was created by well-known scientists and is presented (reproduced) in textbooks and monographs [11-16]. Therefore, the theory looks convincing. But the validity of the theory has not been questioned so far.

In my opinion, the validity of a theory can only be researched (studied, analyzed) within the framework of the correct methodological basis: the unity of formal logic and rational dialectics. The unity of formal logic and rational dialectics represents the only correct criterion of truth. Formal logic is the general science of the laws of correct thinking. Rational dialectics is the general doctrine of universal connection and change in the world. The most important concepts of rational dialectics are the concepts of quality, quantity and measure.

Quality (i.e., the qualitative determinacy) is the unity of properties, essential features of an object. The qualitative determinacy of an object represents the essence (as a set of essential features) of an object. Quantity is the quantitative determinacy of the essence of an object. The quantitative determinacy belongs to the qualitative determinacy of the object (i.e., the quantitative determinacy belongs to the essential feature of the object) and is expressed by dimensional neutral numbers.

The measure of an object is the unity of the qualitative and quantitative determinacy of an object. From this point of view, a correct mathematical relationship represents the unity of qualitative and quantitative determinacy: the left and right sides of the mathematical relationship denote (designate, indicate) an identical qualitative determinacy (i.e., an identical meaning). Therefore, a mathematical relationship is incorrect if the left and right sides of the relationship belong to different qualitative determinacy.

Well-known scientists did not find the correct criterion of truth for mathematical and physical theories. As is known, Albert Einstein and Henri Poincaré were probably the last scientists who tried to find the correct criterion of truth. After Albert Einstein, the problem of truth in science was not studied (researched) by mathematicians and physicists. Scientists worshiped (adored, venerated) the works of the classics of sciences. Scientists believed in the inviolability (firmness, stability) of the foundations of sciences. Therefore, scientists did not question the standard theories. That is why theoretical physics and mathematics contain gross methodological errors and enter into the greatest crisis.

The purpose of the present work is to propose the critical analysis of the standard theory of harmonic oscillations. The methodological basis for analysis is the unity of formal logic and rational dialectics. This way of analysis gives an opportunity to understand the erroneous essence of the theory of harmonic oscillations.

1. Elements of correct kinematics and dynamics [17-20]

As is known, the starting point of correct kinematics is based on the following statements. 1) "The quantity $l^{(M)}(t) - l^{(M)}(t_0)$ is called increment of the length of the path of the material point M over time $\Delta t_0 \equiv t - t_0$ where $\Delta t_0 \neq 0$, t_0 is the initial point of time. The length of the path and the increment of the length of the path are not vector quantities. The quantity

$$\frac{l^{(M)}(t) - l^{(M)}(t_0)}{\Delta t_0} \equiv v^{(M)}(\Delta t_0)$$

is rate of change in the quantity $l^{(M)}$. In other words, the speed of motion of the point M is rate of change in quantity $l^{(M)}(t)$. (Movement is change in general). Therefore, the speed is not a vector quantity. By definition, the speed of the motion of the point M is the average speed over time Δt_0. There is no "instantaneous speed" (i.e., speed at point of time t). The speed of the

motion is the essential feature (property, characteristic) of motion: speed is the rate of the change in quantity. The rate of the change in the quantity $l^{(M)}(t)$ has no a graphical representation in system XOY because the quantity of the rate has no the dimension of "meter (m)". The rate of the change in the quantity $l^{M}(t)$ is not defined and is not characterized by any direction because the quantity $l^{(M)}(t)$ is not defined and is not characterized by a direction of the motion of the point M in the system XOY. Thus, the rate of the change in the path length is independent of a direction of the motion of the point M".

2) "The variable quantity $v^{(M)}(\Delta t_0)$ takes on the values $v_1^{(M)}(\Delta t_{10})$, $v_2^{(M)}(\Delta t_{20})$, $v_3^{(M)}(\Delta t_{30})$ under Δt_{10}, Δt_{20}, Δt_{30}, respectively. If the interval (duration) of time is the variable quantity $\Delta t_0 \equiv t - t_0$, then the quantity $v^{(M)}(\Delta t_0)$ of the speed is a function of the argument $\Delta t_0 \equiv t - t_0$. The conventional concept of speed at point of time (at instant of time) t (or at point of plane XOY) has no scientific and practical sense because the speed of the motion is determined by two (different) positions of the moving point M on plane XOY and by two (different) points of time: movement is change in general; but there is no change in position at point of time t (or at point of plane XOY)".

3) "If the speed of the motion of the point M depends on time, then the quantity

$$\frac{v^{(M)}(\Delta t_0) - v_1^{(M)}(\Delta t_0)}{\Delta t_0} \equiv a^{(M)}$$

is called acceleration of the point M on the path length $l^{(M)}(t) - l^{(M)}(t_0)$ where $v_1^{(M)}(\Delta t_0)$ is certain value of speed, which is experimentally determined. Acceleration characterizes the motion of the point M: acceleration is the essential feature (property, characteristic) of the motion of point M. The quantity of the acceleration of the point M has no graphical representation in the system XOY because the quantity of the acceleration has no dimension of "meter (m)". The quantities $l^{(M)}(t)$ and $a^{(M)}$ are connected by the following relationship:

$$l^{(M)}(t) - l^{(M)}(t_0) = a^{(M)} \cdot (\Delta t_0)^2".$$

If

$$l^{(M)}(t) - l^{(M)}(t_0) = \Delta l^{(M)}(\Delta t_0),$$

$$a^{(M)} = g,$$

then $\Delta t_0 = \sqrt{\frac{\Delta l^{(M)}}{g}}$

where Δt_0 is the free fall time of the material point M in the gravitational field; g is the gravitational acceleration. This expression does not depend on the mass of the material point M and represents a reliable experimental result.

4) The product of mass and speed of the moving object M represents the essential physical property (essential feature) of the moving material object:

$$p^{M}(\Delta t_0) \equiv m^{M} \times v^{M}(\Delta t_0)$$

where the physical quantity $p^{M}(\Delta t_0)$ is called momentum of object M. The dimension of the quantity of the momentum is "$kg\ m\ s^{-1}$". This definition of the momentum satisfies the formal-logical law of identity:

(property of the moving object $"M"$*)* =
= *(property of the moving object* $"M"$*).*

In addition, the definition of the momentum satisfies the formal-logical law of lack (absence) of contradiction:

(property of the moving object $"M"$*)* $\neq$
$\neq$ *(property of the moving object* $"non-M"$*)*

5) The rate of change in the momentum of the moving object M represents the essential

physical property (essential feature) of the motion of the material object M. The rate of change in the momentum of the moving object M is defined as follows:

$$\frac{p^M(\Delta t_0) - p_1^M(\Delta t_0)}{\Delta t_0} = m^M \times \frac{\left[v^M(\Delta t_0) - v_1^M(\Delta t_0)\right]}{\Delta t_0}$$

,

$$\frac{p^M(\Delta t_0) - p_1^M(\Delta t_0)}{\Delta t_0} = m^M \times a^M$$

where $p_1^M(\Delta t_0)$ is a certain value of the momentum, which is experimentally determined. The dimension of the quantity of the rate of change in the momentum is "$kg\ m\ s^{-2}$". The dimension "$kg\ m\ s^{-2}$" characterizes the qualitative determinacy of the quantity of rate of change in the momentum. The definition of the rate of change in the momentum of the moving object satisfies the formal-logical law of identity:

(property of the moving object $"M"$*) =*
= (property of the moving object $"M"$*).*

In addition, the definition of the rate of change in the momentum satisfies the formal-logical law of lack (absence) of contradiction:

(property of the moving object $"M"$*)* $\neq$
$\neq$ *(property of the moving object* $"non-M"$*).*

6) As is known, the starting point of the correct dynamics of the material body S is the following formulation of Hooke's law.

(a) In the case of the spring S stretching, Hooke's law is the following correct expression:

$$\frac{F^D - F_1^D}{F_1^D} = \frac{l^{(spring)} - l_1^{(spring)}}{l_1^{(spring)}},$$

$$F^D = \left(\frac{F_1^D}{l_1^{(spring)}}\right) l^{(spring)},$$

$$F^D \neq m\ddot{l}^{(spring)},\ l^{(spring)} \neq 0$$

where $l^{(spring)} - l_1^{(spring)}$ is the increment of the length of the spring S; the dimension of the force F^D is "kgf", i.e. $[F] = kgf$; F_1^D is a certain value of variable quantity F^D which is the reading of the dynamometer D; $k^{(spring)} \equiv \left(\frac{F_1^D}{l_1^{(spring)}}\right)$ is coefficient of stiffness of the spring S having the dimension "kgf/m". (The coefficient $k^{(spring)}$ does not depend on time t).

Let one, using the dynamometer D, stretch out the spring S to a certain length $l^{(spring)}$ (Figure 1).

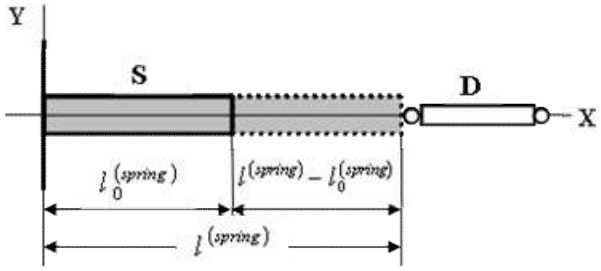

Figure 1: Change of the length of the spring. S. $l_0^{(spring)}$ is initial value of the spring length; $l^{(spruing)} - l_0^{(spring)}$ is the finite value of the spring length. D is a dynamometer, the readings of which are neutral numbers with the dimension "kgf".

As practice shows, the dynamometer D readings are real neutral numbers of the dimension "kgf", but not numbers of the dimension "$kg\,m\,s^{-2}$". If one disconnects the dynamometer D from the spring S, the spring S returns to its original (neutral) state during the relaxation time: $l^{(spring)}(t) \to l_0^{(spring)}$.

(b) In the case of compression of the spring S, Hooke's law is the following correct expression:

$$\frac{F^D - F_1^D}{F_1^D} = \frac{1/l^{(spring)} - 1/l_1^{(spring)}}{1/l_1^{(spring)}},$$

$$F^D = \left(\frac{F_1^D}{1/l_1^{(spring)}}\right)\frac{1}{l^{(spring)}},\ l^{(spring)} \neq 0,$$

7) Mathematical pendulum. In the case of a cycloidal periodic motion of a material circle (solid body), Huygens' experimental result is the following statement: "Ratio of the time of one small oscillation of the circular pendulum to the time of falling on the double length of the pendulum is as ratio of the circumference of the circle to the diameter" (Huygens). In the case of the mathematical pendulum, the Huygens kinematic relationship for the oscillation period has the following form:

$$T^{(pendulum)} = \frac{l^{(circle)}}{r^{(circle)}}\sqrt{\frac{l^{(pendulum)}}{g}}$$

where $l^{(pendulum)}$ is the length of the mathematical pendulum; $l^{(pendulum)} \equiv r^{(circle)}$; g is the gravitational acceleration. The oscillation period in the Huygens formula does not depend on the mass of the pendulum. This result is a reliable experimental fact.
Comparison of the expressions

$$\Delta t_0 = \sqrt{\frac{\Delta l^{(M)}}{g}}$$

and $$T^{(pendulum)} = \frac{l^{(circle)}}{r^{(circle)}}\sqrt{\frac{l^{(pendulum)}}{g}}$$

shows that the kinematics of the mathematical pendulum and the kinematics of free fall of the material point M are qualitatively identical. The quantitative difference between these expressions is determined by the design features of the mathematical pendulum. For example, the dimensionless coefficient

$$\frac{l^{(circle)}}{r^{(circle)}}$$

.is determined by the design features of the mathematical pendulum. Essential meaning of this coefficient is that this coefficient determines the amplitude of oscillations

If the fall (dropping) and lifting of the material point M is repeated continuously several times by some material device, then the quantity $\omega \equiv 1/\Delta t_0$ is the frequency of the periodic movement. The frequency has the dimension "hertz" (i.e., cycle per second). The frequency is measured with a material counter. But if the fall (dropping) and lifting of the material point M is not repeated continuously several times, then the quantity $\omega \equiv 1/\Delta t_0$ has no physical meaning.

STANDARD DIFFERENTIAL EQUATION OF HARMONIC OSCILLATIONS IN THE CASE OF A MATERIAL POINT SUSPENDED ON AN ELASTIC SPRING

In the case of the material point M suspended on the elastic spring S, the displacement of the material point M is motion in the vertical straight line segment – the coordinate ruler X (Figure 2).

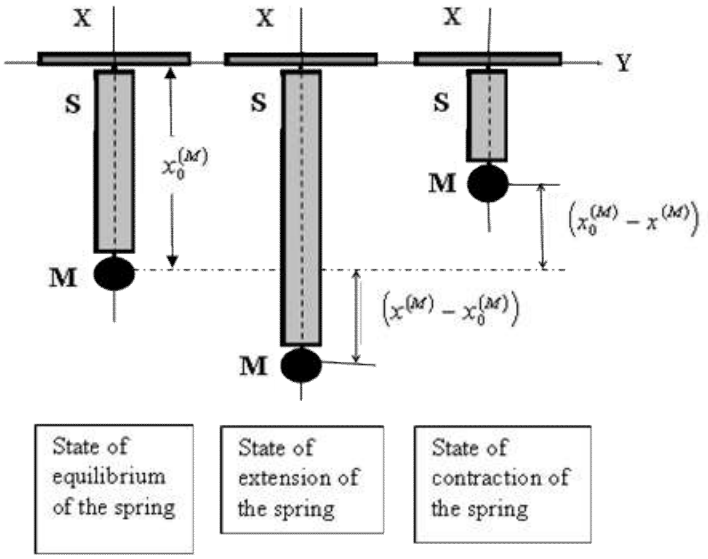

Figure 2: The coordinate $x^{(M)}$ of the oscillating material point M suspended on the elastic spring S.

As is known, the standard equation of harmonic oscillations of the material point M is the following linear differential equation of the second order:

$$\ddot{x}^{(M)} + \omega_0^2 x^{(M)} = 0$$

where $x^{(M)}$ is the displacement of the material point M, having the dimension "m"; $\omega_0^2 = k/m^{(M)}$ is the coefficient (frequency) having the dimension "$1/s^2$"; the mass $m^{(M)}$ of the material point M is the coefficient having the dimension "kg"; the spring stiffness coefficient k is the coefficient having the dimension "$kg\ s^{-2}$". This equation of motion of the material point M is a mathematical consequence of the following expressions:

(a) Lagrange function: $L^{(M,\ spring)} = \frac{m^{(M)}\left(\dot{x}^{(M)}\right)^2}{2} - \frac{k\left(x^{(M)}\right)^2}{2}$ for the "material point M + spring" system;

(b) "Hook's law" (as pseudolaw): $F^{(M)} = -kx^{(M)}$. This expression is not an equation of motion of the material point M;

(c) Newton's second law for the material point M. This expression is the equation of motion of the material point M;

(d) dynamic equation of balance (connection) of forces: $m^{(M)}\ddot{x}^{(M)} = -kx^{(M)}$.

The only meaning of the standard equation is that it is an equation (condition) for the balance of accelerations of the material point M.

OBJECTIONS TO THE STANDARD DIFFERENTIAL EQUATION OF HARMONIC OSCILLATIONS

In the case of the material point M suspended on the elastic spring S, the displacement of the material point M is motion in the vertical straight line segment – the coordinate ruler X (Figure 2). Physical, mathematical and formal-logical objections to the standard theoretical description of the harmonic oscillations of the material point M are as follows.

(a) The first gross error is as follows. The quantities $\ddot{x}^{(M)}$ and $\omega_0^2 x^{(M)}$ in the standard equation $\ddot{x}^{(M)} + \omega_0^2 x^{(M)} = 0$ represent accelerations and have the dimension "m/s^2". These quantities designate numbers. If these quantities take on numerical values and the sum of these quantities (numbers) is equal to zero, then $\ddot{x}^{(M)} \equiv 0$ and $\omega_0^2 x^{(M)} \equiv 0$ in the region of neutral real numbers. Consequently, the standard equation is incorrect;

(b) the second gross error is that the coefficient $\omega_0^2 = k/m^{(M)}$ in the standard equation has the dimension "$1/s^2$". From the point of view of formal logic, the following statement is true: the correct dimension of the quantity ω_0^2 is "kgf/mkg". Really, in the correct relationship $\omega_0^2 = k^{(spring)}/m^{(M)}$, the quantities $k^{(spring)}$ and $m^{(M)}$ have the following meanings: $m^{(M)}$ is mass of the material point M, which does not depend on the characteristics of the spring S and time t; $k^{(spring)} \equiv \left(\frac{F_1^{(spring)}}{l_1^{(spring)}} \right)$ is the coefficient of spring S stiffness, which does not characterize the material point M and does not depend on time t; the coefficient $k^{(spring)} \equiv \left(\frac{F_1^{(spring)}}{l_1^{(spring)}} \right)$ has the dimension "kgf/m". Therefore, the correct dimension of the quantity ω_0^2 is not "$1/s^2$". This means that the coefficient ω_0^2 cannot be contained in the equation of motion of the material point M;

(c) the third gross error is that the quantity ω_0 in the standard relationship $\omega_0^2 = k/m^{(M)}$ is called the frequency of oscillations. The dimension of the quantity ω_0^2 is $1/s^2$ because one uses the formula $F = ma$. But frequency (as the number of iterations of oscillation per unit time) cannot be contained in the equation of motion because the quantity ω_0^2 is

$$\omega_0^2 \equiv \frac{(coefficient\ of\ stiffness\ of\ spring\ S)}{(mass\ of\ the\ material\ point\ M)} =$$
$$= (square\ of\ frequency) = (absurdity).$$

In other words, the quantity

$$\frac{(coefficient\ of\ stiffness\ of\ spring\ S)}{(mass\ of\ the\ material\ point\ M)}$$

cannot depend on time t. This means that the formula $F = ma$ is incorrect, and the quantity ω_0 is not a frequency;

(d) the fourth gross error is that the expression $F^{(M)} = -kx^{(M)}$ (as pseudolaw) contradicts to the following correct formulation of Hooke's law:

$$F^{(Hooke's)} \equiv F^D = \left(\frac{F_1^D}{l_1^{(spring)}} \right) l^{(spring)},$$
$$F^{(Hooke's)} \equiv F^{(spring)} = k^{(spring)} l^{(spring)}.$$

Really, the spring S and the material point M are different (non-identical) objects. This is expressed by the formal-logical law of the lack of contradiction:

"(spring S) $\neq$ (material point M)".

Violation of the formal-logical law of the lack of contradiction is that one replaces the concept "spring S" (which is not characterized by the term "coordinate") by the non-identical concept "material point M" (which is characterized by the terms "coordinate" and "mass"). In other words, the mistake is that one identifies non-identical concepts, i.e.

"(spring S) = (material point M)".

But the coordinate $x^{(M)}$ of the material point M is not the length of the spring S. Consequently, the term $kx^{(M)}$ cannot be contained in the equation $m^{(M)}\ddot{x}^{(M)} = -kx^{(M)}$.

(e) The fifth gross error is that the equation $\ddot{x}^{(M)} + \omega_0^2 x^{(M)} = 0$ is not a logical consequence of the equation $m^{(M)}\ddot{x}^{(M)} + kx^{(M)} = 0$. Really, from the point of view of formal logic, the concepts $\ddot{x}^{(M)}$ and $\omega_0^2 x^{(M)}$ are not identical to the concepts $m^{(M)}\ddot{x}^{(M)}$ and $kx^{(M)}$, respectively.

(f) The sixth gross error is the following expression: $F^{(Newton\ 's)} = F^{(Hooker's)}$. But, from the point of view of formal logic and rational dialectics, $F^{(Newton\ 's)} \neq F^{(Hooker's)}$ because the left and right sides of the quantitative relationship $F^{(Newton\ 's)} = F^{(Hooker's)}$ have different qualitative determinacy, different meanings (i.e., the left and right sides of this relationship do not represent the same physical law). In other words, the gross error is that the expression $F^{(Newton\ 's)} = F^{(Hooker's)}$ violates the formal-logical law of the lack of contradiction:

"(Newton's second law) ≠ (Hooke's law)".

(g) The seventh gross error is the following formula: $F^{(Ntwton's)} \equiv F^{(M)} = m^{(M)}\ddot{x}^{(M)}$. But $F^{(M)} \neq m^{(M)}\ddot{x}^{(M)}$ because Newton's formula $F = ma$ is not a definition of force.

(h) The eighth gross error reveals in the next operation. The operation is based on the correct definition of acceleration. If one represents (interprets) the standard differential equation in the form of the algebraic equation

$$\frac{x^{(M)} - x_0^{(M)}}{\left(t - t_0\right)^2} + \omega_0^2\left(x^{(M)} - x_0^{(M)}\right) = 0$$

(where $x^{(M)} - x_0^{(M)} \neq 0$ is an increment; $\frac{x^{(M)} - x_0^{(M)}}{\left(t - t_0\right)^2}$ is a definition of the acceleration of the material point M), then the standard differential equation will take the following algebraic form:

$$1 = -\omega_0^2\left(t - t_0\right)^2.$$

This algebraic expression is the proof that the standard differential equation is nonsense.

Thus, the standard differential equation of harmonic oscillations represents a gross error.

MATHEMATICAL PENDULUM

In the case of a mathematical pendulum, the displacement of the material point M suspended on an inextensible thread is the angular displacement φ of the inextensible thread (Figure 3).

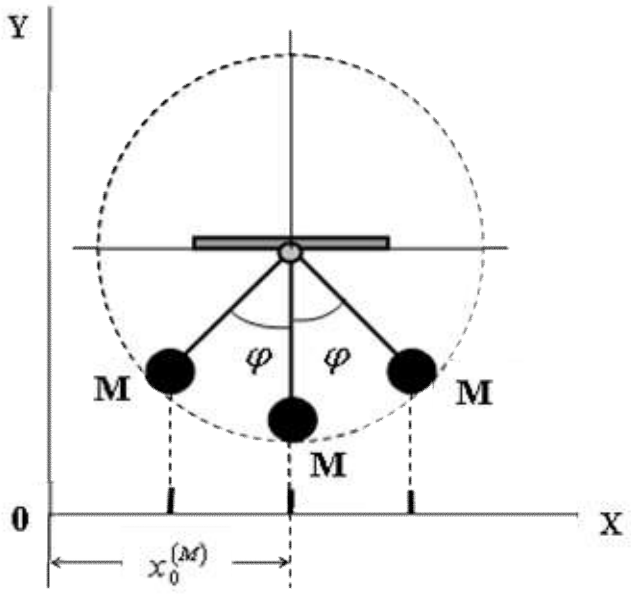

Figure 3: The positions of the oscillating material point M suspended on the inextensible thread in the "mathematical pendulum + coordinate system XOY" system. The quantity $x_0^{(M)}$ is the coordinate of the equilibrium position of the point M. The quantities $\left(x_0^{(M)} - x^{(M)}\right)$ and $\left(x^{(M)} - x_0^{(M)}\right)$ characterize the displaced positions of the material point M. φ is the quantity of the angle of displacement of the pendulum thread from the equilibrium value $\varphi_0 = 270^\circ$. The trajectory of the oscillating point M is the arc of the circle.

The trajectory of the material point M is the arc of the circle. The correct relationship between the length of the arc of the circle and the quantity of the central angle is as follows:

$$l^{(circular\ arc)} = \frac{l^{(circle)}}{360^\circ}\varphi^{(central\ angel)},$$

$$l^{(circle)} = \left(\frac{l_1^{(circle)}}{r_1^{(circle)}}\right) r^{(circle)} \equiv q^{(circle)} r^{(circle)},$$

$$q^{(circle)} = \left(\frac{l_1^{(circle)}}{r_1^{(circle)}}\right),$$

$$l^{(circular\ arc)} = \frac{q^{(circle)}}{360^\circ} r^{(circle)} \varphi^{(central\ angel)},$$

$$l^{(circular\ arc)} \neq l^{(pendulum)} \varphi^{(central\ angel)},$$

$$r^{(circle)} \equiv l^{(pendulum)} = const,$$

$$l^{(circular\ arc)} \equiv l^{(M)},$$

$$\dot{l}^{(M)} = \frac{q^{(circle)}}{360^\circ} r^{(circle)} \dot{\varphi}^{(central\ angel)},$$

$$p^{(M)} \equiv m^{(M)} \dot{l}^{(M)}$$

where $\varphi^{(central\ angel)}$ is the quantity of the central angle leaning (resting) on the arc of the circle; $l^{(circular\ arc)}$ is the length of the arc of the circle; $r^{(circle)}$ is the radius of the circle; $l^{(circular\ arc)} \equiv l^{(M)}$ is the length of the path traveled by the material point M; $l^{(pendulum)}$ is the length of the pendulum thread; $p^{(M)}$ is the momentum of the material point M.

The quantitative relationships between the circumference $l^{(circle)}$ and the radius $r^{(circle)}$ has form of the following proportion:

$$\left(\frac{l^{(circle)} - l_1^{(cirkle)}}{l_1^{(cirkle)}}\right) = \left(\frac{r^{(circle)} - r_1^{(circle)}}{r_1^{(circle)}{}_1}\right),$$

$$l^{(circle)} = \left(\frac{l_1^{(circle)}}{r_1^{(circle)}}\right) r^{(circle)}$$

where the dimensionless coefficient $\left(\frac{l_1^{(circle)}}{r_1^{(circle)}}\right)$ is experimentally determined.

STANDARD DIFFERENTIAL EQUATION OF HARMONIC OSCILLATIONS OF THE MATHEMATICAL PENDULUM

As is known, the standard linear differential equation of harmonic oscillations of the mathematical pendulum (Figure 3) has the following form:

$$\ddot{\varphi}^{(central\ angel)} + \omega_0^2 \varphi^{(central\ angel)} = 0,$$
$$\omega_0^2 = g/l^{(pendulum)}$$

where ω_0 is the frequency having the dimension "$1/s$"; $l^{(pendulum)}$ is the length of the inextensible thread having the dimension "m"; $\varphi^{(central\ angel)}$ is the angle of displacement of the pendulum from the equilibrium position; $g = 9{,}8\,\frac{meter}{\sec^2}$ is the gravitational acceleration, which has the dimension "m/s^2". This equation is a mathematical consequence of the following standard differential equation (i.e. the rotary motion dynamics equation):

$$m^{(M)}\left(l^{(pendilum)}\right)^2 \ddot{\varphi}^{(central\ angel)} = -m^{(M)} g l^{(pendilum)} \sin\varphi^{(central\ angel)},$$
$$\sin\varphi^{(central\ angel)} \approx \varphi^{(central\ angel)}$$

where $m^{(M)}$ is the mass of the material point M; $m^{(M)} g l^{(pendilum)} \sin\varphi^{(central\ angel)}$ is the rotational moment created by the force of gravity; $m^{(M)}\left(l^{(pendulum)}\right)^2$ is the moment of inertia of the pendulum; $m^{(M)}\left(l^{(pendulum)}\right)\dot{\varphi}^{(central\ angel)}$ is the momentum; $m^{(M)}\left(l^{(pendulum)}\right)^2 \dot{\varphi}^{(central\ angel)}$ is the angular momentum (moment of momentum); $\ddot{\varphi}^{(central\ angel)}$ is the angular acceleration.

The standard meaning of this dynamic equation is the following standard statement: the rate of change of angular momentum (i.e., $\dot{J}^{(M)} = m^{(M)}\left(l^{(pendilum)}\right)^2 \ddot{\varphi}^{(central\ angel)}$) is equal to the moment of the acting force (i.e., $N^{(M)} = -m^{(M)} g l^{(pendilum)} \sin\varphi^{(central\ angel)}$). In other words, this equation expresses the condition of balance of the rate of change of the angular momentum (moment of momentum) and the moment of the acting force.

OBJECTIONS TO THE STANDARD DIFFERENTIAL EQUATION OF HARMONIC OSCILLATIONS OF THE MATHEMATICAL PENDULUM

(a) The first gross error is that the dimensions of the quantities $\sin\varphi^{(central\ angel)}$ and $\varphi^{(central\ angel)}$ are different: the values of the quantity $\sin\varphi^{(central\ angel)}$ are dimensionless numbers, and the values of the quantity $\varphi^{(central\ angel)}$ have the dimension "degree".

(b) The second gross error is that the quantity $l^{(pendilum)} \sin\varphi^{(central\ angel)}$ represents the imaginary side of the non-existent right-angled triangle.

(c) The third gross error is that the standard expression $m^{(M)}\left(l^{(pendulum)}\right)\dot{\varphi}^{(central\ angel)}$ contradicts to the following correct definition of the momentum of the material point M:

$$p^{(M)} \equiv m^{(M)} \dot{l}^{(M)},\quad l^{(circular\ arc)} \equiv l^{(M)},$$
$$l^{(circular\ arc)} = \frac{l^{(circle)}}{360^\circ}\varphi^{(central\ angel)},$$
$$l^{(circular\ arc)} \neq l^{(pendulum)} \varphi^{(central\ angel)}.$$

(Explanation: The correct definition of the momentum of the material point M is based on the following fact: the trajectory (path) of the motion of the material point M is the arc of the

circle. The length of the arc of the circle is not a vector quantity. Change in the length of the arc of the circle determines the speed, acceleration and momentum of the material point M).

(d) The fourth gross error is the assertion that the rate of change of momentum (i.e., $m^{(M)}\left(l^{(pendilum)}\right)^2 \ddot{\varphi}^{(central\ angel)}$) is equal to the moment of the acting force (i.e,, $-m^{(M)} g l^{(pendilum)} \sin\varphi^{(central\ angel)}$). But, from the point of view of formal logic and rational dialectics,

$$m^{(M)}\left(l^{(pendilum)}\right)^2 \ddot{\varphi}^{(central\ angel)} \neq -m^{(M)} g l^{(pendilum)} \sin\varphi^{(central\ angel)}$$

because the left and right sides of the quantitative relationship have different qualitative determinacy (i.e., different measures, different meanings). In other words, the left and right sides of the standard relationship represent quantitative changes under non-identical qualitative determinacy. Really, the physical concepts "momentum of the material point M " and "moment of the force acting on the material point M " have different meanings, different qualitative determinacy, different measures. From the point of view of formal logic, the identification of the concepts "momentum" and "moment of force" is a violation of the law of the lack of contradiction:

"(momentum) ≠ (moment of force)".

Consequently, the relationship

$$m^{(M)}\left(l^{(pendilum)}\right)^2 \ddot{\varphi}^{(central\ angel)} = -m^{(M)} g l^{(pendilum)} \sin\varphi^{(central\ angel)}$$

represents a gross error.

(e) The fifth gross error is that the equation

$$\ddot{\varphi}^{(central\ angel)} + \omega_0^2 \varphi^{(central\ angel)} = 0$$

is not a logical consequence of the equation

$$m^{(M)}\left(l^{(pendilum)}\right)^2 \ddot{\varphi}^{(central\ angel)} = -m^{(M)} g l^{(pendilum)} \sin\varphi^{(central\ angel)}$$

.

Really, from the point of view of formal logic, the concepts $\ddot{\varphi}^{(central\ angel)}$ and $\omega_0^2 \varphi^{(central\ angel)}$ are not identical to the concepts $m^{(M)}\left(l^{(pendilum)}\right)^2 \ddot{\varphi}^{(central\ angel)}$ and $m^{(M)} g l^{(pendilum)} \sin\varphi^{(central\ angel)}$, respectively.

(f) The sixth gross error manifests itself in the following. The quantities $\ddot{\varphi}^{(central\ angel)}$ and $\omega_0^2 \varphi^{(central\ angel)}$ in the standard equation $\ddot{\varphi}^{(central\ angel)} + \omega_0^2 \varphi^{(central\ angel)} = 0$ represent the accelerations and have the dimension "degree/s² ". If these quantities take numerical values and the sum of these values is equal to zero, then $\ddot{\varphi}^{(central\ angel)} \equiv 0$ and $\omega_0^2 \varphi^{(central\ angel)} \equiv 0$ in the region of neutral real numbers. Consequently, the standard equation is incorrect.

(g) The seventh gross error manifests itself in the next operation. The operation is based on the correct definition of acceleration. If one represents the standard differential equation in the form of the algebraic equation

$$\frac{\varphi^{(central\ angel)} - \varphi_0^{(central\ angel)}}{\left(t - t_0\right)^2} + \omega_0^2\left(\varphi^{(central\ angel)} - \varphi_0^{(central\ angel)}\right) = 0$$

, $\varphi_0^{(central\ angel)} = 270^\circ$

(where $\varphi^{(central\ angel)} - \varphi_0^{(central\ angel)} \neq 0$ is the increment of the quantity of the angle; $\frac{\varphi^{(central\ angel)} - \varphi_0^{(central\ angel)}}{\left(t - t_0\right)^2}$ is the definition of acceleration), then the standard equation will take the following form:

$$1 \equiv -\omega_0^2\left(t - t_0\right)^2, \quad \omega_0^2 = g / l^{(pendulum)}.$$

This algebraic expression is the proof that the standard differential equation represents nonsense.

Thus, the standard differential equation of harmonic oscillations of the mathematical pendulum is a gross error.

DISCUSSION OF THE SOLUTION OF THE STANDARD DIFFERENTIAL EQUATION

Thus, the standard differential equation of harmonic oscillations is incorrect because the equation does not satisfy the laws of formal logic and rational dialectics. This fact means that the solution of the incorrect equation cannot be a scientific truth. Really:

1) As is known, the standard solution of the standard differential equation $\ddot{x}^{(M)} + \omega_0^2 x^{(M)} = 0$ is found as follows. Substitution of the expression $x^{(M)} = a\exp(\lambda t)$ into the standard differential equation leads to the characteristic equation $\lambda^2 + \omega_0^2 = 0$ where the parameter λ and the constant a are not in a logical connection with the quantities $x^{(M)}$ and ω_0^2.

From the point of view of rational dialectics and formal logic, the standard mathematical (quantitative) expression $x^{(M)} = a\exp(\lambda t)$ contradicts to the following assertions (statements, points) of the methodological basis: (a) the dialectical category of measure; (b) the formal-logical law of identity and the law of the lack of contradiction because the left and right sides of the mathematical (quantitative) expression $x^{(M)} = a\exp(\lambda t)$ do not have identical qualitative determinacy (measures). In other words, the right side of the quantitative (mathematical) expression $x^{(M)} = a\exp(\lambda t)$ is not a feature of the material point M (i.e., $a\exp(\lambda t)$ does not characterize the object M). Therefore, the standard mathematical operation of change of the variable (i.e., $x^{(M)} = a\exp(\lambda t)$) is a gross methodological error.

From the point of view of formal logic, if $\lambda^2 + \omega_0^2 = 0$, then $\lambda^2 \equiv 0$ and $\omega_0^2 \equiv 0$ in the region of neutral real numbers because letters in mathematics designate (indicate, denote, denominate, mean) numbers. Therefore, the expression $\lambda^2 + \omega_0^2 = 0$ is a gross error.

From the standard point of view, the characteristic equation $\lambda^2 + \omega_0^2 = 0$ has imaginary roots: $\lambda_1 = +i\omega_0$, $\lambda_1 = -i\omega_0$. In this case, the standard general solution of the equation $\ddot{x}^{(M)} + \omega_0^2 x^{(M)} = 0$ is:

$$x^{(M)} = (a/2)\left(\exp\left[i(\omega_0 t + \alpha)\right] + \exp\left[-i(\omega_0 t + \alpha)\right]\right) = a\cos(\omega_0 t + \alpha)$$

where a and α are arbitrary constants that do not characterize the material point M. This solution leads to the following contradiction:

$$x^{(M)} = a\exp(\lambda t) = a\cos(\omega_0 t + \alpha).$$

From the mathematical point of view, $\exp(\lambda t) \neq \cos(\omega_0 t + \alpha)$ because an exponential function is not a periodic function. Therefore, the general solution of the equation $\ddot{x}^{(M)} + \omega_0^2 x^{(M)} = 0$ is a gross error.

The standard equation $\ddot{x}^{(M)} + \omega_0^2 x^{(M)} = 0$ of harmonic oscillations is a special case of the standard equation of the general oscillatory motion. This means that the solution of the standard equation of the general oscillatory motion is a gross error.

2) In the case of the mathematical pendulum, the standard linear differential equation of harmonic oscillations of the mathematical pendulum has the following standard form:

$$\ddot{\varphi}^{(central\ angel)} + \omega_0^2 \varphi^{(central\ angel)} = 0,$$
$$\omega_0^2 = g/l^{(pendulum)}$$

This equation is analogous to the equation $\ddot{x}^{(M)} + \omega_0^2 x^{(M)} = 0$. Therefore, the analysis of the solution of the equation $\ddot{\varphi}^{(central\ angel)} + \omega_0^2 \varphi^{(central\ angel)} = 0$ leads to a similar conclusion: the solution of the equation $\ddot{\varphi}^{(central\ angel)} + \omega_0^2 \varphi^{(central\ angel)} = 0$ is a gross error.

3) In my works [21-69], the following statements are proved:
(a) the differential and integral calculus represents a gross error;
(b) the numbers are neutral numbers; positive and negative numbers do not exist;
(c) pure mathematics, standard trigonometry, complex number theory, and vector calculus represent gross errors.
(d) Newton's second and third laws represent gross errors.

Consequently, the standard general theory of oscillations using standard trigonometry, complex number theory, vector calculus, Newton's laws, etc. is unfounded, groundless, unreasonable one because it represents gross error in science.

A particular (special) scientific theory cannot be substantiated (validated, well-founded, grounded) within the framework of particular (special) sciences because particular (special) sciences do not contain a criterion of truth. Moreover, the criterion of truth cannot be formulated within the framework of particular (special) sciences. The criterion of truth can only be formulated within the framework of the general sciences. The general sciences are formal logic and rational dialectics. Therefore, the unity of formal logic and rational dialectics represents the correct criterion of truth and the methodological basis for particular (special) sciences. Consequently, the substantiation (validation) of particular (special) scientific theories should be carried out within the framework of the correct methodological basis. The existence of methodological errors in particular (special) scientific theories means the collapse of these theories.

CONCLUSION

Thus, the critical analysis of the foundations of the standard theory of harmonic oscillations within the framework of the unity of formal logic and rational dialectics leads to the conclusion that this theory represents gross error. The substantiation (validation) of this statement is the following main results.

I. In the case of the material point suspended on the elastic spring, the linear differential equation of harmonic oscillations is the equation (condition) of balance of Newton's force (Newton's second law) and "Hooke's force" ("Hooke's law" as pseudolaw). This equation contains the following gross methodological errors:

(a) the differential equation of motion of the material point does not satisfy the dialectical principle of the unity of the qualitative and quantitative determinacy of physical quantities (i.e., Newton's force and Hooke's force). In other words, the left and right sides of the differential equation (i.e., the equation of balance of the forces) have no identical qualitative determinacy: the left side of the the equation of balance of the forces represents Newton's force, and the right side of the the equation of balance of the forces represents the "Hooke's force" (as pseudolaw).

(b) the sum of Newton's force and the "Hooke force" (as pseudolaw) in the the equation of balance of the forces is equal to zero. This means that the sum of the numerical values of Newton's force and "Hooke's force" (as pseudolaw) is equal to zero. Consequently, the numerical values of Newton's force and "Hooke's force" (as pseudolaw) are equal to zero in the region of neutral real numbers. This means that the equation of balance of the forces is incorrect.

(c) "Hooke's force" (as pseudolaw) in the equation of balance of the forces represents the product of the spring constant (coefficient of stiffness of the spring) and the coordinate of the material point. In this case, "Hooke's force" (as pseudolaw) does not represent Hooke's law. "Hooke's force" (as pseudolaw) contradicts to Hooke's law because the coordinate of rhe material point does not determine the spring constant (coefficient of stiffness of the spring). "Hooke's force" (as pseudolaw) has the dimension of Newton's force. But, as the practice of measurement of Hooke's force with the help of a dynamometer shows, the dynamometer readings are real neutral numbers with the dimension "kilogram-force".

(d) the mathematical operation of division of the equation of balance of the forces by the mass of the material point leads to the linear equation of the balance of the accelerations of the material point. In this case, the mathematical operation gives rise to the term "frequency": (spring stiffness coefficient)-to-(mass) ratio is "squared frequency". But the spring stiffness coefficient is the constant that does not define the concept of frequency. Therefore, the quantity of the acceleration of the material point does not define the concept of the frequency of periodic motion.

(e) the solution of the linear differential equation of balance of the accelerations of the material point has imaginary roots. This leads to the following contradiction: the coordinate of the material point is both an exponential function and a trigonometric function.

II. In the case of oscillations of the mathematical pendulum, the linear differential equation of harmonic oscillations of the material point suspended on the inextensible thread represents a mathematical description of the angular displacement of the inextensible thread in the Cartesian coordinate system. This equation is a mathematical consequence of the standard differential equation of the rotational motion dynamics and contains the following gross methodological errors:

(a) the differential equation of motion of the material point suspended on the inextensible thread does not satisfy the dialectical principle of the unity of the qualitative and quantitative determinacy of physical quantities (i.e., the physical quantity of rate of change of the angular momentum (moment of momentum) and the physical quantity of moment of the acting force). This equation expresses the condition of balance of the rate of change of the angular momentum (moment of momentum) and the moment of the acting force. Gross error is that the left and right sides of the balance equation have no identical qualitative determinacy: the left side of the balance equation is the rate of change of the angular momentum (moment of momentum), and the right side of the balance equation is the moment of the acting force.

(b) the sum of the rate of change of the angular momentum and the moment of the acting force is equal to zero in the balance equation. This means that the sum of the numerical values of the rate of change of the angular momentum and the moment of the acting force is equal to zero. Consequently, the numerical values of the rate of change of the angular momentum and the moment of the acting force are equal to zero in the region of neutral real numbers. This means that the balance equation is incorrect.

(c) the mathematical operation of division of the equation of the balance of the rate of change of the angular momentum and the moment of the acting force by the mass of the material point and the square of the thread length results in the equation of balance of the angular accelerations. In this case, the mathematical operation results in the term "frequency" ("squared frequency"). But the quantity of the angular acceleration does not determine the frequency of the periodic motion;

(d) the linear differential equation of balance of the angular accelerations is analogous to the linear differential equation of balance of the accelerations of the material point suspended on the spring. Therefore, the solution of the linear differential equation of balance of the angular accelerations has imaginary roots and leads to the following contradiction: the angle of displacement of the pendulum from the equilibrium position is both an exponential function and a trigonometric function.

REFERENCES

[1] E. Madelung. (1957). Die Mathematischen Hilfsmittel Des Physikers. Berlin, Gottingen, Heidelberg: Springer-Verlag.

[2] D.J. Struik. (1987). A Concise. History of Mathematics. New York: Dover Publications.

[3] C.B. Boyer. (1991). A history of mathematics" (Second ed.). John Wiley & Sons, Inc. ISBN 0-471-54397-7.

[4] M. Hazewinkel (2000). Encyclopedia of Mathematics. Kluwer Academic Publishers.

[5] R. Nagel (2002). (ed.). Encyclopedia of Science. (2nd Ed.). The Gale Group.

[6] W.B. Ewald. (2008). From Kant to Hilbert: A source book in the foundations of mathematics. Oxford University Press, US. ISBN 0-19-850535-3.

[7] Robert M. Besançon (1990). The Encyclopedia of Physics. (eBook ISBN978-1-4615-6902-2. Springer, New York.

[8] George L. Trigg (2004). Encyclopedia of Applied Physics. John Wiley. ISBN: 978-3-527-40478-0.

[9] Rita G. Lerner, George L. Trigg. (2005). Encyclopedia of physics. (Edition: 3rd ed. completely rev.). Wiley-VCH, Weinheim.

[10] Mary L. Boas. (2006). Mathematical Methods in the Physical Sciences. (3rd ed.), Hoboken, [NJ.]: John Wiley & Sons. ISBN 978-0-471-19826-0.

[11] R.P. Feynman, R.B. Leighton, M. Sands, (1963). The Feynman Lectures on Physics. Vol. 1 – Mechanics. ISBN 978-0-201-02116-5.

[12] C. Kittel, W.D. Knignt, A. Ruderman. (1964). Berkeley Physics Course. V. 1 – Mechanics. McGraw-Hill Book Company.

[13] L.D. Landau, E.M. Lifshitz. (1972). Course of Theoretical Physics. Vol. 1 – Mechanics. Franklin Book Company. ISBN 0-08-016739-X.

[14] D. Kleppner, R.J. Kolenkow. (1973). An Introduction to Mechanics". McGraw-Hill. ISBN 0-07-035048-5.

[15] M. Alonso, J. Finn. (1992). Fundamental University Physics. Addison-Wesley.

[16] H. Goldstein, P.P. Charles, L.S. John. (2002). Classical Mechanics. (3rd ed.). Addison Wesley. ISBN 0-201-65702-3.

[17] T.Z. Kalanov. (2017). On the correct formulation of the starting point of classical mechanics. Advances in Physics Theories and Applications, 64, 27-46.

[18] T.Z. Kalanov. (2017). On the correct formulation of the starting point of classical mechanics. International Journal of Advanced Research in Physical Science. 4(6), 1-22.

[19] T.Z. Kalanov. (2017). On the correct formulation of the starting point of classical mechanics. International educational scientific research journal. 3(6), 56-73.

[20] T.Z. Kalanov (2010). On a new analysis of the foundations of classical mechanics. I. Dynamics. Bulletin of the Amer. Phys. Soc. (April Meeting), 55(1).

[21] T.Z. Kalanov (2011). Critical analysis of the foundations of differential and integral calculus. MCMS (Ada Lovelace Publications), 34-40.

[22] T.Z. Kalanov (2011). Logical analysis of the foundations of differential and integral calculus. Indian Journal of Science and Technology, 4(12).

[23]] T.Z. Kalanov (2011). Logical analysis of the foundations of differential and integral calculus. Bulletin of Pure and Applied Sciences, 30E (2), 327-334.

[24] T.Z. Kalanov (2012). Critical analysis of the foundations of differential and integral calculus. International Journal of Science and Technology, 1(2), 80-84.

[25] T.Z. Kalanov (2012). On rationalization of the foundations of differential calculus. Bulletin of Pure and Applied Sciences, Vol. 31E (1), 1-7.

[26] T.Z. Kalanov (2012). On logical error underlying classical mechanics. Bulletin of the Amer. Phys. Soc., (April Meeting), 57(3).

[27] T.Z. Kalanov (2013). Critical analysis of the mathematical formalism of theoretical physics. I. Foundations of differential and integral calculus". Bulletin of the Amer. Phys. Soc., (April Meeting), 58(4).

[28] T.Z. Kalanov (2013). On the logical analysis of the foundations of vector calculus. International Journal of Scientific Knowledge. Computing and Information Technology, 3(2), 25-30.

[29] T.Z. Kalanov (2013). On the logical analysis of the foundations of vector calculus. International Journal of Multidisciplinary Academic Research, 1(2).

[30] T.Z. Kalanov (2013). On the logical analysis of the foundations of vector calculus. Journal of Computer and Mathematical Sciences, 4(4), 202-321.

[31] T.Z. Kalanov (2013). On the logical analysis of the foundations of vector calculus. Journal of Research in Electrical and Electronics Engineering (ISTP-JREEE), (ISSN: 2321-2667), 2(5), 1-5.

[32] T.Z. Kalanov (2013). On the logical analysis of the foundations of vector calculus. Research Desk, (ISSN: 2319-7315), 2(3), 249-259.

[33] T.Z. Kalanov (2013). The foundations of vector calculus: The logical error in

mathematics and theoretical physics. Unique Journal of Educational Research, 1(4), 054-059.

[34] T.Z. Kalanov (2013). On the logical analysis of the foundations of vector calculus. Aryabhatta Journal of Mathematics & Informatics, (ISSN: 0975-7139), 5(2), 227-234.

[35] T.Z. Kalanov (2013). Critical analysis of the mathematical formalism of theoretical physics. II. Foundations of vector calculus". Unique Journal of Engineering and Advanced Sciences (UJEAS, www.ujconline.net), 1(1).

[36] T.Z. Kalanov (2013). Critical analysis of the mathematical formalism of theoretical physics. II. Foundations of vector calculus. Bulletin of Pure and Applied Sciences, 32E (2), 121-130.

[37] T.Z. Kalanov (2014). Critical analysis of the mathematical formalism of theoretical physics. II. Foundations of vector calculus. Bulletin of the Amer. Phys. Soc., (April Meeting), 59(5).

[38] T.Z. Kalanov (2014). On the system analysis of the foundations of trigonometry. Journal of Physics & Astronomy, (www.mehtapress.com), 3(1).

[39] T.Z. Kalanov (2014). On the system analysis of the foundations of trigonometry. International Journal of Informative & Futuristic Research, (IJIFR, www.ijifr.com), 1(1), 6-27.

[40] T.Z. Kalanov (2014). On the system analysis of the foundations of trigonometry. International Journal of Science Inventions Today, (IJSIT, www.ijsit.com), 3(2), 119-147.

[41] T.Z. Kalanov (2014). On the system analysis of the foundations of trigonometry. Pure and Applied Mathematics Journal, 3(2), 26-39.

[42] T.Z. Kalanov (2014). On the system analysis of the foundations of trigonometry. Bulletin of Pure and Applied Sciences, 33E (1), 1-27.

[43] T.Z. Kalanov (2014). Critical analysis of the foundations of the theory of negative number. International Journal of Informative & Futuristic Research (IJIFR, www.ijifr.com), 2(4), 1132-1143.

[44] T.Z. Kalanov (2015). Critical analysis of the mathematical formalism of theoretical physics. IV. Foundations of trigonometry. Bulletin of the Amer. Phys. Soc., (April Meeting), 60(4).

[45] T.Z. Kalanov (2015). Critical analysis of the mathematical formalism of theoretical physics. V. Foundations of the theory of negative numbers. Bulletin of the Amer. Phys. Soc., (April Meeting), 60(4).

[46] T.Z. Kalanov (2015). Critical analysis of the foundations of the theory of negative numbers. International Journal of Current Research in Science and Technology, 1(2), 1-12.

[47] T.Z. Kalanov (2015). Critical analysis of the foundations of the theory of negative numbers. Aryabhatta Journal of Mathematics & Informatics, 7(1), 3-12.

[48] T.Z. Kalanov (2015). On the formal–logical analysis of the foundations of mathematics applied to problems in physics. Aryabhatta Journal of Mathematics & Informatics, 7(1), 1-2.

[49] T.Z. Kalanov (2016). On the formal-logical analysis of the foundations of mathematics applied to problems in physics. Bulletin of the Amer. Phys. Soc., (April Meeting).

[50] T.Z. Kalanov (2016). Critical analysis of the foundations of pure mathematics. Mathematics and Statistics (CRESCO, http://crescopublications.org), 2(1), 2-14.

[51] T.Z. Kalanov (2016). Critical analysis of the foundations of pure mathematics. International Journal for Research in Mathematics and Mathematical Sciences, 2(2), 15-33.

[52] T.Z. Kalanov (2016). Critical analysis of the foundations of pure mathematics. Aryabhatta Journal of Mathematics & Informatics, 8(1), 1-14 (Article Number: MSOA-2-005).

[53] T.Z. Kalanov (2016). Critical Analysis of the Foundations of Pure Mathematics. Philosophy of Mathematics Education Journal, ISSN 1465-2978 (Online). Editor: Paul Ernest), No. 30 (October 2016).

[54] T.Z. Kalanov (2017). On the formal–logical analysis of the foundations of mathematics applied to problems in physics. Asian Journal of Fuzzy and Applied Mathematics, 5(2), 48-49.

[55] T.Z. Kalanov (2017). The formal-logical analysis of the foundation of set theory.

Bulletin of Pure and Applied Sciences, 36E(2), 329 -343.

[56] T.Z. Kalanov (2017). The critical analysis of the foundations of mathematics. Mathematics: The Art of Scientific Delusion. LAP LAMBERT Academic Publishing (2017-12-05). ISBN-10: 620208099X.

[57] T.Z. Kalanov (2018). On the correct formulation of the starting point of classical mechanics. Physics & Astronomy (International Journal). 2(2), 79-92.

[58] T.Z. Kalanov (2018). The formal-logical analysis of the foundation of set theory. Scientific Review, 4(6), 53-63.

[59] T.Z. Kalanov (2019). Hubble Law, Doppler Effect and the Model of "Hot" Universe: Errors in Cosmology". Open Access Journal of Physics (USA), 3(2), 1-16.

[60] T.Z. Kalanov (2019). Definition of Derivative Function: Logical Error in Mathematics. MathLAB Journal, 3, 128-135.

[61] T.Z. Kalanov (2019). Definition of Derivative Function: Logical Error in Mathematics. Academic Journal of Applied Mathematical Sciences, 5(8), 124-129.

[62] T.Z. Kalanov (2019). Definition of Derivative Function: Logical Error in Mathematics. Aryabhatta Journal of Mathematics & Informatics, 11(2), 173-180.

[63] T.Z. Kalanov (2019). Vector Calculus and Maxwell's Equations: Logic Errors in Mathematics and Electrodynamics. Open Access Journal of Physics, 3(4), 9-26.

[64] T.Z. Kalano (2019). Vector Calculus and Maxwell's Equations: Logic Errors in Mathematics and Electrodynamics. Sumerianz Journal of Scientific Research, 2(11), 133-149.

[65] T.Z. Kalanov (2020). Definition of work: Unsolved Problem in Classical Mechanics. Bulletin of Pure and Applied Sciences (Section D –Physics), 39D (1), 137-148.

[66] T.Z. Kalanov (2020). Definition of work: Unsolved Problem in Classical Mechanics. Open Access Journal of Physics, 4(1), 29-39.

[67] T.Z. Kalanov (2021). Formal-logical analysis of the starting point of mathematical logic. Aryabhatta Journal of Mathematics & Informatics, 13(1), 01-14.

[68] T.Z. Kalanov (2022). On fundamental errors in trigonometry. Bulletin of Pure and Applied Sciences (Section - E - Mathematics & Statistics), 41E(1), 16-33.

[69] T.Z. Kalanov (2022). Theory of complex numbers: gross error in mathematics and physics". Bulletin of Pure and Applied Sciences (Section - E - Mathematics & Statistics), 41E(1), 61-68.

****

Bulletin of Pure and Applied Science
Physics, Vol.41D No.2,
July-December 2022 P.111-115
Short Communication

Print version ISSN 0970 6569
Online version ISSN 2320 3218
DOI: 10.5958/2320-3218.2022.00018.5
Available online at www.bpasjournals.com

A Short Communication on Progress and Problems of ITER Fusion Project

[1]Victor Christianto*, [2]Florentin Smarandache

Author's Affiliations:
[1]Malang Institute of Agriculture, Indonesia. Halton Arp Institute, affiliated to International Mariinskaya Academy, St. Petersburg
E-mail: victorchristianto@gmail.com
[2]Dept. Mathematics & Sciences, University of New Mexico, Gallup, USA.
E-mail: smarand@unm.edu

***Corresponding author:**
Victor Christianto
Malang Institute of Agriculture, Indonesia. Halton Arp Institute, affiliated to International Mariinskaya Academy, St. Petersburg
E-mail: victorchristianto@gmail.com

Received on 22.04.2022
Revised on 20.08.2022
Accepted on 30.10.2022
Published on 15.12.2022

ABSTRACT

In recent years, it becomes clear that ITER project in France, as one of the largest experimental fusion reactors underway, is far away from achieving net energy production. In this review article, we presented a short communication this week with Robert Neil Boyd, a senior physicist who happens to have his own working design of fusion reactor in the past. We hope that this transcript of our communication with him (as per 15-17th Nov. 2021) may be found useful for younger scientists.

KEYWORDS ITER Fusion project, Hydrogen-based economy

How to cite this article: Christianto V., Smarandache F. (2022). A Short Communication on Progress and Problems of ITER Fusion Project. *Bulletin of Pure and Applied Sciences- Physics,* 41D (2), 111-115.

INTRODUCTION

As we know, many people and scientists believe that fusion energy is our hope for clean source of energy in the future. But whether there is real ground for such a hope, or it is just another techno-fantasy, we shall find out. In recent years, it becomes clear that ITER project in France, as one of the largest experimental fusion reactors underway, is far away from achieving net energy production. According to W. Wayt Gibbs: "Major fusion projects such as ITER in France and NIF in the U.S. have consumed billions of dollars and are nowhere close to generating enough energy to even sustain their own operation much less create commercial power. Smaller, simpler designs are now being explored, in some cases by private companies. Preliminary results have raised hopes that there might be more practical, less expensive paths to fusion power plants."[1] In this article, we presented a short communication this week with

Robert Neil Boyd, PhD, a senior physicist who happens to have his own working design of fusion reactor in the past. He is now associated with Princeton Biotechnology Corp., New Jersey. We hope that this transcript of our communication with him (as per 15-17th Nov. 2021) may be found useful for younger scientists.

RECENT PROGRESS OF ITER PROJECT

As the story goes, for future power generation, fusion reactors have unique benefits. Unlike conventional nuclear reactors, fusion reactors cannot melt down and do not produce radioactive material that can be weaponized or that requires special disposal. Safety and environmental concerns with fusion reactors are minimal, and the deuterium and lithium required for fuel can be extracted from seawater. A fusion power plant can, in aspiration, be built at a competitive capital cost and have virtually no input cost beyond operating expenses.[2] For readers not quite familiar with the progress of ITER, allow us to quote W. Wayt Gibbs again: "Right now the pragmatists have people's attention because the academics have hit practical dead ends: enormous reactors that have clarified some fusion science but are not on track to pump electricity into the grid by midcentury. One example is the National Ignition Facility (NIF) at Lawrence Livermore National Laboratory. "NIF fires just a few hundred shots a year," Binderbauer says in his Austrian lilt. A power plant would have to fire tens of thousands of times a day. Two years ago Livermore pulled the plug on designing a prototype power plant. The second discouraging example is ITER, a 10-story-high machine under construction in France by a consortium of nations. It will rely on giant superconducting magnets to control a plasma burning at roughly 150 million degrees C for minutes at a time. Even if it succeeds, ITER will make no electricity."[1]

NEIL BOYD'S REMARK AND VC'S RESPONSE

Note: RNB stands for Robert Neil Boyd, and VC stands for one of these authors. RNB: "Similar and related events are seen in this Aureon-produced video: https://vimeo.com/453152469. The striations which arise from the plasma discharge are due to quantization of the electric field. Here is an example of a larger Natural version of the instrumented results of the Safire experiments, as observed in by astrophysical instruments, such as this Hubble telescope image of the "Cat's Eye" Nebula. The point of this is that if one looks closely at the full moon, which has been surrounded by a rainbow ring for more than 7 consecutive years, you can see similar circular radial behaviors of light as it arises from the surface of the moon. However, the electric field caused directly by solar and stellar radiation is not sufficiently large to cause such layered radiation sources.

...By the way, "*free electricity*" was discovered and proved, long ago, by Faraday during one of his experiments regarding electric and magnetic field behaviors. Faraday's result got stopped and it was never published in any of the journals of those days. But Faraday still recorded it and kept it among his personal effects, for posterity." VC: "Thank you. Thanks also for the story of Michael Faraday." RNB: "Plasmas exhibit "double layers" which form *Birkeland currents*, plasma "cells" and multiple boundary layers, due to charge separation, exactly as we can see in the Aureon video. This happens when all the electrons go to one side of the given volume, while the positive charges (typically protons) are separated away from the electrons at another wall in the given volume, usually because protons and positively charged atomic nuclei are much more massive than electrons, so they have a lot more inertia and resistance to moving, and tend not to move very much or very fast. The force developed between the positive and the negative portions are measurably huge, and eventually the positive and negative charges will meet and neutralize, if nothing about the existing configuration changes. Eventually the plus charges will start moving slowly towards the negatively charge volume. Or the electrons will flash over to where the positive charges are. Many energetic events can happen, associated with that kind of behavior. The Aureon results demonstrate some of the above discussion. I started my research in plasma physics back in 1966 and continued until the late 1990s. I designed the third energy-

gaining thermonuclear fusion reactor in history. It was built and tested by DoE and I was notified of the success of the design back in 1989. They did an in-house video interview with me, but very few have any awareness of it aside from me. Bogdan Maglich designed and tested the second energy-gaining fusion reactor. I corresponded personally with Maglich for a while. He was really frustrated because nobody would fund him to build a power plant using his fusion reactor design, which had been publicly proven. Philo Farnsworth, who designed most of the components of the old tube-style television, made the first energy-gaining fusion reactor, based on a "multipactor tube", a very unusual tube he had developed during his TV researches. In 1965 his "Fusor Mark IV" was producing 50 giga-neutrons per second, due to huge numbers of fusion reactions occurring in a fusion confinement volume the size of a grapefruit. The 4th demonstrated fusion reactor was designed and constructed by a group of college kids in someone's basement. They got a patent of the device. The patent was sold to Chrysler-Daimler and never heard from again. I was in touch with them for a while too. I guess they got some good income from selling their patent, but they stopped talking to me soon after the patent issued. So where are any of these functional fusion reactors?" VC: "Thank you for your story, and also Maglich and Farnsworth's designs for real fusion reactor. I am skeptical on ITER project. I heard that only a Japanese team wrote honestly that the real purpose of ITER project is to improve gain function, not to obtain net energy production."

OTHER POTENTIAL CREATIVE ENERGY BREAKTHROUGH - TOWARD HYDROGEN AGE

Allow us to make a quick note about the potential for breakthrough energy towards a hydrogen-based economy (cf. Capra, 2009), as follows: There are indeed some leaders of technology companies, such as Elon Musk, who are skeptical of the fuel cell, and call it: "*fool sell*." It may be that fuel cell technology is not economical in today's context, but let us briefly mention that since the 1980s-1990s, efficient water electrolysis technology has been discovered by Dr. Andrija Puharich, and what's interesting is that a few months after his electrolysis patent was accepted by the US patent office, he seems to have inspired Stanley Meyer's experiments on his known *water-fueled car design* (and a more efficient electrolysis process).

Recently, there are various debates in online channels on Indonesian version of the alternative fuel research for the motorbikes, which has become one of the hot topics, from the findings of H. Aryanto Misel from Lemahabang, Cirebon (Indonesia), which he calls Nikuba (according to him from the Javanese expression, "*niku banyu*"; trans. it's water). There has been controversy over these findings, and this is quite reasonable, considering that the electrolysis method has long been known in the field of chemistry.

What is interesting is that standard textbooks state that the electrolysis process is not efficient, because it takes a lot of energy to separate H_2O into H-H-O. In addition, among mechanical engineers, one other issue is corrosion that must be prevented. Maybe that's why the Nikuba electrolysis design, practically designed by Aryanto, Misel uses stainless steel. In addition, to achieve an efficient electrolysis process, it seems that he did not use the usual catalysts such as NaCl etc., but he used a special homemade catalyst. This is an interesting innovation, compared to the available information regarding the findings of the electrolysis process by Dr Andrija Puharich, around the 80s, which opens up the possibility of efficient processes, including: (a) ordinary electrolysis, (b) pulsed electrolysis, (c) gated-pulsed electrolysis with a type of source wave called a waveform. The fourth innovative breakthrough made by Stan Meyer is to add a fourth alternative method to achieve an efficient electrolysis process, namely: (d) resonance electrolysis. From discussions among others in cyberspace, there is information that perhaps what is meant by resonance here is not the resonant frequency of water molecules, which are on the order of MHz, but ordinary electric resonance in the range of 280 Hz or about 495 Hz.

Another interesting piece of information is that Stan Meyer triggered the resonance using a *bifilar coil source*, which can be traced back to Nikola Tesla's inventions. H. Aryanto's findings can be considered as the fifth innovation for an efficient electrolysis process because it uses a catalyst, so we can call it in more scientific terms: "catalytic-aided electrolysis generator." Of course it will be interesting, if the research can be continued further by developing alternative combinations between the catalytic method coupled with the bifilar coil / resonance: who knows maybe we will achieve a dramatic increase in efficiency, above 100% of the performance of current water electrolysis machines. Thus presumably the process of scientific discovery can continue. What is interesting is not only the concept of resonance which has long been known in physics, but also bifilar coil. Besides bifilar coil, there is also a so-called *Rodin coil*, which may be rarely known (cf. Boyd & Smarandache, 2022) [12]. Rodin coil has the potential not only to have a good effect on health (Schumann resonance), but can also be engineered to create a magnetic levitation machine. These things would be interesting if there are researchers who are interested in conducting experiments on aerial vehicles for the future.

Summarizing, in addition to developing a transportation ecosystem based on electrical energy (EV) as many countries begin to develop, it may also be time for us to prepare for the next stage of transformation: i.e. towards hydrogen energy age; cf. Capra, 2009 [13]. It is worth to mention here, that around two decades ago, Prof Pm. Kanarev from Kuban State University has proved that hydrogen economy era has come, especially with his finding of nuclear water electrolysis (Kanarev & Mizuno, 2001; Mizuno, 2001) [9,8].

DISCUSSIONS

As we pointed above, the Japanese ITER team is the only participating group to clearly and transparently state the power capability of ITER: "Will ITER make more energy than it consumes? . . . ITER is about equivalent to a zero (net) power reactor, when the plasma is burning."[4] Other than that, the problem is more accute, not only that Tokamak-based fusion includes complicated MHD problems which are highly nonlinear; cf. ref. [7], but also confusion in messages to public. As S. Krivit wrote: "Members of your fusion science community promoted ITER with language that made it appear to laypersons as designed for Q-engineering=10, rather than Q-fusion=10. They did this for three decades. Nobody said a word."[6] At this point, some readers may ask:"So, what are our choices for future energy?" We can cite T. Linden here, that there are: "relatively small and compact devices compared to tokamaks decreases the costs and building time of the reactors and this has allowed some private companies to enter the field, like EMC2, General Fusion, Helion Energy, Lockheed Martin and LPP Fusion."[3] Alternatively, one may also consider Prof. Ph. M. Kanarev's method of water electrolysis reactor. [10-11]

Last but not least, we can also argue that actually fusion process can happen even from classical electromagnetic considerations, see our paper at JCMNS, 2017 [8]. In other words, we may expect that fusion process can happen at relatively low temperature, such as from biological transmutation (see J. Biberian's papers in JCMNS).

CONCLUDING REMARKS

In this paper, we began by citing from W. Wayt Gibbs, that actually our hope for plentiful energy based on fusion, is not based on actual progress of present experimental reactors. But as Linden, Gibbs, and Kanarev wrote, there are actually more hope on the so-called *'fusion underground*," or small fusion ex periments carried out by independent scientists. [1] We recall comment by a senior scientist at Russia, that there is a different culture of science between Russia and USA scientists; is that scientist in Russia is allowed to do small experiments at any type of inquiry that they like in their basement or houses more or less freely. Such a culture seems quite lacking, but it seems CF report by Pons-Fleischmann around 80s began to inspire other physicists, to do small basement-scale experiments at their own. Then

such a small-scale experiment can be scaled up later on. All in all, for the time being, renewable energy sources (such as: WWS, geothermal, biofuels, etc.) may be expected to meet the world energy demands, at least partially, until that energy abundance days come. See for instance Mark Z. Jacobson's book [16]. Also ref. [15].

And in latter part, we discuss other potential energy breakthroughts, especially if we consider seriously going toward hydrogen age, cf. Pm. Kanarev (2001, 2002), F. Capra (2009).

Acknowledgement

These authors wish to express sincere gratitude to Robert N. Boyd, for contribution and dialogue in various subjects according to his deep experiences in experimental physics such as a working design of fusion reactor. Many thanks also go to our colleagues, Volodymyr Krasnoholovets and Yunita Umniyati, especially for contributing in a joint paper at JCMNS (2017).

REFERENCES

[1] W. Wayt Gibbs (2016). *Fusion underground*, Scientific American.

[2] D. Kauffman (2017). *The uncertain future of fusion energy*, http://energypost.eu/the-uncertain-future-of-fusion-energy.

[3] T. Linden (2015). *CERN Colloquium 26th of March 2015.*

[4] New Energy Times (2017). *Eurofusions role in the ITER power deception.*

[5] http://news.newenergytimes.net/2017/11/07/eurofusions-role-in-

[6] S. Krivitt (2017.) *The ITER 500 megawatt power amplification myth* url:http://news.newenergytimes.net/2017/10/06/the-iter-power- amplification- myth/

[7] R.D. Hazeltine J.D. Meiss (1992). *Plasma confinement* Basic Books, USA.

[8] V. Christianto, Y. Umniyati, V. Krasnoholovets (2017). On plausible role of classical electromagnetic theory and submicroscopic physics to under- stand and enhance low energy nuclear reaction: A preliminary review. *Journal of Condensed Matter Nuclear Science*, 2017, 22, pp. 27–34. http://www.iscmns.org

[9] T. Mizuno (2000). Experimental Confirmation of the Nuclear Reaction at Low Energy Caused by Electrolysis in the Electrolyte. *Proceedings for the Symposium on Advanced Research in Energy Technology 2000*, Hokkaido University, March 15, 16 and 17, 2000, pp. 95-106.

[10] Ph. M. Kanarev (2001). Water as a new energy source. *Weinfelden 2001 Lecture. New hydrogen technologies and space drive*, June 2001.

[11] Ph. M. Kanarev & T. Mizuno (2002). *Cold fusion by plasma electrolysis of water*. Published 20-12-2002. url: https://www.researchgate.net/publication/237276063_COLD_FUSION_BY_PLASMA_ELECTROLYSIS_OF_WATER

[12] Robert N. Boyd & F. Smarandache (2022). Remark on Project Greenglow and Rodin coil: Letter to Editor. *J. Cosmology, Filaments and Astrobiology* Vol. 1 Issue 2, July 2022.

[13] Fritjof Capra (2009). Hidden connections. Kata pengantar: Husain Heriyanto. Cet. III. Yogyakarta: Penerbit Jalasutra.

[14] Edward de Bono (2018). *Conflicts: a better way to resolve them.* London: Vermilion.

[15] Mark Z. Jacobson (2020). *100 percent Clean, Renewable Energy and Storage for Everything* 1st ed. Cambridge: Cambridge University Press. (Note: online course at Stanford Univ. Based on this book: CEE 176B/276B.) url: https://web.stanford.edu/group/efmh/jacobson/WWSBook/WWSBook.html

****

Instructions to Authors

Submission to the journal must comply with the Guidelines for Authors.

Non-compliant submission will be returned to the author for correction.

Submission of article

You can submit your article through mail across our mail id.

E-mail: bpaspublications@gmail.com

To access the online submission system and for the most up-to-date version of the Guide for Authors please visit:

http://www.bpasjournals.com

For online Submission go through link
http://www.bpasjournals.com/article-submit.php

Alternatively, please contact the Journal's Editorial Office for further assistance.

Editorial Manager
BPAS PUBLICATIONS
115-RPS- DDA Flat, Mansarover Park,
Shahdara, Delhi-110032, India
Mob: +91- 9212200909
E-mail: bpaspublications@gmail.com
Website: www.bpasjournals.com

Bulletin of Pure and Applied Sciences
Section-D-Physics

Library Recommendation Form
If you would like to recommend this journal to your library, simply complete the form below and return it to us. Please type or print the information clearly. We will forward a sample copy to your library, along with this recommendation card.

Please send a sample copy to:
Name of Librarian
Name of Library
Address of Library

Recommended by:
Your Name/ Title
Department
Address

Dear Librarian,
I would like to recommend that your library subscribe to the **Bulletin of Pure and Applied Sciences Section-D-Physics**. I believe the major future uses of the journal for your library would provide:

1. useful information for members of my specialty.
2. an excellent research aid.
3. an invaluable student resource.

I have a personal subscription and understand and appreciate the value an institutional subscription would mean to our staff.

Should the journal you're reading right now be a part of your University or institution's library? To have a free sample sent to your librarian, simply fill out and mail this today!

Stock Manager
BPAS PUBLICATIONS
115-RPS- DDA Flat, Mansarover Park,
Shahdara, Delhi-110032, India
Mob: +91- 9212200909
Email: editorbulletin8@gmail.com, bpaspublications@gmail.com
Website: www.bpasjournals.com

Subscription Information

Institutional (1 year) INR3200/USD100

Here is payment instruction for your reference.

For Bank transactions: (RTGS, IMPS and NEFT transactions)
Complete Bank Account No. 916020035086217
Beneficiary Name: BPAS PUBLICATIONS
Bank & Branch Name: AXIS BANK Ltd. Laxmi Nagar, Delhi-110092
MICR Code: 110211163
SWIFT Code: AXISINBB166
IFSC Code: UTIB0002685 (used for RTGS and NEFT transactions)

For Bank Cheque/ Demand Draft:
Please send the US dollar check from outside India and INR check from India made
Payable to '**BPAS PUBLICATIONS'** at **Delhi**.

Online Payment Method (By Payment Gateway):
https://online.bpasjournals.com/payment/

**Please kindly add bank charge at your side if you pay by check or wire transfer.
Payment, orders and all correspondences should be sent to;

Mail all orders to
Subscription and Marketing Manager
BPAS PUBLICATIONS
115-RPS- DDA Flat, Mansarover Park,
Shahdara, Delhi-110032, India
Mob: +91- 9212200909
E-mail:
editorbulletin8@gmail.com
bpaspublications@gmail.com
bpassubscriptions@gmail.com
Website:
www.bpasjournals.com

Subscription Form

I want to renew/subscribe international class journal
"Bulletin of Pure and Applied Sciences Section-D-Physics"
of BPAS PUBLICATIONS.

Subscription Rates:
• Institutional: INR3200/USD100
Name and complete address (in capitals):
……
Payment methods:
Cheque/DD:
Please send the US dollar check from outside India and INR check from India made:
Payable to '**BPAS PUBLICATIONS'**.
Drawn on Delhi branch
Credit Card:
We accept Visa or MasterCard.
Wire transfer: (RTGS, IMPS and NEFT transactions)
Complete Bank Account No. 916020035086217
Beneficiary Name: BPAS PUBLICATIONS
Bank & Branch Name: AXIS BANK Ltd. Laxmi Nagar, Delhi-110092
MICR Code: 110211163
IFSC Code: UTIB0002685 (used for RTGS and NEFT transactions)

1. Advance payment required by Demand Draft payable to BPAS PUBLICATIONS payable at Delhi.
2. Cancellation not allowed except for duplicate payment.
3. Agents allowed 10% discount.
4. Claim must be made within six months from issue date.

Mail all orders to
Subscription and Marketing Manager
BPAS PUBLICATIONS
115-RPS- DDA Flat, Mansarover Park,
Shahdara, Delhi-110032, India
Mob: +91- 9212200909
E-mail: editorbulletin8@gmail.com, bpaspublications@gmail.com
Website: www.bpasjournals.com

ANNUAL SUBSCRIPTION FORM 2023

(Online subscription order form available at: https://online.bpasjournals.com/subscription-order-form/)

To,
Managing Editor,
BPAS Publications
115-RPS- DDA Flat, Mansarover Park,
Shahdara, Delhi-110032, India

Subject: Annual Subscription request for January-December 2023

Dear Sir/Madam

With reference to your valuable Research Journals, we invite your kind attention on the following ticked (√) Journals, Please arrange bill in duplicate /triplicate towards the annual subscription for the following ticked (√) Research Journals for **January – December 2023 (complete volume).**

A. SUBSCRIPTION CHARGES

Select Journal	Name of the Journal	Vol.	Freq.	Annual Subscriptions Charges		
				India (INR)		Foreign (USD)
				Print	Online	Print/Online
	Bulletin of Pure and Applied Sciences *Section-A-Zoology* **pISSN-0970-0765, eISSN 2320-3188**	**42A**	**Half-yearly**	**3200**	**2000 + 18% GST**	**100**
	Bulletin of Pure and Applied Sciences *Section-B-Botany* **pISSN-0970-4612, eISSN 2320-3196**	**42B**	**Half-yearly**	**3200**	**2000 + 18% GST**	**100**
	Bulletin of Pure and Applied Sciences *Section-C-Chemistry* **pISSN-0970-4620, eISSN 2320-320X**	**42C**	**Half-yearly**	**3200**	**2000 + 18% GST**	**100**
	Bulletin of Pure and Applied Sciences *Section-D-Physics* **pISSN-0970-6569, eISSN 2320-3218**	**42D**	**Half-yearly**	**3200**	**2000 + 18% GST**	**100**
	Bulletin of Pure and Applied Sciences *Section-E-Math & Stat.* **pISSN-0970-6577, eISSN 2320-3226**	**42E**	**Half-yearly**	**3200**	**2000 + 18% GST**	**100**
	Bulletin of Pure and Applied Sciences *Section-F-Geology* **pISSN-0970-4639, eISSN 2320-3234**	**42F**	**Half-yearly**	**3200**	**2000 + 18% GST**	**100**
	Bio-Science Research Bulletin *(Multidisciplinary Journal of Biological and Medical Sciences)* **pISSN-0970-0889, eISSN 2320-3161**	**39**	**Half-yearly**	**3200**	**2000 + 18% GST**	**100**
	Library Progress International *(Library & Information Science)* **pISSN-0970-1052, eISSN 2320-317X**	**43**	**Half-yearly**	**3200**	**2000 + 18% GST**	**100**

B. SUBSCRIPTION INFORMATIONS

SUBSCRIBER TYPE: (Check one) Library / Institution / Individual Date:.....

Name/Institution:.....

Full Address:.....

City:..... **Pin / Zip code:**.....

State:.....**Country:**.....

Phone (with STD/ISD code):.....

E-mail:.....

PAYMENT OPTIONS (Check one)

Cheque /DD is enclosed (Payable to "***BPAS Publications,*** **Delhi**")

Amount:.....**Cheque / DD No. :**..... **Dated:**.....

Drawn on Bank:.....

Terms & Conditions:

- Agency Discount applicable **10%** for Subscription Agent, there is not any discount for individual Subscription.
- Online Journals also include **18% GST** charges.
- All deliveries to be made by **Speed Post** only.
- Limited back volumes are available at the same rates.
- All legal disputes subject to Delhi jurisdiction only.
- Cancellations are not accepted orders once processed.
- No claims will be entertained if not reported within 6 months of the publishing date.
- Subscription period is accepted on calendar year basis (i.e. Jan to Dec). However orders may be placed any time throughout the year

For RTGS, IMPS and NEFT transactions:
Complete Bank Account No. 916020035086217
Beneficiary Name: BPAS PUBLICATIONS
Bank & Branch Name: AXIS BANK Ltd. Laxmi Nagar, Delhi-92
IFSC Code: UTIB0002685, MICR Code: 110211163
For Bank Cheque/Demand Draft:
Make payable to 'BPAS PUBLICATIONS' at Delhi.
For Online Payment Method:
https://online.bpasjournals.com/payment/

(Seal & Signature of the subscriber)
Date:..... (DD/MM/YYYY)

Please send complete Order Form with payment to:

BPAS PUBLICATIONS
115-RPS- DDA Flat, Mansarover Park, Shahdara, Delhi-110032, India
Mob:+91- 9212200909,
Email : editorbulletin8@gmail.com, bpaspublications@gmail.com **website :** www.bpasjournals.com

EXCELLENT Research Solutions

THE EXCELLENT Solutions

Research and Scientific Publication Support Services

(For Authors of Research, Scientific and Academic Documents)

THE EXCELLENT Solutions

- Editing & Proofreading
- Plagiarism Checking
- Plagiarism Correction
- English Translations
- Research Data Support
- Publication Support
- Journal/ Book Design and Layout
- Graphic Design
- Publish Conference Proceeding / Special Issue
- Publish Article, Dissertation and Thesis

EXCELLENT Research Solutions

- Article Writing
- Synopsis Writing
- Ph.d Thesis Writing
- M.Phil Thesis Writing
- Dissertation Writing
- Data Analysis
- Statistical Service
- Questionnaire Design
- Reference style Corrections

Editing & Proofreading Services for all Research, Scientific and Academic Documents such as Journal Articles, Scientific Papers, Journals, Books, Manuscripts, Theses, Dissertations, Reports

Submit your manuscripts to:
theexcellentsolutions@gmail.com

For Online Submission:
https://www.theexcellentsolutions.com/submit-manuscript/

Website:
https://www.theexcellentsolutions.com/

Registered with the Registrar of News Papers for Govt of India, Regd.No.UPENG/1982/02321

Annual Subscriptions Charges 2023

Name of the Journal	Vol.	Freq.	Annual Subscriptions Charges		
			India (INR)		Foreign(USD)
			Print	Online	Print/Online
Bulletin of Pure and Applied Sciences *Section-A-Zoology* **pISSN-0970-0765, eISSN 2320-3188**	**42A**	**Half-yearly**	**3200**	**2000 + 18% GST**	**100**
Bulletin of Pure and Applied Sciences *Section-B-Botany* **pISSN-0970-4612, eISSN 2320-3196**	**42B**	**Half-yearly**	**3200**	**2000 + 18% GST**	**100**
Bulletin of Pure and Applied Sciences *Section-C-Chemistry* **pISSN-0970-4620, eISSN 2320-320X**	**42C**	**Half-yearly**	**3200**	**2000 + 18% GST**	**100**
Bulletin of Pure and Applied Sciences *Section-D-Physics* **pISSN-0970-6569, eISSN 2320-3218**	**42D**	**Half-yearly**	**3200**	**2000 + 18% GST**	**100**
Bulletin of Pure and Applied Sciences *Section-E-Math & Stat.* **pISSN-0970-6577, eISSN 2320-3226**	**42E**	**Half-yearly**	**3200**	**2000 + 18% GST**	**100**
Bulletin of Pure and Applied Sciences *Section-F-Geology* **pISSN-0970-4639, eISSN 2320-3234**	**42F**	**Half-yearly**	**3200**	**2000 + 18% GST**	**100**
Bio-Science Research Bulletin *(Multidisciplinary Journal of Biological and Medical Sciences)* **pISSN-0970-0889, eISSN 2320-3161**	**39**	**Half-yearly**	**3200**	**2000 + 18% GST**	**100**
Library Progress International *(Library & Information Science)* **pISSN-0970-1052, eISSN 2320-317X**	**43**	**Half-yearly**	**3200**	**2000 + 18% GST**	**100**

Subscription Agencies:

M/S U B S Publishers & Distributors, 5-Ansari Road, New Delhi-110002
M/S D.K. Agencies (P) Ltd, A/15-17, Mohan Garden, Najafgarh Road, New Delhi-110059
M/S Central News Agencies Pvt Ltd, 4E/15 Jhandewalan Extn, New Delhi-110005
M/S Total I T Solutios Pvt Ltd, WZ-248- 2nd Floor, Plot No. 07, Inderpuri, New Delhi-110012
M/S D K Books & Periodicals, 109/662, Ananda Vihar, Nugaon Road, Sisupal garh, Odisha-751002
M/S Higgibothames Pvt Ltd, 116 (Old No. 814) Anna Salai, Chennai-600002
M/S IBH Publications Pvt Ltd, Gr. Flr, Tejkiran Co-operative Society, 2nd Dadiseh Cross Lane, Chowpatty Bandstand (Nr. Babulnath), Mumbai-400 007 (MS)
M/S Mother India Associates, Post Box 7361, AP-B-818, Ist Floor,I-street, G-Block, 11th Main Road, Anna Nagar, Chennai-600040 (TN)
M/S International Book House Pvt Ltd, Indian Mercantile Mansion (Extn), Madam Cama Road, Colaba, Mumbai-40001
M/S Vardhaman Agency, 1-Mahavir Complex (Near ICICI Bank), Kalawad Road, Rajkot (Gujurat)-360001
M/S Globe Subscription Agency, 3-4-870/1, Barkatpura, Hyderabad-500027

For details, please contact- editorbulletin8@gmail.com, bpassbuscriptions@gmail.com
Printed, published and owned by: A K Sharma, Modinagar, Ghaziabad, U.P., India.